INSTITUTO SUPERIOR DE ENGENHARIA DO PORTO

MESTRADO EM ENGENHARIA MECÂNICA

isep

STUDY ON FEASIBILITY AND VIABILITY OF APPLYING ECO-FRIENDLY MATERIAL FOR THE ?BE?-CAR BONNET FOR A SUSTAINABLE AUTOMOTIVE PART

DILIPKUMAR SELVARAJ

novembro de 2018

POLITÉCNICO
DO PORTO

STUDY ON FEASIBILITY AND VIABILITY OF APPLYING ECO-FRIENDLY MATERIAL FOR THE "BE"-CAR BONNET FOR A SUSTAINABLE AUTOMOTIVE PART

DILIPKUMAR SELVARAJ

2018

ISEP – School of Engineering, Polytechnic of Porto

Department of Mechanical Engineering

POLITÉCNICO
DO PORTO

STUDY ON FEASIBILITY AND VIABILITY OF APPLYING ECO-FRIENDLY MATERIAL FOR THE "BE"-CAR BONNET FOR A SUSTAINABLE AUTOMOTIVE PART

Dilipkumar Selvaraj

1161863

Dissertation presented to ISEP – School of Engineering to fulfill the requirements necessary to obtain a master's degree in Mechanical Engineering, carried out under the primary guidance of Prof. Dr. Francisco Jose Gomes da Silva and Co-Supervised by Prof. Dr. Raul Duarte Salgueiral Gomes Campilho, Adjunct Professors at ISEP – School of Engineering, Polytechnic of Porto.

2018

ISEP – School of Engineering, Polytechnic of Porto

Department of Mechanical Engineering

JURY

President

Luís Carlos Ramos Nunes Pinto Ferreira, PhD

Adjunct Professor, ISEP – School of Engineering, Polytechnic of Porto

Supervisor

Francisco Jose Gomes da Silva, PhD

Adjunct Professor, ISEP – School of Engineering, Polytechnic of Porto

Second supervisor

Raul Duarte Salgueiral Gomes Campilho, PhD

Adjunct Professor, ISEP – School of Engineering, Polytechnic of Porto

Examiner

Fernando Jorge Lino Alves, PhD

Associate Professor, FEUP – Faculty of Engineering, University of Porto

ACKNOWLEDGMENT

First and foremost, I would like to express my sincere gratitude to my principal supervisors Prof. Francisco Jose Gomes da Silva and Jose Silva. It was my prerogative to be guided by two of the amazing minds I have known and gained knowledge from their experience.

Thanks to CEIIA for providing such a fantastic opportunity to work in one of their futuristic projects and gave freedom to express my thoughts and ideas since the beginning and pushing me to think and achieve more. A special thanks to CEIIA's engineer Gustavo Burmester who helped me in every aspect for my work and thanks to engineers Renato Machado and Ines Martins for their support.

A special thanks to ISEP and especially Prof. Raul Campilho for all his motivation and guidance provided to me. Thank you for all my work colleagues.

To all my friends who stood by me in all my ups and downs and encouraged follow my passion

To my Father Selvaraj Sivalingam, for being such a wonderful father and believing in me in any situation. A lovely thanks to my mother, UshaRani Selvaraj for trusting me blindly and supported and backed me up at any cause. To my brother Jagadeesh Selvaraj thanks for always being there for me.

Finally, to the superior power beyond us which is behind us and this universe.

KEYWORDS

Sustainability, Bonnet, NCAP, Safety, CEIIA, Eco-friendly, NFRPs, Testing, Composite recycling.

ABSTRACT

The usage of plastic parts and metals parts in automotive industries is causally related to the negative impact on the environment. The fact behind using plastic auto parts is that they give the same strength as metal parts in minimal weight. However, the plastic parts are non-biodegradable, and the extraction of mineral ores lead to the polluted environment, physical landscape disturbances, and substantial harms.

Thus, this research is to find an alternative solution for such kind of problems. To begin with, attempts were performed in order to analyze the feasibility and viability of using natural fiber composites for a semi-structural or small structural auto part. In this study, the part to be studied is an automotive bonnet. Two significant parts comprise the bonnet system, the skin and the supporting frame. The objective is to replace the plastic/metal bonnet skin with an NFRP (Natural Fiber Reinforced Plastic) so that the part can be sustainable and eco-friendly. The bonnet is one of the critical components in an automobile. They have to fulfill many pedestrian safety requirements in order to successfully be certified by the NCAP, apart from being an engine cover.

This research is concerned about the bonnet of a new car called “Be”, which CEIIA is developing for a sustainable automotive future. Based on brief studies on the bonnet system, the NFRPs, and the safety requirements for the bonnet system, the use of sustainable materials and corresponding manufacturing process selection was carried out. Using the selected material, a composite laminate is manufactured using a suitable manufacturing process to produce a sustainable and eco-friendly composite.

To answer many of the significant questions such as strength and the sustainability of the composite part, various mechanical testing and numerical simulations were performed and checked with the requirement matrix. Two kinds of the recycling process are carried out, and the composite was successfully recycled to prove its sustainability. This investigation has been performed as a “CEIIA - Product Development Project,” and as a master thesis for “Instituto Superior de Engenharia do Porto,” during February-October 2018.

Man needs his difficulties because they are necessary to enjoy success...

-Dr. A. P. J Abdul Kalam

Anything that can be dreamt of will eventually be built...!!

-Dilipkumar Selvaraj

LIST OF SYMBOLS AND ABBREVIATIONS

List of abbreviations

A	Bending test samples without additives
AB	Bending test samples with additives
ADAS	Advanced Driver Assistance Systems
AHSS	Advanced High Strength Steel
AI	Artificial Intelligence
ANSI	American National Standards Institute
ASTM	American Society for Testing and Materials
AT	Tensile test of samples with additives
AW	Moisture absorption test samples with additives
BEV	Battery Electrical Vehicles
BIW	Body-in-White
BPP	Bipolar Plates
CAD	Computer-Aided Design
CAE	Computer-Aided Engineering
CFRP	Carbon Fiber Reinforced Plastics
CLT	Classical Laminate Theory
DBTT	Ductile to Brittle Transition Temperature
DCB	Dichlorobenzene
DCPD	Dicyclopentadiene
DCT	Dual Clutch Transmission
DOE	U.S. Department of Energy
DOF	Degree of Freedom
ELV	End of Life Vehicle
EOL	End of Life
EU	European Union
EWE	Effective Moisture Equilibrium
FCV	Fuel Cell Vehicles
FM	Flexible Manufacturing
GDP	Gross Domestic Product
GE	General Electric
GFRP	Glass Fiber Reinforced Plastics
GHG	Green House Gases
GM	General Motors
GMT	Glass-Mat Thermoplastic
HDPE	High-Density Poly Ethylene

HIC	Head Injury Criteria
HSLA	High Strength Low Alloy
HSS	High Strength Steel
ICT	Information and Communication Technology
IoT	Internet of Things
MAPE	Maleic Anhydride Polymer
MEA	Membrane Electrode Assembly
MIL	Military Standards
MS	Mild Steel
NAMII	National Additive Manufacturing Innovation Institute
NFRP	Natural Fiber Reinforced Polymer
OEM	Original Equipment Manufacturer
OPEFB	Oil Palm Empty Fruit Bunch Fiber
PEEK	Polyether Ether Ketone
PEMFC	Proton Exchange Membrane Fuel Cells
PLA	Poly-Lactic Acid
POV	Point of View
PPS	Polyphenylene Sulfide
PS	Polystyrene
RLW	Remote Laser Welding
RTM	Resin Transfer Molding
SAE	Society of Automotive Engineering
SCRP	Sugarcane Reinforced Polymer
SEA	Specific Energy Absorption
SEM	Scanning Electron Microscope
SLM	Selective Laser Melting
T	Tensile test samples without additives
TSP	Tamarind Seed Powder
UDF	Uni-Directional Fiber
UHSS	Ultra-High Strength Steel
UP	Unsaturated Polyester
UUT	Under Unit Testing
V2V	Vehicle to Vehicle
VARTM	Vacuum Aided Resin Transfer Molding
W	Moisture absorption test samples without additives
WHO	World Health Organization
Wt.	Weight

List of units

^{0}C	Degree Celsius
deg	Degree-Angle
g/cc	Gram per cubic centimeter
GPa	Giga Pascal
J	Joule
kg	Kilogram
kJ	Kilo Joule
kJ/m^2	Kilo Joule per square meter
kmph	Kilometer per hour
kWh	Kilo Watt hour
min	Minute
mm	Millimeter
MPa	Mega Pascal
m/s	Meters per second-velocity
m/s^2	Meter per second square-Acceleration
N	Newton
Âµu	Angstrom micro unit

List of symbols

%	Percentage
€	Euro
$	Dollar
ε	Strain
ρ	Density
σ	Stress
ν	Poisson's ratio
μ	Friction coefficient
A	Average Acceleration
A_v	Resultant Acceleration
E	Young's Modulus
E'	Storage Modulus
E''	Loss Modulus
G	Shear modulus
I	Moment of inertia
L	Length
Li	Lithium
m	Mass
M_f	Fiber mass fraction
T	Thickness
V_f	Fiber volume fraction
W	Width
1D	One dimension

GLOSSARY OF TERMS

Benzoylation	A reaction that introduces a benzoyl group into a molecule
Biodegradability	The ability of organic substances and materials to be broken down into simpler substances through the action of enzymes from microorganisms
Body-in-White	Automobile manufacturing in which a car body's sheet metal components have been welded together
Bonnet	A car hood is a part that covers the engine/motor of an automobile
Composite Material	The material made of two or more distinct material with distinct properties
Crashworthiness	The degree to which a vehicle will protect its occupants from the effects of an accident
Embodied energy	The sum of energy needed to produce any product, from the mining and processing of natural resources to manufacturing, transport, and product delivery
End-of-life	A term used to show that the product is at the end of its useful life
Exothermic reaction	The chemical reaction releases energy in the form of heat or light
Head Injury Criteria	It is a measure of the likelihood of head injury arising from an impact
Micromechanics	Analysis of composite or heterogeneous materials on the level of the individual constituents present in that materials
Natural fiber	Fibers that are produced by plants, animals, and geological processes
Orthotropic material	The material properties vary along three mutually-orthogonal two-fold axes of rotational symmetry
Scutching	Scutching is a step in the processing of cotton or the dressing of flax or hemp in preparation for spinning
SEA	Energy absorbed per unit mass
Strain	The ratio of change in length to the original length
Stress	Force applied per unit area to the material
Sustainability	Avoidance of the depletion of natural resources to keep an ecological balance
Tensile testing	It is a fundamental engineering test in which a sample is subjected to a controlled tension until failure
Thermoplastic	Type of plastic polymer which becomes soft when heated and hard when cooled
Thermoset plastic	Thermoset plastic is a plastic which becomes irreversibly hardened upon being cured
Tribology	The study of friction, wear, lubrication, and the design of bearings; the science of interacting surfaces in relative motion
Ultimate stress	The maximum Stress a material can withstand before it breaks
Yield stress	The stress at which the material will deform permanently

FIGURES INDEX

TABLES INDEX

INDEX

INTRODUCTION

1 INTRODUCTION

This chapter is describing the thesis work on introducing Eco-Friendly materials (NFRPs) in automotive components to develop a sustainable part, to promote green initiative and to reduce the negative environmental impacts caused by conventional metal and non-eco-friendly plastic parts.

1.1 *Background*

The bonnet system is an access panel to the combustion engine/electrical motor compartment to enable maintenance of powertrain, drive belts, battery, fluid levels, and lamp units. It is fundamentally a reinforced skin panel with many safety and quality requirements. Weight reduction of the cars, especially on the front side of the vehicle, is crucial in any car to lower the fuel consumption and the emissions. To overcome these concerns, many automotive industries such as Volvo, Aston Martin, BMW, etc., started using composite materials such as CFRPs and GFRPs over metals. The exhaust emissions emitted from a passenger car has for the last decades a significant negative impact factor on the environment. However, the next big problem is an increase in usage of CFRP and GFRP composites. These composites are non-biodegradable and have a substantial negative impact on the environment. To overcome this situation, an improved knowledge in the area is needed, new thinking and finding a new technical solution is necessary. That new solution will be based on the use of eco-friendly materials, such as Natural fibers and sustainable resins, which can be recycled with less energy than other materials, allowing the production of an Eco-friendly composite.

1.2 *Aim*

This thesis aims to reach a first step in the investigation of using natural composite materials for the car bonnet. The new material needs to match the demands and requirements and lower the weight of the car bonnet, which leads to lower fuel/energy consumption and more environmentally friendly car and abet some necessary and vital human safety criteria as a complete part. Since both the natural fiber and the natural resin have low strength compared to the synthetic counterparts, it is evident in this stage to go for the semi-natural product, but the resin must be easily recyclable and must have low embodied energy as possible.

1.3 *The Challenge*

Currently there is no sustainable bonnet system in the market. In fact, there are only a few available composite bonnet systems in the industry, which are used mostly in high-end model cars. Thus, the challenge here is to create a sustainable and eco-friendly automotive bonnet system which will be later implemented in the next prototype of “Be,” the autonomous car which is under development in CEIIA. Replacing the conventional material is hard in any application, being particularly tricky in the case of the bonnet, since the bonnet system has various requirements to fulfill in order to get certified for the market use.

1.4 *Structure of the work*

In this section, the structure of the work is explained in a graphical way using Figure 1.

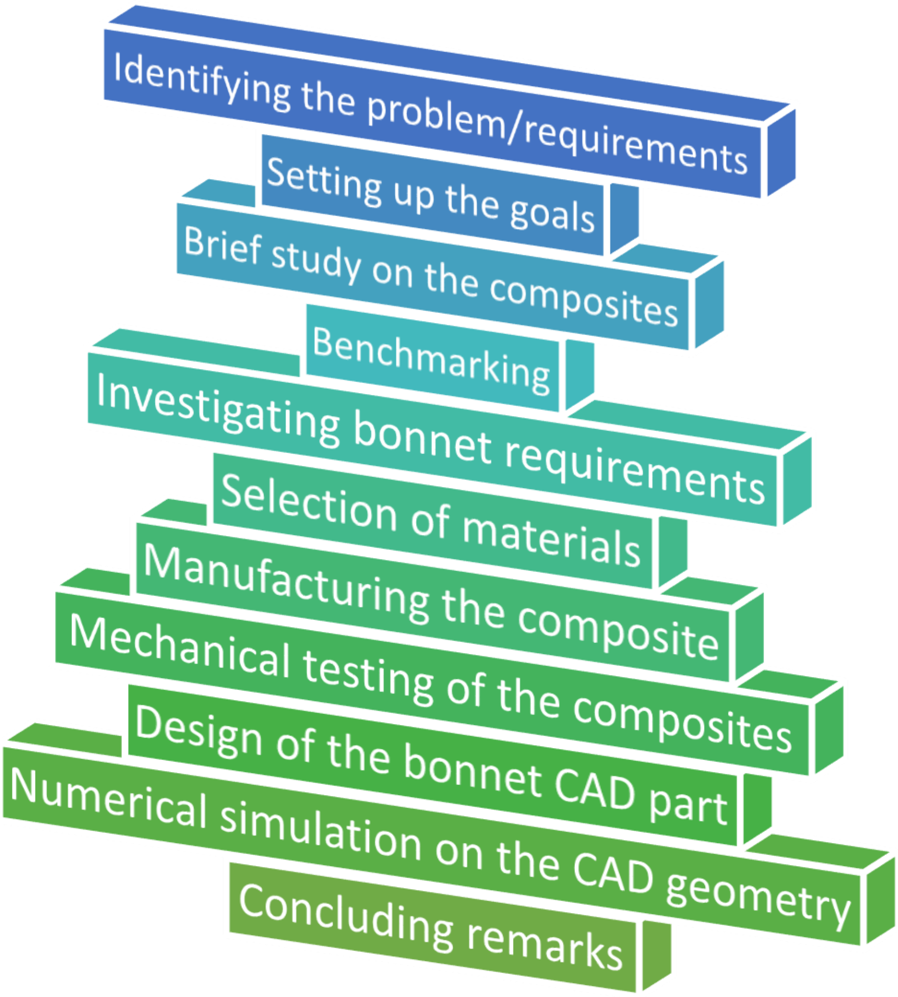

Figure 1 Work structure

STATE OF THE ART

2.1 Importance of the automotive industry
2.2 Materials usually used in the automotive industry
2.3 Composites
2.4 Benchmarking
2.5 Composite recycling

2 STATE OF THE ART

2.1 *Importance of the automotive industry*

An era of automotive industry began in the 1880s with hundreds of manufacturers that instigate the animal-less carriage. More than one hundred years ago, the United States led the world in total automobile production. Later countries like Japan, Germany, and China have been dominating the sector. Currently, China is the world's biggest vehicle manufacturer according to 2017 statistical record by producing 32,118,794 units [1].

2.1.1 *Importance of the automotive industry*

The importance of the automotive sector can be expressed in some crucial ways:

- Links to other sectors - the automotive trade encompasses essential multiplier factor impact within the economy. It is essential for upstream industries like steel, chemicals, and textiles, likewise as downstream industries like ICT (Information and communication Technology), repair, and quality;
- Employment - EU automotive sector provides a job for 12 million people distributed as follows: Manufacturing - 3million jobs, Sales and maintenance - 4.3 million jobs, and Transport - 4.8 million jobs;
- Economy - Around 6.8% of European GDP is contributed by Auto industries [2].

2.1.2 *Economic relevance*

Across the globe, there were about 806 million cars and light trucks on the road in 2007, consuming over 980 billion liters of petrol and diesel annually. The automobile is the backbone for most of the developed sectors. An American multinational management consulting firm called Boston Consulting Group's Detroit branch of predicted that, in 2014, one-fourth of the global demand will be in the four markets Brazil, Russia, India, and China (BRIC) [3]. Next, some details are provided about the automotive industry importance:

Powering economic growth

- 6.8% of EU GDP is from Automotive industries turnover;
- The automobile industry has ripple effects all over the economy, supporting a vast supply chain and generating an array of business services.

Creating skilled jobs

- 13 million people - or 6% of the EU workforce - are employed in the sector;
- The 3.3 million jobs in automotive manufacturing represent 11% of EU manufacturing.

EU Manufacturing

- 'Vehicle manufacturing' is a strategic industry in the EU, where the manufacturers are producing 19.2 million cars, vans, trucks, and buses per year;
- Automobile manufacturers run some 302-vehicle assembly and production plants in more than 26 countries in Europe.

Exporting worldwide

- The European auto industry is a global player, delivering quality 'Made in Europe' products around the world, and bringing in a €90 billion trade surplus.

Generating government revenue

- Motor vehicles account for €396 billion in tax contributions in just 15 EU countries.

Spurring innovation

- The auto trade is that the most significant private capitalist in R&D in Europe, with over €50 billion invested with annually. In 2016, about 8,000 patents were granted to the automotive sector by the EPO [3] [4].

According to the ACEA (European Automobile Manufacturing Association) Economic Market Report, European car production growth is minuscule over the 1st three quarters of 2017; the rate is 1.4% than in 2016. This growth rate is due to increased production in Ukraine, Turkey, and Russia. Those increasing rates are 128.1%, 19.4% and 14.5%, respectively. The production in the US declined slightly by 2.6%. South America recovered from a massive production drop from earlier quarters, and they managed to show a growth of 1.1%. In Asia, the four major producers India, China, Japan, and South Korea showed significant growth of 8.8%, 3.3%, 4.5%, and 2.4%, respectively. China kept contributing 26% of the global production [5], which is illustrated in Figure 2.

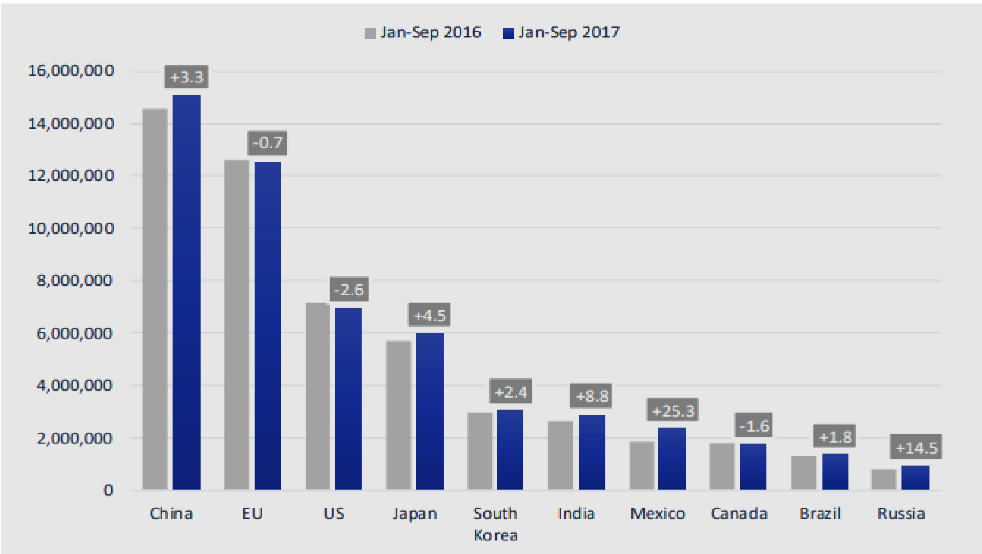

Figure 2 World passenger car production [4]

2.1.2.1 Trade

In 2017 EU car exports increased than earlier years, regarding both value (+2.3%, 4.2M cars) and volume (+4.7%, €94.5 Billion). At the same time, passenger car imports also increased (9.5%, 2.3M units) and by the value of 0.1% (€64.6 Billion) [5]. More statistical data about car vehicles trade can be seen in Annex 6.1.1.

2.1.2.2 Imports

The global import statistics in terms of value and units is increased by a considerable percentage than the earlier year. Regarding the value, Japan leads with €5,719 million, and by units, Turkey imports the most (551,776 units) [5]. More import statistics can be seen in Annex 6.1.2.

2.1.2.3 Exports

The global Export statistics in terms of value and units is increased by a considerable percentage than the earlier year. Regarding value and units, the United States top the table by exporting 828,846 units and earning €27,398 Million [5]. More statistical data about exports can be seen in Annex 6.1.3.

2.1.3 Technical evolution

Technology is one of the few things with which we humans are never satisfied with what we have now. Thus, based on our needs we keep on developing new technologies every moment we live to make our life simpler and more accessible. Computers are one of the most significant technological evolution, which changed our history. Over the decades, we expressed cars as everything from horseless carriages to hot rods, and now we are starting to think of them as smart, connected, and even someday, freeways to get around.

On the other hand, automobile technologies are considered a beacon for technology. Each step of the car's evolution has signified the achievement of engineers and innovators. It is easy to appreciate just how many times and ways this has happened within the auto industry. The following milestones in the timeline help us to understand the automotive milestones that profoundly moved the world forward [6].

Table 1 Important Car Tech Evolution [6]

S. No	Technology	Description
1	 1908 - Model T	Ford motors released the Model T to the public. The mass-produced commercial auto becomes the technological start line for the automotive as not solely a thing people could go out and buy, however additionally as a medium for brand new concepts with which future developers could work.
2	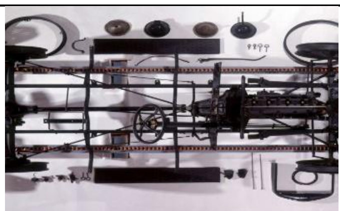 1911 - Electric Starters	Starting the car gets a lot easier, and safer. The cumbersome cranks that once fired back and killed the driver in 1910. A year later, the electric ignition debuts with a safe self-starting technology. Thus, electrical starters revolutionized the ignition system.
3	 1929 - Four-Wheel Brakes	In 1920s stopping the car safely was the biggest problem. However, by the end of the decade, some 99% of automobiles worked with brakes on each wheel. It is a humble precursor to the anti-lock braking systems that would revolutionize stopping power later in the century.
4	 1930 - Car Radio	In the 1930s for less than 130 $ one can get a radio broadcaster and receiver, which was understandably a big deal for the automobile owner and will fuel late-night parking for generations of teenagers to come.
5	 1934 - Coil Spring Suspension	Shimmying wheels and rough road conditions put more than one car into a ditch because of lousy suspension. Independent coil spring suspension comes into its own in '34 — first in the front, later for the back wheels, too. The improved handling saves aggravation and lives.
6	 1949 - Up, Up (and Away)	A decade of automotive optimism hits a momentary high with the creation of the world's first flying car. The Aero car never really took off (apparently), but one did recently appear on the market.

7	 1956 - Power Steering	An invention on the drawing boards of carmakers for decades, power steering finally becomes a standard feature in the post-War autos of the '50s. By the decade's end, one in four drivers are making turns with the help of hydraulics.
8	 1969: 3-Speed Automatic Transmission	A demand for automatic transmissions arose in the 1950s, and the ways they worked became more straightforward and more powerful. By the end of the '60s, it is a standard inclusion in many makes and models. Also, in a small victory for beleaguered mammals, manufacturers stop using whale oil in the transmission fluid.
9	 1973 - Catalytic Converter	We could all breathe a little easier. The first production catalytic converter is introduced, scrubbing tailpipe emissions and getting around a cleaner proposition. Thanks to new federal regulations, adoption of the devices is well underway by the mid-'70s.
10	 1982 - Electronic Fuel Injection	For most of the auto's history, there is not a genuinely standard approach to how the vehicle mixes air and fuel to get the most out of its engines. However, sensors and microprocessors change the playing field, starting in the early '80s, and automotive design begins to set a new baseline for the process.
11	 1984 - Air Bags	There is a common thread throughout the history of autos. Inventions seldom take root right away, and they happen in many ways and places, overlapping. After many tries, by 1984 manufacturers are figuring out cost-effective and safe ways to deploy airbags. They start to become standard features for the first time.
12	 1994 - On-Board Diagnostics	On-board computer-assisted diagnostics have been a thing for some time, but starting in about '94, the 16-pin connector that garage mechanics will come to know so well begin to appear increasingly frequently under the dash.

13	 1995 - Navigation Systems	GPS navigation makes mostly reliable possible for drivers, but the first system appears a half-decade before the 2000's.
14	 2000 - Hybrid Cars	Changing the fuel that cars use in the first place could be one of the most profound potential steps in automotive evolution. Hybrid electric vehicles get their first mass-production shot at the turn of the century. While there are still challenges ahead, it does not yet look like they will go away.
15	 2000–now - Connected and 'Smart' Cars	In the coming decade, our auto may well be just another part of the fully connected consumer experience. Optimizing their performance and maintenance is one thing, but the potential to move into a realm where cars navigate, brake, avoid collisions and hazards on their own. The smart cars are the future of automotive industry.

Apart from these technologies, there are some other essential technologies. These techs are the most important achievements and milestones of the last three decades [7].

Electronically Controlled Torque Vectoring Differential

Mitsubishi was one of the first manufacturers to offer an electronically controlled differential. The system was called Active Yaw Control and was available on its high-performance Evolution model in the late 1990s. Today, one can find active differentials that use electronics to send torque across an axle in many high-performance cars. If equipped in both the front and rear axles of an all-wheel-drive car, these sophisticated differentials can direct the vehicle's torque to any wheel in any amount at any moment. That not only improves handling when the driver is pushing hard, but it also improves the around town drivability and traction in foul weather, without any drawbacks (Figure 3).

The Smart Key

In 1998, Mercedes-Benz was the first to offer the tech. Some of the first versions were card-sized slivers of plastic, but those evolved into the fobs one has today. A modern smart key is shown in Figure 4 [8].

Dual Clutch Transmission

DCT offers the benefits of a traditional automatic transmission with none of the drawbacks. On a six-speed DCT gearbox, for instance, one clutch shifts the odd gears (1, 3 and 5) and the other one handles even gears (2, 4 and 6). The twin clutches, which can be seen in Figure 5, the driver shift gears seamlessly with incredible speed. The result is something as easy to use an automatic, but with quicker shifts than a manual.

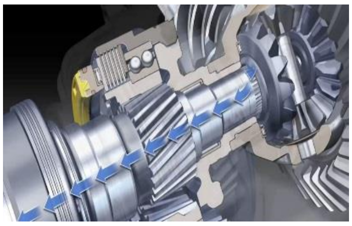

Figure 3- EC Torque Vectoring Differential [8]

Figure 4- The Smart key [8]

Figure 5 Dual Clutch Mechanism [8]

Advanced Turbocharging

The use of turbos on production cars is usual since the 1960s. These compressors, driven by the vehicle's exhaust gases, force more air into the cylinders. When combined with more fuel, that results in more power. Turbos can make a small engine perform like a much larger one.

Both GM (General Motors) and Ford introduced small turbocharged engines in the 2008-2009 timeframe, that signaled the tech had matured enough to install in the company's least-expensive cars. Now, automakers could use smaller, more efficient turbo engines and retain (or even exceed) the power levels of larger engines which can be seen in Figure 6. Today, every manufacturer has downsized its engines to smaller turbocharged ones with a boost in performance and fuel economy.

Mandatory Tire Pressure Monitoring (TPM)

There are two types of systems. The indirect TPMS (Time-Pressure Monitoring System) uses the anti-lock braking system and wheel speed sensors to notice if tires are spinning faster than they should, showing reduced air pressure. Light illuminates when the tire is 25 percent below a pressure threshold. The direct TPMS is far more correct and uses pressure sensors inside each wheel to measure tire pressure and send it to our vehicle's information center. A typical TPM can be seen in Figure 7.

Rear View Backup Camera

In 2002, Infiniti launched a lifesaver with the first backup camera available in the new Nissan Q45. With a camera mounted below the trunk lid and a monitor in the dash, these early systems saved lives and made parking far easier for thousands of car owners. Later in the decade, Nissan introduced its Around View Monitor, which used multiple cameras to produce a 360-degree perimeter picture of the area around the car. Some of the best systems, like the one in the new Mercedes-Benz E-Class, even give enough detail such as the proximity of nearest object etc. when parking (Figure 8).

Figure 6- Turbo Charge [8]

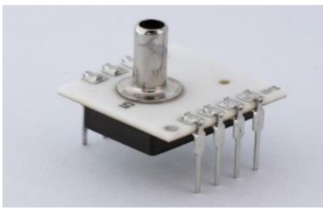

Figure 7- Tire Pressure monitor [8]

Figure 8- Rear view camera [8]

GM EV1, the First Highway-Capable Mass-Produced Electric Vehicle

In 1991, GM launched the fully electric EV1. This car looked and drove like the future, but it was not without faults. The EV1 had long charge times, and though it promised 70-90 miles on a charge, Popular Mechanics' real-world testing at the time saw ranges closer to 50-60 miles. The EV1s were all leased vehicles and famously crushed upon their return to GM, and to some, it seemed like the crushing of EV (Electrical Vehicles) resurgence along with them. However, it was the pioneering efforts of GM and others, along with advancements in battery technology, which set the stage for the EV revolution which began a decade later. We have heard all about Tesla, no doubt. However, the more established car companies are taking EVs more seriously than ever. GM's new brainchild is the Bolt, an affordable car that delivers 240 miles on a single charge.

Bluetooth Integration

The significance of Bluetooth's wireless technology to the automobile industry was not clear when it was launched in the late 1990s. However, by 2001 it had its first application in-car kit for talking on mobile phone hands-free. Today, this technology is in about every car and installed on about every mobile phone. It is so ubiquitous one rarely thinks about the fact that one did not use it a couple of years ago. However, to legally talk on our phone in the car in the EU, a hands-free connection must be set up between the phone and the car. Moreover, Bluetooth is the way to make that happens.

Radar-Based Cruise Control

As technology has advanced, it has gotten more ambitious. This same radar tech system used in many vehicles in collision avoidance systems that warn a driver when he/she is in danger, apply full brake power automatically. Mercedes-Benz added the ability to steer the vehicle some years ago automatically, and last year Tesla enabled its controversial autopilot with fully autonomous control. Someday in the future, when car does the whole driving, remember that it all started with a small improvement in cruise control.

Stability Control

Electronic Stability Control (ESC), which helps correct a skid if your car begins to slide, was the final step in a technical progression that began with anti-lock brakes in the 1970s and 1980s.

As computing power increased, and sensors improved (and got cheaper), automakers could apply the brakes to individual wheels to reduce wheel slip and increase traction. Thus, traction control was born. What stability control added was a yaw sensor to decide whether the car was sliding. If ESC detects a slide, the system will apply the brakes on individual wheels to help control the skid and straighten the car's path. Some ESC systems control the throttle to manage power going to the wheels.

Toyota Prius and the Hybrid Drivetrain

No drivetrain advancement has improved fuel economy more dramatically than the hybrid-electric powertrain, and today hybrids are so conventional that it is hard to imagine a time before them. They are just now old enough to vote.

Toyota was the first to market with a mass-produced hybrid in the form of the 1998 Prius. It combined a dinky 1.5-liter gas engine with an electric motor and nickel-metal hydride battery pack. Few embraced the tech early on, but the idea was revolutionary and changed the face of the car industry—nearly every automaker has a hybrid or plug-in hybrid in the lineup. Moreover, while few loved the frumpy body of the first Prius, Toyota soon replaced it with the cars natural futuristic look. Since the 1990s, Toyota has sold 4 million Prius liftback and now has a full lineup of Prius-badged hybrids.

In 2018 the technology that trends in the automotive industry is listed below [9].

Autonomous Driving

Most innovative research and development in the auto industry today is already focused on enabling self-driving transport. In 2017, Nvidia has introduced a chipset to support Level 5 autonomy, and new driver-assisted technologies (ADAS – Advanced Driver Assistance Systems) are already gradually seeping down into today’s vehicles.

Full autonomy is not extremely far off either: the race for the first Level 5 autonomous car is expected to result in fully functional driverless vehicles hitting the road as early as 2020. In the meantime, the development of new wireless communication technologies (5G) and AI (Artificial Intelligence) is evolving fast to enable full autonomy.

Big Data

Multiple sensors and wireless V2V communication over the IoT (Internet of Things) are fundamental pillars of self-driving automotive technology. All data they generate and send a brand-new source of revenue for automotive companies: Big Data is expected to be the next big thing in the industry. Coupling Big Data with AI could have significant implications for the auto and transport industries. The combination of V2V communication, Big Data, and AI could contribute to a variety of feature and service innovations including more efficient traffic systems, customized insurance policies, etc.

2.1.4 *Evolution of Electric Cars*

Electric vehicles first appeared in the mid-19th century. An electric vehicle held the vehicular land speed record until around 1900. The high cost, low top speed, and short range of battery electric vehicles, compared to later internal combustion engine vehicles, led to a worldwide decline in their use; although using of electric vehicles has continued to be in the form of electric trains and another niche uses.

At the beginning of the 21st century, interest in electric and other alternative fuel vehicles has increased due to growing concern over the problems associated with hydrocarbon-fueled vehicles, including damage to the environment caused by their emissions, and the sustainability of the current hydrocarbon-based transportation infrastructure, as well as improvements in electric vehicle technology. Since 2010, joint sales of all-electric cars and utility vans achieved 1 million units delivered globally until September 2016 [10].

The birth of the electric vehicle

It is difficult to spot the invention of the electric car to a person or country. Instead, it was a breakthrough in the 1800s that lead to a first non-combustion powered vehicle on the road. In the early part of the century, innovators in Hungary, the Netherlands and the United States began toying with the concept of a battery-powered vehicle and created some of the first small-scale electric cars. Moreover, Robert Anderson, a British inventor, made a first crude-electric carriage. In the US, the first successful car was launched around the 1890s.

Over the next few years, different manufacturers will launch electric vehicles. Nowadays, there are more than 200 electric taxis in NY city. During the next ten years, they continue to show strong sales.

The early rise and fall of the electric car

To understand the popularity of electric vehicles during the 1900s, it is essential to understand other options that were available at that time. At the beginning of the 20th century, the horse was still the primary mode of transportation. However, in America, they started inventing new motor vehicles to get around.

Steam was the actual energy source, powering factories and trains. However, they are not suited for personal vehicles since they needed long startup times and would need to be refilled with water, limiting their range. Then there is the arrival of electric vehicles along with steam or gasoline powered vehicles.

Gasoline cars needed much manual effort, and they produce huge noise, and the exhaust was unpleasant. Electric cars did not have any of these issues. They are quiet and less pollutant. It was Henry Ford's mass-produced Model T that dealt a blow to electric cars. Introduced in 1908, the Model T made gasoline-powered cars widely available and affordable. By 1912, the gasoline car cost only $650, while an electric roadster had been sold for $1,750.

Gas shortages spark interest in electric vehicles

Fast forward to the late 1960s and early 1970s, soaring oil prices and gasoline shortages created a growing interest in lowering the U.S.'s dependence on foreign oil and finding homegrown sources of fuel.

Around this same time, many big and small automakers began exploring options for alternative fuel vehicles, including electric cars. For example, General Motors developed and displayed a prototype for an urban electric car at the Environmental Protection Agency's First Symposium on Low Pollution Power Systems Development in 1973, and the American Motor Company produced electric delivery jeeps that the United States Postal Service used in a 1975 test program. Even NASA helped raise the profile of the electric vehicle when its electric Lunar rover became the first human-crewed vehicle to drive on the moon in 1971 [11].

Environmental concern drives electric vehicles forward

In the 20 years since the long gas lines of the 1970s, interest in electric vehicles had mostly died down. During this time, automakers began changing some of their popular vehicle models into electric vehicles, which meant that electric vehicles now achieved speeds and performance much closer to gasoline-powered vehicles, and many of them had a range of 60 miles. One of the most popular electric cars during this time was GM's EV1. Instead of changing an existing vehicle, GM designed and developed the EV1 from the ground up. With a range of 80 miles and the ability to accelerate from 0 to 50 miles per hour in just seven seconds, the EV1 quickly gained a cult following. However, because of high production costs, the EV1 was never commercially viable, and GM discontinued it in 2001.

A new beginning for electric cars

While all the starts and stops of the electric vehicle industry in the second half of the 20th century helped show the world the promise of the technology, the true revival of the electric vehicle did not happen until around the start of the 21st century.

The first turning point many have suggested was the introduction of the Toyota Prius. Released in Japan in 1997, the Prius became the world's first mass-produced hybrid electric vehicle. The worldwide release of the Prius in 2000, made it an instant success with celebrities helping to raise the profile of the electric car.

The other event that helped reshape electric vehicles was the announcement in 2006 that a small Silicon Valley startup, Tesla Motors, would start producing a luxury electric sports car that could go more than 200 miles on a single charge.

Tesla's announcement and later success spurred many big automakers to accelerate work on their electric vehicles. In late 2010, the release of the Chevy Volt and the Nissan LEAF in the U.S. market happened. Automakers and other private businesses also installed their chargers in more than 8,000 different locations with more than 20,000 charging outlets [11].

At the same time, new battery technology began hitting the market, helping to improve a plug-in electric vehicle's range. Consumers now have more choices than ever when it comes to buying an electric vehicle. Today, there are 23 plug-in electric and 36 hybrid models available in a variety of sizes with more than 234,000 plug-in electric vehicles and 3.3 million hybrids on the road in the U.S.

The future of electric cars

It is hard to tell where the future will take electric vehicles, but it is clear they hold much potential for creating a more sustainable future. Many governments and many private research centers and Industries are spending billions and billions in electric vehicles to develop a futuristic and reliable alternate fuel consuming vehicles [11].

2.2 *Materials usually used in the automotive industry*

2.2.1 *Requirements for materials in automotive*

The materials used in the automotive industry must satisfy several benchmarks before being approved. Some of them are the results of regulation and legislation with environmental and safety concerns, and some are customer requirements. In many occasions, different factors are conflicting, so an optimized and balanced solution is achieved only by a successful design.

Lightweight

As there is a high accentuate on greenhouse gas reductions and improving fuel efficiency in the transportation sector, all car manufacturers, suppliers, assemblers, and part producers are investing materially in lightweight materials research, development, and commercialization. All are moving towards the use of lightweight materials and achieving more market penetration by manufacturing components and vehicle structures made from lightweight materials. Automakers have been investigating the replacement of steel with aluminum, magnesium, composites, and foams to achieve lightweight construction, without compensating on stiffness (Table 2) [12].

Some of the facts about lightweight materials are listed below [13]:

- HSS (High Strength Steels) account for the most significant percentage of total tons of lightweight materials consumed, followed by aluminum and plastics. In value terms, plastics with their high unit prices are the largest market segment.
- The consumption of lightweight materials around the globe used in transportation equipment was 146.8 million tons/$180.5 billion in 2012 and will increase to 168.5 million tons/$206.4 billion by 2017.
- Motor vehicles, particularly passenger cars and light trucks, are by far the largest end-user segment. Shipbuilding was the second largest consumer of lightweight materials, while the aircraft industry ranks second in the value of the lightweight materials consumed.

Table 2- Alternative materials, potential weight savings versus cost

	Steel (kg)	Aluminium (kg)	Magnesium (kg)	%Weight (Part)	Reduction (Vehicle)	%cost increase
Body in White (BIW)	285	218	N/A	23.5	3.9 (Vehicle mass of 1700 kg)	250
Bonnet	14.5	8.3	N/A	44	0.48 (Vehicle mass of 1350 kg)	300
IP Beam	15.7	9.5	N/A	39	0.40 (Vehicle mass of 1500 kg)	275
Panel support	11.4	N/A	6.3	45	0.33 (Vehicle mass of 1500 kg)	350

Source 1: Corus Automotive Eng., 2010

Cost

One of the most critical consumer-driven factors in the automotive industry is the cost. Comparing the cost of new material to the material that presently employed in a product, it is one of the most critical variables that decide whether any new material has an opportunity to be selected for a vehicle part. Cost includes three components: the actual cost of raw materials, manufacturing value added, and the cost to design and test the product. This test cost can be significant since it is only through successful vehicle testing that the product and manufacturing engineers can achieve a 'level of comfort" to choose newer materials for application in a high-volume production program.

Aluminum and magnesium alloys are indeed costlier than the currently used steel and cast irons that they might replace. Based on their reduced manufacturing cycle times, better machinability, ability to have thinner and more variable wall dimensions, closer dimensional tolerances, reduced number of assemblies, more efficiently produced to near net shape. Since cost may be higher, decisions to select light metals must be justified based on improved functionality. Government regulations mandate reductions in exhaust emissions, improved occupant safety, enhanced fuel economy, reductions in workplace emissions, increased safety requirements, and requirements for toxic materials handling and disposal. Also, the high cost is one of the significant barriers in use of the composite materials.

Safety, crashworthiness

The ability to absorb impact energy and be survivable for the passengers is called the ''crashworthiness'' of the structure in a vehicle. There are two crucial safety concepts in the automotive industry to consider, crashworthiness and penetration resistance. Crashworthiness is the potential of absorption of energy through controlled failure modes and mechanisms that give a gradual decay in the load profile during absorption. However, penetration resistance is concerned with the total absorption without allowing projectile or fragment penetration.

The current trend of materials in the car industry is towards replacing metal parts increasingly by polymer composites to improve the fuel economy and reduce the weight of the vehicles. Considering several aspects of design for improved crashworthiness, including the geometrical and dimensional aspects, which have a crucial role in different stages of the crash. However, the materials deformation and progressive failure behavior regarding stiffness, yield, strain hardening, elongation and strain at break are also especially significant in the energy absorption ability of the vehicle [14].

Recycling and life cycle considerations

One of the major growing concerns in all the industries, including automotive, is an increased awareness of the environmental concerns. Issues such as the protection of resources, reduction of CO_2 emissions and recycling, are topics with increasing interest.

The End of Life Vehicles (ELV) Directive from the environment agency aims at reducing the scrap rate waste produced by vehicles. Around two million vehicles reach the end of their life in the UK each year. The directive needs ELV treatment sites to meet stricter environmental standards. The Certificate of Destruction should be issued to the last owner of a vehicle, and they must be able to dispose of their vehicle free of charge. Vehicle manufacturers and importers must cover all or most of the cost of the free take-back system. It also sets higher reuse, recycling, and recovery targets and limits the use of hazardous substances in both new vehicles and replacement vehicle parts [15].

2.2.2 Evolution of the materials and manufacturing processes

The introduction of new materials with better performance characteristics into vehicles has been taken for various reasons, but primarily for improving crashworthiness, noise, and vibration, overall cost, and fuel economy. The regulatory pressure to improve fuel economy is expected to accelerate the evolutionary rate of the introduction of lightweight materials into vehicles [16].

Key Enabling Factors

- **Fuel Economy:** Lighter materials will lead to lighter vehicles that need less fuel for propulsion. Fuel economy is an attractive selling feature for customers, so automakers will try to satisfy this demand;
- **Vehicle Emission Reduction:** Legislative requirements may force automotive manufacturers to improve fuel economy to lower greenhouse gas (GHG) emissions;
- **Autonomous Vehicles:** Self-driving vehicles have significantly more components than driver-required vehicles. Thus, offset this extra weight and space through the lighten of the other parts;
- **Electric Powertrain:** Electric engines and batteries weight more than modern internal combustion engines. The switch to electric powertrains needs other materials to be lighter to compensate;
- **Added Content:** Drivers expect improved vehicle features each new model. Components need to become lighter over time, or else fuel economy will suffer.

Threatening Factors for this evolution

- **Mixed Material Joining:** Innovating the traditional welding techniques since there is a difference in melting points between materials;
- **Corrosion:** Exposure to moisture can break down new materials over time, causing failure of vehicle systems;
- **Thermal Expansion:** As parts enter to paint ovens, parts made of some materials may expand or be coated differently than other materials;
- **Cycle Time:** Parts made of innovative materials need to be manufactured at a similar speed as a traditional technique to ensure a similar throughput;
- **Cost:** New materials, such as carbon fiber, can cost significantly more than traditional materials;
- **Supply Chain:** Manufacturers across the world must be able to supply materials and keep the equipment to process it. More complex materials are challenging to reproduce across the world, leading to supply chain disruptions;
- **End-of-life Recycling:** Automotive materials should be recyclable upon the retirement of a vehicle. Some advanced materials do not meet recycling requirements;
- **Repair:** Repair costs are higher with more complex materials, which increases the cost of ownership including ongoing maintenance fees;
- **Talent Gap:** Training the engineers and manufacturing plant workers need to work on new complex materials and processes.

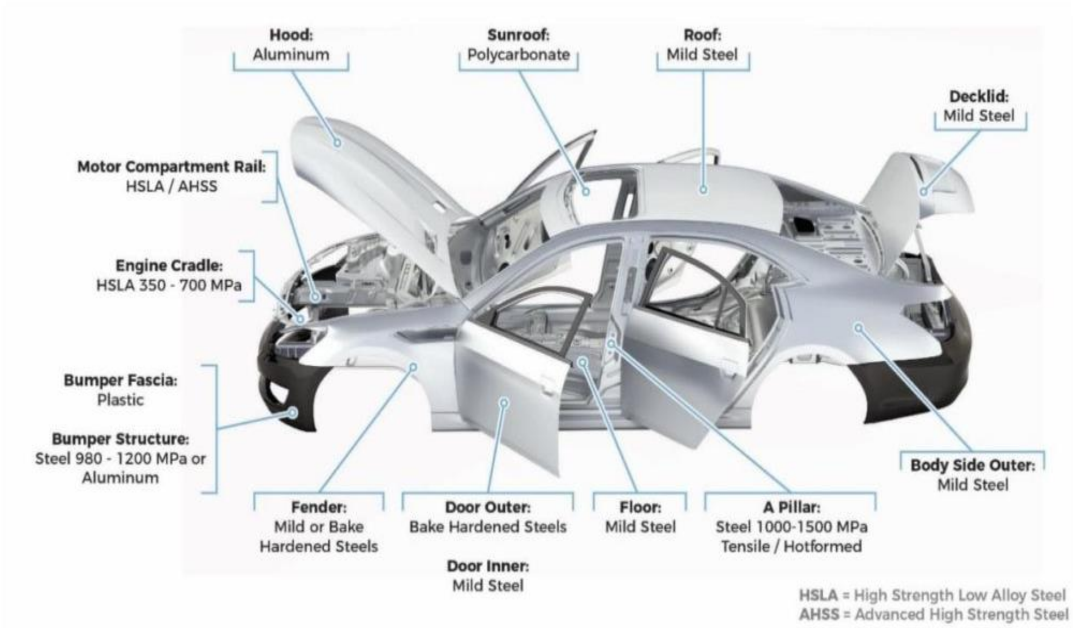

Figure 9 Materials used most commonly for major vehicle structure components in the current fleet [17]

Today, and shortly, the most commonly used automotive materials include:

MS: Mild steels are easy to form, which makes them a top choice for automotive parts manufacturers, using cold stamping and other dated manufacturing processes. They have a tensile strength of 270 MPa.

HSS: High strength steels use traditional steels and remove carbon during the baking cycle. Thus, softer steels can be formed, then treated into harder metals. Typical tensile strength grades range from 250 to 550 MPa.

HSLA: HSLAs (High Strength Low Alloys) are carbon manganese steels strengthened with the addition of a microalloying element such as titanium, vanadium, or niobium. These have a tensile strength up to 800 MPa and can still be press formed.

AHSS: Advanced High Strength Steels (AHSS) yield strength levels more than 550 MPa. They are composites made of multiple metals, then heated and cooled throughout the manufacturing process to meet a part's specifications.

UHSS: Ultra-High Strength Steels (UHSS) follow similar properties as AHSS but keep strength levels of at least 780 MPa.

Boron/Martensite: Martensite is the hardest and most durable form of steel, but it is also the least formable. It shares properties with boron, which has a tensile strength of around 1,200 to 1,800 MPa. These are usually combined with softer steels to form composites.

Aluminum 5000/6000 (AL 5000/6000): Alloying 5000-series aluminum with magnesium. 6000-series aluminum has both silicon and magnesium which forms magnesium silicide and makes the aluminum alloy heat-treatable.

Magnesium: Magnesium is an attractive material for automotive use because of its lightweight. When alloyed, magnesium has the highest strength-to-weight ratio of all structural metals.

Carbon Fiber Reinforced Plastic (CFRP): CFRPs are extremely strong and light plastics, which have carbon fibers to increase strength. They are expensive to produce but will have a growing demand in the future automotive industry.

As depicted above, the composition of vehicles is quickly changing and becoming incredibly diverse. In the 10-year period from 2010 to 2020, mild steel use will be cut in half and replaced with higher-strength steels, aluminum, and composites. This trend will continue to unfold well into the future as automotive materials become more advanced and cost-competitive with traditional steels [17].

Natural Fiber Reinforced Polymers (NFRP):

Natural fibers come from plants which include coir, jute, basalt, cotton, banana, bamboo, hemp, and so on. These fibers are eco-friendly, lightweight, renewable, cheap and bio-degradable. These fibers are used to reinforce both thermosetting and thermoplastic matrices. Using thermosetting resins such as epoxy, polyester, polyurethane, phenolic, better mechanical properties can be achieved, such as stiffness and strength, at low-price levels [18].

Core technologies for future automotive production

The following figures shows some of the technological evolution in automotive components production. Figure 10 shows the manufacturing of Li-ion battery which is used in cars nowadays where Figure 11 show the advance battery technology such as fuel cell technology used in an automotive vehicle. The fuel cells are place along with the frame which is used to activate the actuators. Figure 12 shows the BIW manufacturing unit of a ford car. This system is known for its efficiency and precision in assembly unit.

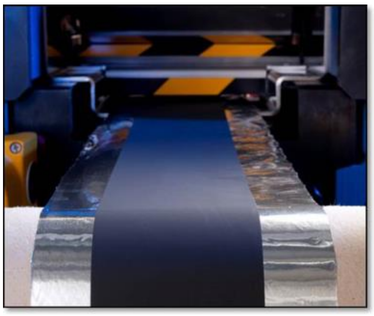

Figure 10 Development of automotive batteries [24]

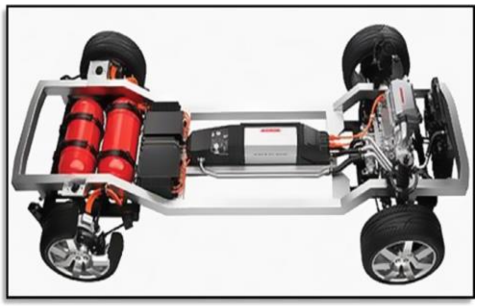

Figure 11 Fuel cells [24]

Figure 12 Robots with flexible tools, Internet-based control (Source 2 Ford)

Table 3 Summary of current trends and roads to achieve future goals

Topic	2014	2017	2020	2025	Goal
Battery Technology [19] [20].	Li-Ion pouch cells	Electrochemical models, quality characteristics	Li-Sulphur and Li-Polymer		***Li-Air***
Fuel-cell Technology [21][22][23] [24]	Novel catalysts, batch production of metallic bipolar plate	Batch production of MEA and plates, partially automated assembly of the stack	Mass production of fuel cell stacks	Highly integration and automation of fuel cells	***competitive costs and hydrogen infrastructure***
Hybrid Lightweight construction [25] [26] [27] [28]	Al, HSS, CFRP (RTM, Low automation)	AHSS 3rd gen., Al, Mg, High-performance RTM for CFRP, automated placement of hybrid structures, organic sheets, advanced joining		Metallic body structure planked with sheets of diverse materials.	***System-oriented, function-integrated multi-material-mix***
Additive manufacturing Flexible manufacturing of BIW [29] [30] [31] [32]	Rapid tooling	The increase of build-up-rate in SLM and 3D- printers, new material models, quality assurance and reproducibility		One-shot production of whole modules	***New design paradigm Manufacturing for "Functionally."***
Autonomous final assembly [33] [34]	Strict sequence inflow	Human-machine collaboration	Flexible in routs	Continuous rescheduling of work-load	***Labor and technology-flexibility***
Re-Manufacturing [35][36] [37] [38]	"Recover end-of-life products to as-good-as-new."	Advancement in inspection and non-destructive disassembly	Re-man activities adaptive to machine state	The universal re-man standard for multiple product models	***Cradle-to-cradle production design for remanufacturing***

2.2.3 *Material Selection Methodology*

Material selection is one of the significant parts of *Product designing*, correlating with other parameters such as the manufacturing method, the working environment employed and so on. To understand it completely, one should know about the designing process.

According to Ashby "Design starts with market needs. The need is analyzed, expressing it as a set of design requirements". Ways to meet these are sought, developed and refined, to give a product specification. The process and material selection process evolve in parallel. The selection strategy involves four steps, namely:

1. Translation;
2. Screening;
3. Ranking;
4. Documentation.

2.2.3.1 The Design Process

Classifying the design process is into two types based on the concept that one is an original design, and another is redesign.

Original Design:

Original design starts from scratch with a new concept and develops the necessary information to implement it, involving a new idea or working principle. New materials can be used to stimulate the original design. Sometimes new material suggests the new product. Sometimes, instead, the new product, demands the development of new material.

Redesign:

Redesign starts with an existing product and looks to change it in ways that increase its performance, reduce its cost, or both. Most design is not 'original' in the sense of starting from a new idea. It is a redesign, starting with an existing product and correcting its shortcomings, refining it, enhancing its performance or reducing its cost, without discarding the principles behind its creation.

Here are some scenarios that call for a redesign.

- **Product recall** - Released product did not meet safety standards, often material failure;
- **Poor value for money** - Product works safely but shows poor performance, at an average price;
- **Inadequate profit margin** - When the cost of manufacturing exceeds the bearable market price;
- **Stay ahead of the competition** - Designing the old model leads to redesigning.

The designing process is explained graphically using Figure 13, where the required information about materials at each stage entails different levels of breadth and precision. The broken lines suggest the iterative nature of the original design and the path followed in the redesign [39].

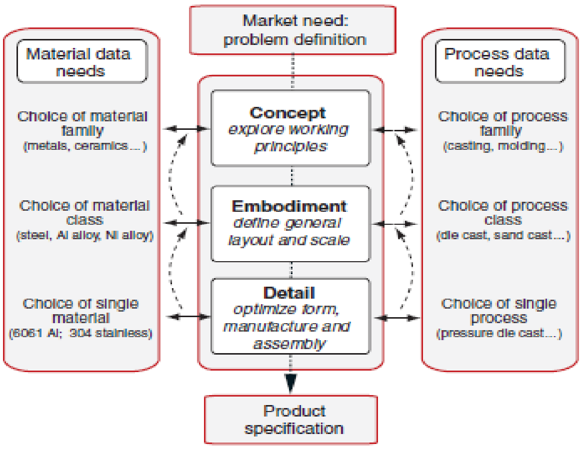

Figure 13 Design process flowchart [39]

2.2.3.2 The strategy: translation, screening, ranking, and documentation

Selection involves seeking the best match between the attribute profiles of the materials and processes—bearing in mind that these must be mutually compatible—and those needed by design. The same strategy can be adapted to select the process.

Translation

Any engineering part has one or more functions: to have pressure, to support heat and this must be achieved by constraints. Translation is the process of converting the design requirements into material choice prescription, which helps in finding the constraints that material must meet and the aims that the design must fulfill. Distinguishing between constraints and aims is essential. Meeting the constraint is an essential condition. Sorting out an aim is a quantity for which an extreme value cost, mass or volume, etc.

Screening

Screening is the step where the elimination of materials or a process that cannot do the job at all because one or more of its attributes lies outside the limits set by the constraints.

Ranking

The material that survives the screening is ranked based on their material indices. Performance is sometimes limited by a single property, sometimes by the combination of them. Thus, for buoyancy material with the lowest density, ρ; for thermal insulation the one with the smallest values of the thermal conductivity, λ. Often, though, it is not one but a group of properties that are relevant. Thus, the best materials for a light, stiff tie-rod are those with the highest value of the specific stiffness, E/ρ, where E is Young's modulus. The best materials for spring are those with the most significant value of σ_y^2/E, where σ_y is the yield strength. The property or property group that maximizes performance for a given design is called its material index. There are many such indices, each associated with maximizing some aspect of performance.

Documentation

The outcome of the steps so far is a ranked short-list of candidates that meet the constraints and is able to maximize or minimize the criterion of excellence, whichever is needed. Figure 14 is a schematic representation of screening and ranking methods in material selection.

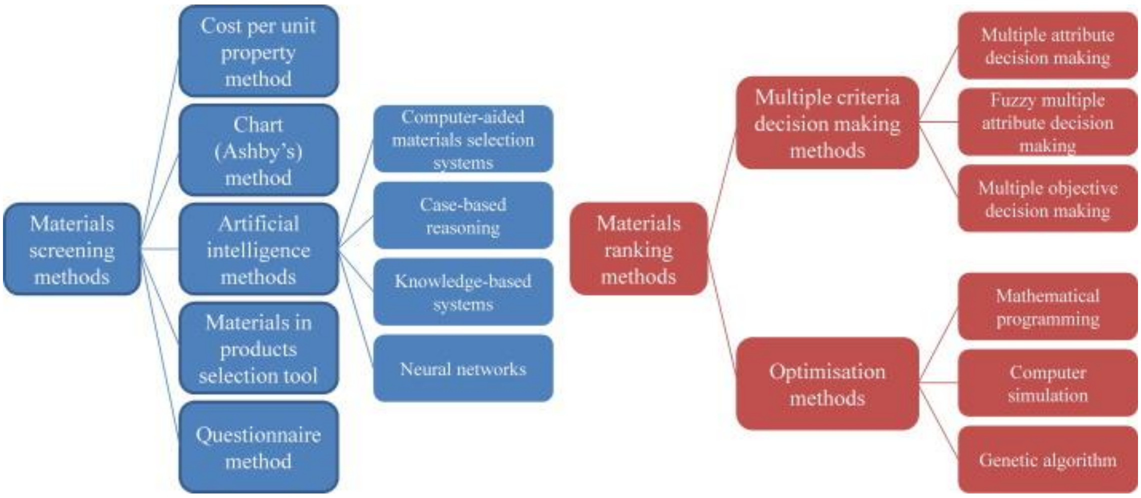

Figure 14 Classification of screening and ranking methods in materials selection [40]

2.2.3.3 The relation between Materials Selection and Design Process

Materials selection enters at every stage of the total design process. To reach the desired goal in the design process, it should typically go through certain stages, as mentioned before. Ashby developed a model describing the function of material choice in product design as shown in Figure 13. The materials needed at each stage of the design process differed. At the concept level of design, there is a broad consideration of all materials and processes. The designer needs approximate property values for the broadest range of material. Therefore, the precision of property data needed is low, and to make an innovative choice of material, it should be at this stage because too many decisions have been made to allow for a radical change in the later stages of the design. During the embodiment design, the designer will have decided on a class of materials and processes. The material properties must be known to a higher level of precision. The required data needed is found in more specialized handbooks and software, which deal with a single class of material. Finally, at the detail design, the decision will have narrowed to a single material and only a few manufacturing processes. Depending on how critical the part is, material properties have a high level of precision. The data sheets issued by the supplier present the precision of the material producers.

2.2.3.4 Ashby Method

Ashby scatters plots, created by Professor Michael Ashby of Cambridge University, display two or more properties of a material or material classes. These charts are useful to compare the ratio between the properties. This property ratio helps in deciding the material for the desired application. For example, if a plate with high stiffness and less weight is needed, one must consider the material index to be $E^{1/3}/\rho$ since the plates bending stiffness is rated as its thickness cubed. Thus, applying the cube root to the stiffness, and the density of the material divides it. Density is directly proportional to the weight of the material [39].

Utilizing an "Ashby chart" is a conventional method for choosing the right material. First, one must find three different sets of variables:

- Material variables are the inherent properties of a material such as density, modulus, yield strength, and many others;
- Free variables are quantities that can change during the loading cycle, for example, applied force;
- Design variables are limits imposed on the design, such as how thick the beam can be or how much it can deflect.

Next, an equation for the performance index is derived. This equation numerically quantifies how desirable the material will be for a specific situation. By convention, a higher performance index denotes a better material. Lastly, one selects the performance index on the Ashby chart. Visual inspection reveals the most desirable materials. Mapping those materials on the Ashby Charts and that mapped area is called as *"Area of interest."* There may be some materials in the mapped area. As an engineer, one must decide and sort out the material list and choose the "*best fit material"* for the desired application. The best-fit materials are then subjected to a quantitative method of selection, where the various properties of the materials essential for the application, are assigned with an importance value and compared with each other to form a matrix. From the matrix, the performance index of all the materials can be calculated. Then the material with high-performance index Υ is chosen for the required application. This method of material selection is one of the efficient, effective and simple way.

2.3 *Composites*

Composite materials are materials made up of two or more than two distinct materials with varying physical or chemical properties that, once combined, form a material utterly different. Both components add strength to a composite, and the combination often compensates for weaknesses in the individual components. Composites are different from alloys, such as brass or bronze, forming alloys in such a way that it is impossible to separate one part from the other. Some common composite materials include concrete, fiberglass, mud bricks, and natural composites such as rock and wood. Composites are of different types depending on the type of constituent which is combined to form a durable composite material. Composites are now extensively used for rehabilitation/strengthening of pre-existing structures that must be retrofitted to make them seismic resistant, or to repair damage caused by seismic activity. Unlike conventional materials (e.g., steel), one can design the composite properties considering the structural aspects of the composites. The design of a structural part using composites involves both material and structural design, giving rise to properties such as stiffness, thermal expansion, and so on. A careful selection of reinforcement type can achieve any desired material for almost any specific engineering requirement.

2.3.1 *Characteristics of the composites*

A composite material consists of two phases: one or more than one discontinuous phase encapsulated in a continuous phase. The discontinuous phase, which is called reinforcement, is usually harder and stronger than the continuous phase called the matrix phase. The matrix is usually more ductile, and binders the dispersed phase together share the load with it. One of these three basic material types (polymers, metals or ceramics) is chosen as a matrix. The dispersed phase embedded with the matrix is usually harder and stronger than the continuous phase. It improves the overall mechanical property of the composite and carries most of the applied load.

Properties of composites are strongly dependent on the matrix, and the dispersed phase properties, their distribution and the interaction among them. Apart from these, the geometry of the reinforcement (shape, size and size distribution) influences the properties of the composite. Also, factors such as fiber orientation, concentration and the working temperature influences the mechanical properties.

There are two types of FRPs (Fiber Reinforced Plastics), single-layer or multi-layer. A single-layer composite type consists of several layers in a stacking sequence with the material orientation in the same direction. A multi-layer composite type consists of several layers in a stacking sequence with fibers orientation in different directions. Each ply (layer) can be unidirectional and oriented in the different direction. The reason having plies with different fiber orientation is to achieve different properties in different directions of the laminate.

As mentioned previously FRP has anisotropic properties. However, layered FRPs are orthotropic. Orthotropic means that the properties are different in the three perpendicular directions as is visualized in Figure 15. The definition of the orthotropic directions is as follows: the longitudinal fiber direction as 1, the transverse direction as 2, the out of plane direction as 3. These different directions differ for each ply in a stacking sequence. If the laminate shares the same properties in all transverse directions to the fiber, the material is transversely orthotropic material.

The mechanical properties of a UD (unidirectional) ply highly depend on the fiber fraction. The properties regarding stiffness of a ply are figured out by combining the stiffness of fiber and matrix by the rule of mixture. The fiber fraction finds in no small extent the longitudinal and transverse stiffness of the ply. When stacking plies with different fiber orientations, the contributions from each layer are transformed to follow a global coordinate system, as it is shown below in Figure 16.

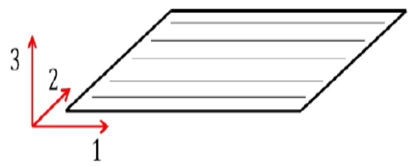

Figure 15 Illustrating the orthotropic directions

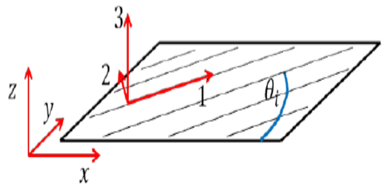

Figure 16 Illustration of the relationship between material orientation and coordinate system

During the transformation for each ply, the property contributions from each ply can be summed up in three different matrices, the extensional stiffness matrix, coupling stiffness matrix and bending stiffness matrix (A, B and D). The contribution from each ply in the B and D matrices depends on the distance to the mid-plane of the laminate. The matrices are what couples force and moments to strains and curvatures in the laminate which can be seen in Equation 2.1.

$$\begin{bmatrix} N_x \\ N_y \\ N_{xy} \end{bmatrix} = [A] \begin{bmatrix} \varepsilon_x^0 \\ \varepsilon_y^0 \\ \gamma_{xy}^0 \end{bmatrix} + [B] \begin{bmatrix} k_x \\ k_y \\ k_{xy} \end{bmatrix}, \quad \begin{bmatrix} M_x \\ M_y \\ M_{xy} \end{bmatrix} = [B] \begin{bmatrix} \varepsilon_x^0 \\ \varepsilon_y^0 \\ \gamma_{xy}^0 \end{bmatrix} + [D] \begin{bmatrix} k_x \\ k_y \\ k_{xy} \end{bmatrix} \qquad \textbf{2.1}$$

**Where N-forces in newton, M-moments in Nm., k- curvatures in m-1, ε0-mid-plane strains, [A]-Membrane extensional stiffness matrix, [B]- strain-curvature coupling stiffness matrix, [D]-Flexural stiffness matrix

2.3.2 *Natural Fiber Composites*

Fibers are hair-like materials that are a continuous thread or discrete elongated pieces, while there are two types of fibers: natural fibers and human-made or synthetic fibers. Natural fibers come from plants which include coir, jute, basalt, cotton, banana, bamboo, hemp and so on. These fibers are eco-friendly, lightweight, renewable, cheap and bio-degradable. These fibers are used to reinforce both thermosetting and thermoplastic matrices. Thermosetting resins such as epoxy, polyester, polyurethane, and phenolic are used because they give enough mechanical properties, stiffness, and strength at low-price levels. Various natural fibers that are available today in can be seen in Figure 17.

Source 3 Journal of Cleaner Production

Figure 17 Different types of natural fibers

Natural fiber composites are attractive to industry because of their low density and environmental advantages over conventional composites. These are gaining importance due to their non-carcinogenic and biodegradable properties. Natural fiber composites are cost effective materials in building and construction, packaging, automobile, railway coach interiors, and storage devices. These composites act as a replacement of high-cost glass fiber for low load bearing applications.

All plant fibers, whether from wood or non-wood origin, are composed of three main cell wall polymers such as cellulose, lignin and matrix polysaccharides (such as pectin and hemicellulose) associated with cellulose and lignin in the cell wall. A high percentage of cellulose in the fiber correlates positively with desirable characteristics. The main disadvantages of natural fibers are high moisture absorption, which can be reduced by chemical treatment.

2.3.3 *Introduction to natural fibers*

An in-depth and targeted review has been administrated on these topics and therefore the threat of global warming and the rising awareness of new environment-initiated pushing analysis activities towards bio-products. The environmental laws of different countries and therefore the client awareness of eco-friendly products also emphasize the need for manufacturing reclaimable and bio-degradable composite materials. Natural fibers have the advantage of eco-friendliness, low density, high specific strength, biodegradability, and cost-effectiveness. The rising environmental concern of the globe has currently created a paradigm transformation of applying natural fibers as reinforcements replacing artificial fibers in polymers notably within the field of automotive production. The lingo-cellulosic natural fibers of the plants and fruits do not have an abundant industrial price.

Natural fiber could also be a resource that will be adult and created among a quick quantity. The unlimited convenience of natural fibers exists once place next to the traditional glass and carbon fiber for making advanced composites. The natural fibers, once mixed with polymers, are used for making light-weight structural and bio-medical products. The properties of these natural fibers will think about the kind of the plant, extraction technique and thus the setting throughout that the plant grew, and this makes it difficult to predict the natural fiber's mechanical properties.

Malkapuram et al. [41] studied the recent development of natural fiber reinforced polypropylene composites. Natural fibers are known to be low-cost, eco-friendly and recyclable materials. The review highlighted the fact that the matrix-fiber adhesion influences the mechanical properties of composites. Chemical and physical modification methods were incorporated to enhance the matrix-fiber adhesion characteristics. They considered jute, flax, and coir fibers to describe the processing techniques to develop natural fiber reinforced composites.

2.3.3.1 Chemical Composition of Natural Fibers

The chemical composition of natural fibers varies depending upon the type of fibers. The chemical composition (Table 4), as well as the structure of the plant fibers, is complicated [42]. Plant fibers are a composite material designed by nature. The fibers are a rigid, crystalline cellulose microfibril-reinforced amorphous lignin and with hemicellulose matrix. Most plant fibers, except for cotton, are composed of cellulose, hemicellulose, lignin, waxes, and some water-soluble compounds, where cellulose, hemicelluloses, and lignin are the major constituents. The properties of the constituents contribute to the overall properties of the fiber. Hemicellulose handles the biodegradation, micro absorption and thermal degradation of the fiber as it shows least resistance, while lignin is thermally stable but prone to UV degradation. The percentage composition of each of these components varies for different fibers. The fiber holds 60-80 % cellulose, 5-20 % lignin, and up to 20 % moisture. The cell wall of the fibers undergoes a chemical treatment (pyrolysis) with increasing processing temperature and contributes to char formation. These charred layers help to insulate the lignocellulose from further thermal degradation [43]. The chemical composition of various natural fibers is listed in Table 4.

Table 4 Chemical composition, moisture content, and micro-fibrillar angle of natural fibers [43]

Fiber	Cellulose (Wt.%)	Hemi-celluloses (Wt.%)	Lignin (Wt.%)	Pectin (Wt.%)	Moisture content (Wt.%)	Waxes	Micro-fibrillar angle (Deg)
Flax	71	18.6-20.6	2.2	2.3	8-12	1.7	5-10
Hemp	70-74	17.9-22.4	3.7-5.7	0.9	6.2-12	0.8	2-6.2
Jute	61.1-71.5	13.6-20.4	12-13	0.2	12.5-13.7	0.5	8
Kenaf	45-57	21.5	8-13	3-5			
Ramie	68.6-76.2	13.1-16.7	0.6-0.7	1.9	7.5-17	0.3	7.5
Sisal	66-78	10-14	10-14	10	10-22	2	10-22
Coir	32-43	0.15-0.25	40-45	3-4	8		30-49

2.3.3.2 Mechanical properties of natural fiber and its elucidation

The attractive characteristics of plant fibers, treatments, fiber adhesion characteristics, their physical, chemical, mechanical properties, and behaviors are described as follows [44], reporting that the critical fiber length range of natural fiber composites in between 1–10 mm and would lessen with an added coupling agent. [44] also pointed out that if the critical fiber length is smaller than the reinforcing fiber length, then fiber matrix adhesion would be low. T, there will not be any increase in mechanical properties by using long fibers above 10 mm.

In [45] it is possible to observe physical, chemical and tensile properties of the Mudar fibers. The fibers have good length, fineness, strength, uniformity and excellent moisture absorption properties. The study highlighted the difficulties in spinning 100% Mudar yarn. Subsequently, a 25/75 Cotton/Mudar blend was spun successfully in a cotton spinning system, and the results were analyzed. The yarns have enough potential in natural fiber reinforced composites and other textiles and industrial application.

Bessadok et al. [46] have investigated Alfa fiber for various chemical treatments. Treating the fibers with different chemicals agents such as styrene, acrylic acid, and maleic anhydride and the effects on the fiber by infrared spectroscopy has been studied, such as surface energy, and microscopy, showing that treatments reduced the overall water uptake of Alfa fiber.

Symington et al. [47] conducted tensile tests on the fiber jute, kenaf, flax, abaca, sisal, hemp, and coir. The fibers were exposed to severe conditions such as room temperature and humidity, 65% moisture content, 90% moisture content, soaking. The effect of alkalization using 3% NaOH solution on fibers such as kenaf, sisal, kenaf, and abaca fibers was studied. The results pointed out that excess treatment could hurt the base fiber properties.

Polarized light microscopy and a Scanning Electron Microscopy were used to study the 'Sansevieria cylindrica' fiber's mechanical properties, microstructural, physical, and chemical properties. The study revealed a hierarchical cell structure that consisted of a primary wall, a secondary wall, a fiber lumen, and middle lamellae. The cross-sectional area is 24500 $\mu m^{2,}$ and the porosity fraction of the fiber was estimated at 37% [48].

Elastomers must be able to stretch a long distance and still bounce back. Most of them can stretch from 500 to 1000 % elongation and return to their original lengths without any trouble. Composites are hybrid materials made of a fiber reinforcing the polymer resins, combining the high mechanical and physical performance of the fibers and the appearance, bonding together and enriching the physical properties of polymers. The environmental impact is smaller since the natural fiber can be thermally recycled and fibers come from a renewable resource. Their moderate mechanical properties restrain the fibers from using them in high-tech applications but, for many reasons, natural fibers can compete with synthetic fibers for their biodegradability [49]. Using the agriculture residues as reinforcement in the development of polymer composites can be a vital alternative solution to solve this problem.

In recent years, due to concerns about the disposal of plastics, polymer scientists have been strongly encouraged to develop new biodegradable polymer composite materials from renewable resources. Mixing of natural fiber with is finding increased applications. Sathaye [50] developed sisal glass fiber reinforced epoxy composites, and evaluating their mechanical properties such as tensile strength, compression strength, flexural strength, and impact strength. Due to the low density and high specific properties of these natural fibers, composites based on these fibers may have extremely good implications in the automotive and furniture industry.

2.3.3.3 Mechanical properties of NFPCs

The adhesion between the matrix and the reinforcement influences the mechanical properties of the composites. Reinforcing the matrix with the fiber, a robust fiber-matrix bond has ensured the effective load transfer. The alkali treatment of the fibers removes the surface impurities and makes the fiber surface rough. This rough surface eases better mechanical interlocking of the fiber with resin, and hence the fiber matrix adhesion property improved. Nair et al. [51] examined the thermal and dynamic mechanical analysis of sisal fiber/polystyrene composites. Untreated fibers have poor thermal property than the treated natural fibers. Around 3.34% of initial weight loss between 60 °C-100 °C concern to the heat of water vaporization.

The tensile and flexural behavior of pineapple leaf fiber reinforced polypropylene composites was investigated as a function of the volume fraction [52]. The tensile modulus and tensile strength are increased concerning the increase in fiber content. The increase in volume fraction of the matrix increases flexural modulus and flexural stress of the composites, but the values were lower when compared to the results from other researches. The lower values of flexural properties are due to the presence of voids, maybe the outcome of the fiber-to-fiber interaction, and dispersion problems.

Favaro et al. [53] made the composites from post-consumer high-density polyethylene (PE) reinforced with different concentrations of rice husk. PE and rice husk were chemically changed to improve their compatibility in composite preparation. Rice husk was mercerized with NaOH solution and acetylated. Flexural and impact tests showed that PE/Rice husk composites improved mechanical performance compared to the pure polymer matrix.

2.3.3.4 Thermal behavior of NFPCs

Nowadays polymeric materials are used in all the applications because of their specific characteristics such as lightweight, self-lubricating, and reduced noise. The abundant availability of natural fibers and the ease in composite manufacturing has triggered the interest among researchers to study their thermal behavior under reinforcement in polymers. During the thermal applications like leaf springs, vehicle bodies, doors, etc., the primary failure mechanism was due to the thermal failure only.

The thermal behavior of short sisal fiber reinforced with polystyrene composites was investigated by [51]. The thermal stability of the composites was higher than sisal fiber, and the PS matrix composites, evaluating the effects of fiber loading, fiber length, fiber orientation and fiber modification on the dynamic mechanical properties of the composites. Fiber modifications were carried out by Benzoylation, polystyrene-maleic anhydride coating and acetylation of the fiber and the treatments improved the fiber-matrix adhesion. PS and sisal fiber are proven to be less thermally stable than PS/Sisal composite. The addition of 10% fiber increased the modulus, and the increase is found to be useful to carry higher fiber loadings.

Liliana et al. [54] studied the thermal degradation and fire resistance of different natural fiber composites. On using Unsaturated Polyester (UP) and changed acrylic resins (Modar) as matrix composites, thermal degradation showed that the Modar matrix composites were more resistant to temperature than the composites with UP matrix. Flax fiber, due to their low lignin content, showed the best thermal resistance among the natural fibers studied.

In the presence of a flame, burning of composites takes place in five different steps as shown below [55]:

a) Heating;
b) Decomposition;
c) Ignition;
d) Combustion;
e) Propagation.

2.3.3.5 Dynamical behavior of NFPCs

Mohanty et al. [56] studied the dynamic mechanical and thermal properties of MAPE treated jute/HDPE composites. On investigating the variations in mechanical strength, E', E'', and damping parameter (tan δ) with the addition of fibers and coupling agents, it was seen that the tensile, flexural and impact strengths increased with the increase in fiber loading up to 30%, above which there was a significant deterioration in the mechanical strength. Further, the composites treated with MAPE showed enhanced properties in contrast to the untreated composites. Dynamic mechanical analysis data showed that the treated composites have higher storage modulus [56].

The effect of jute fiber loading on tensile and dynamic mechanical properties of oil palm epoxy composites was studied by Majeedab et al. [57]. Hybrid composites were prepared by reinforcing epoxy with jute and oil palm fibers by hand lay-up technique. The tensile properties increase with an increase in jute fiber loading in this hybrid composites, compared to oil palm–epoxy composite. The examination of the nature of the fiber/matrix interface was performed through scanning electron microscopy of tensile fracture samples. Addition of jute fibers to oil palm composite increases the storage modulus while damping factor shifts towards higher temperature region [58]. A Cole–Cole analysis was made to understand the composite samples phase behavior after failure.

2.3.3.6 Biodegradability of NFPCs

Natural fiber reinforcement in polymers results in high strength composites, which also gives extra or improved biodegradability, low cost, lightweight, and enhanced properties related to mechanical structure [59]. At temperatures as high as 240 °C, degradation starts in natural fibers whereas constituents of fiber, such as hemicelluloses, cellulose, lignin, and others, degrade at different levels of temperature. For example, at 200 °C lignin starts to decompose whereas at temperatures higher than this other constituent will also degrade [60].

Since the thermal stability of the fibers is dependent on the structural constituents of fibers, it can be improved if the structural constituents or concentration levels are entirely removed or modified, such as lignin and hemicelluloses, which can be achieved with the help of chemical treatments. Development of fibers and materials are two important aspects, which should be considered while degradation of natural fibers [60]. Natural fibers have a short life with the least environmental damage upon degradation while plastic ones affect the environment due to pollution. Over fifty percent weight of jute or natural composite is lost after precisely 1500 days of burial [61].

2.3.3.7 Energy Absorption of the NFPCs

The composite materials with high strength, energy absorption, and stiffness are widely used in the automotive and motorsport sectors of the industry due to the property of mass reduction. Enhanced energy absorption is clear from the increased volume fraction that is only possible in the presence of low speed (2.5 m/s) [62]. On the other hand, at high speed of 300 m/s, jute, hemp, and flax showed similar performance, but jute revealed brittleness and low strength for fibers. Flax, jute, and hemp are manufactured by the Vacuum Assisted Resin Transfer Molding (VARTM) technique to study their properties and features. Various values showed by different kinds of materials were recorded to analyze SEA.

2.3.3.8 Tribological Properties of NFPCs

Since every material has some friction and wear properties concerning the degradation over time, the tribological loadings are essential to consider for an improved mechanical part design. Around 90% failure is obtained due to a contrast in tribological loading conditions which revamp their wear and friction properties. Studies on different kinds of tribological analysis have been carried out on many NFRPs, including kenaf/epoxy; betel nut fiber reinforced polyester, sisal/phenolic resin, sugarcane fiber reinforced polyester (SCRP), and cotton/polyester. Improvement in wear performance of PLA was apparent due to the addition of natural fibers in which the wear rate of composites was quite low in comparison to wear rate at higher loads on neat PLA [63].

Kenaf fibers reinforced with epoxy composite is studied by China et al. [64] for a bearing application, in which they showed that the wear performance of the composite part is increased by 85%. Wear and friction features of polyester/glass (GRP) and polyester/sugarcane

(SCRP) were studied by El-Tayeb [65] with different parameters, including speed, loads applied, and the time taken to test. The research results concluded SCRP as a suitable replacement for GRP composite. On studying the same characteristics for sisal fiber reinforced resin brake composites, showing that sisal fiber could be used instead of asbestos in brake pads [66]. Developing laminated composites with the help of three different natural fibers such as grewia, nettle, and sisal, Bajpai et al. [67] studied the connection of natural fibers using hot plate compression to produce three different materials in a PLA resin. Friction and wear features of the composites were investigated in different situations such as dry contact condition with varying operating parameters. Due to a choice of variable operating parameters, the applied load was varied in between the range of 10 to 30 N with speed ranging from 1 to 3 m/s and sliding distance of thousand to three thousand meters. The research results showed that an infusion of natural fiber mats in the PLA matrix could enhance the wear and frictional behavior of neat polymers. An approximate reduction of 10–44% in the friction coefficient with a more significant reduction of 70% of specific wear rate in developed composites was achieved and correlated to neat PLA [63].

2.3.3.9 Relaxation Behavior of the NFPCs

Natural fibers have an intrinsic relaxation behavior which has the primary function in the stress relaxation of NFPCs. Thus, the tensile stress relaxation of the fiber must be reviewed in detail. For instance, Sreekala et al. [59] did such a study focusing on the characteristics of individual OPEFB fiber, and examined the fiber surface modification effects, aging, and strain level on the fiber relaxation behavior. The surface treatments significantly lessened the fibers stress relaxation, like latex modification, and thus decreasing resulting physical interaction between the fiber exterior and the latex particles. Also, water and thermal aging reduce the rate of relaxation for the oil palm fiber; the rate of stress relaxation of the OPEFB is optimized at 10% strain level which is shown in Figure 18, while the relaxation modulus values for the fiber show similar trends as in the case of stress relaxation in (Figure 19).

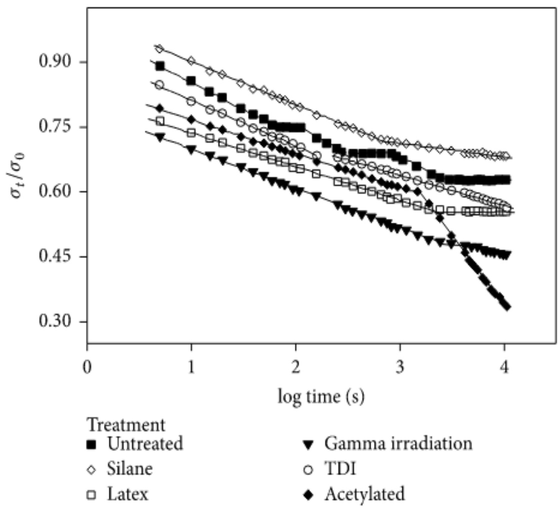

Figure 18 Stress relaxation curves of untreated and treated OPEFB fiber at 10% strain [59]

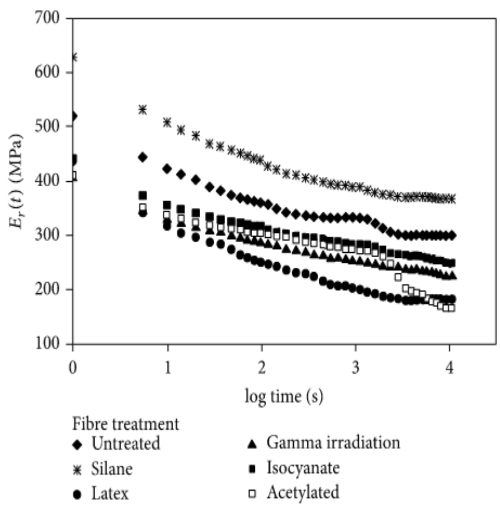

Figure 19 Relaxation modulus curves of untreated and treated OPEFB fiber at 10% strain [59]

2.3.3.10 Water Absorption Characteristics of the NFPCs

Natural fibers work well as polymer reinforcement. However, the main weakness of their application is their susceptibility to moisture. The mechanical properties of polymer composites depend on the interface adhesion between the fiber and the polymer matrix. Natural fibers are rich on hydroxy one groups such as cellulose, hemicellulose lignin, and pectin; that is, they are usually hydrophilic sources, while polymers show significant hydrophobicity. Thus, there are significant challenges of suitability between the matrix and fiber that weakens the interface region between matrices and natural fibers [68].

Woven pandanus/banana fabric composites absorb more water compared to woven banana fabric composites because of higher lignin content and hemicellulose, as well as the presence of defects in the composite system [69]. Furthermore, the temperature can affect the percentage of water absorption of the composites. At 65 % humidity at 21 °C, one can see the equilibrium moisture content of some natural fiber in Table 5. Natural fibers such as Milk Wire fiber and Borassus absorb moisture at a rate of 34 % and 63 %, respectively (Untreated) at 105 ^{0}C [70].

Table 5 Equilibrium moisture content of different natural fiber at 65% relative humidity (RH) and 21°C [69]

Fiber	Equilibrium moisture content (%)
Sisal	11
Hemp	9.0
Jute	12
Flax	7
Abaca	15
Ramie	9
Pineapple	13
Coir	10
Bamboo	8.9

2.3.3.11 NFPCs and Applications

Composite materials are preferred in engineering applications due to their fundamental property of high strength to weight ratio. The synthetic fibers are conventionally used as reinforcements in composite materials. Unfortunately, the synthetic fibers are non-degradable, causing severe environmental concern and it has triggered the researchers to find new eco-friendly natural fibers for these applications, wherever possible. In recent years, there have been many research developments in the field of natural fiber composite materials.

Natural fiber composites are environmentally superior to the glass fiber reinforced composites regarding the following reasons:

(1) Natural fiber production has lower environmental impacts;

(2) Natural fiber composites have higher fiber content for equivalent performance, reducing more polluting base polymer content [71].

Joshi et al. [72] also conveyed that the natural fiber based lightweight composite material improves fuel efficiency in automobile applications.

Davoodi et al. [73] manufactured and studied the mechanical properties of hybrid kenaf/glass reinforced epoxy composite passenger car bumper beam. The results showed that the tensile strength, Young's modulus, flexural strength, and flexural modulus were like glass mat thermoplastics. However, the impact strength of the bumper beam was still low. The impact property could be improved by perfecting the structural design parameters like thickness, beam curvature, strengthening ribs and through material improvement.

2.4 *Benchmarking*

2.4.1 *Natural Fibers*

The concerns about using GFRP, CFRP, and metals in the automotive industries are increasing daily due to their negative environmental impact. Natural fibers are the best solution for those concerns. The general thought that appears among everyone when they heard about NFRP is that they have less strength compared to metals, GFRP or CFRP. However, this may not be entirely accurate. Many of the natural fibers like jute, hemp, and flax are almost as strong as synthetic fibers and metals. Specific chemical treatments achieve this strength to the fiber or altering the matrix or adding some additives. This section is about the natural fibers which are used in structural and non-structural applications in automotive components.

Bast fibers (flax, hemp, jute, kenaf, ramie)

In general, the bast consists of the stem, which has a wooden core. Within the stem, there are many fiber bundles, each having individual fiber cells or filaments. Lignin or pectin matrix together bond the cellulose and hemicellulose filaments. The pectin surrounds the stem holding it together with the fiber. The pectin is removed during the retting, allowing separation of the fiber bundles from the rest of the stem.

During the composite making process, the fiber is impregnated with the resin. During this process, the matrix replaces the weakest part (Lignin) between the individual cells of the material. Particularly in the case of flax, a stronger composite is obtained when the fiber bundles are pre-treated in the way either boiling separates the cells in alkali or any other method.

Flax delivers strong and stiff fibers, and it can be grown in temperate climates. The fibers can be spun into yarns for textile (linen). Other bast fibers are grown in warmer climates. The most common is jute, which has reasonable strength, resistance to rupture, and costs less. Jute is used for packaging (sacks and bales). As far as composite applications are concerned, flax and hemp are two crucial fibers that have replaced glass in many components, especially in German automotive industries [74].

Leaf fibers (sisal, abaca (banana), palm)

In general, leaf fibers are coarser than bast fibers. Applications are ropes and coarse textiles. Within the total production of leaf fibers, sisal is the most important. It is obtained from the agave plant. The stiffness is high, and it is often applied as binder twines.

As far as composites are concerned, sisal is often applied with flax in hybrid mats, to provide good permeability when the mat must be impregnated with a resin. In some interior applications, sisal is preferred because of its low level of smell compared to fibers like flax. Especially when using manufacturing processes at increased temperatures, fibers like flax can cause stinky smell [74].

Seed fibers (cotton, coir, kapok)

Cotton is the most common seed fiber which is used in textile industries all over the world. Other seed fibers are applied in less demanding applications such as stuffing of upholstery. Coir is an exception to this. Coir is the fiber extracted from the husk of the coconut. Coir is thick and coarse but durable fiber used for making ropes, matting, and brushes.

With the rise of composite materials, there is a renewed interest for natural fibers. Their moderate mechanical properties restrain the fibers from using them in high-tech application, but, for many reasons, they can compete with glass fibers [74].

2.4.1.1 Jute Fiber

Jute (Corchorus capsularis) is known as the ‘Golden Fiber’ due to its golden-brown color and its importance. Regarding usage and production, jute is second only to cotton. It is the fiber used to make sacks and garden twine. Jute is environmentally friendly as well as available at an affordable price; jute plants are easy to grow, have a high cultivation rate and require fewer pesticides and fertilizers. Jute is a bast fiber, where the stems are processed to obtain the fibers.

Jute is an annual crop grown in India and Bangladesh in the fertile Ganges Delta. It is classified in the family of lime tree (Tiliaceae) by Kew Royal Botanic Gardens, but jute has sometimes been placed in with cotton, Malvaceae family. Jute is part cellulose, part lignin, where many natural fibers have a significant part of cellulose (plant fiber) or lignin (wood fiber). This makes jute as both wood and textile fiber. Jute fiber has high strength, low cost, and durability. It is one of the essential natural fiber which has a wide range of application in both structural and non-structural components [75]. Jute cannot be grown in European climatic conditions since they need tropical rainfall, high humidity, and warm weather. It can be planted closer together since they grow as tall as 2.3 to 3.5 meters with the thickness of a finger and straight thence it does not need a large area to cultivate a vast quantity. The harvest period is four to six months [75].

On average, in an acre of field jute can yield four times than flax. The fiber is extracted by submerging the jute bundles in water for a few days until the fibers come loose and are ready for stripping from the stalk, they are washed and dried. This is because the fibers lie beneath the bark around the woody core. This process is called retting [76].

The mechanical, physical and thermal properties evaluation of jute fiber composite is carried out by various researchers with different kind of matrixes such as epoxy, polypropylene vinyl ester, etc. [77]. The tensile strength of Jute/Epoxy composite is 216 MPa whereas Young's modulus is 31 GPa and strain to failure is approximately 0.78 %. The flexural strength in the longitudinal direction is 158 MPa while in the transverse fiber direction is around 25.7 MPa. According to Dilipkumar et al. [70], the untreated waste sack/vinyl ester composite (raw jute fiber used for packing and transporting in Asia) has a tensile strength of 39 MPa, the flexural strength is 3.44 MPa in the transverse direction, and the impact strength is 0.7 kJ. The difference in the results of two different experiments shows the impact of chemical treatment on natural fibers.

Alves et al. [78] designed a bonnet for an off-road vehicle called buggy using Jute fiber. The primary goal of them was to achieve a sustainable bonnet and to promote eco-design in automotive manufacturing.

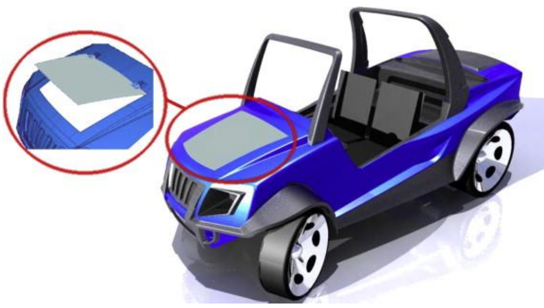

Figure 20 Frontal bonnet of the buggy [78]

2.4.1.2 Flax Fiber

Cultivated flax (linum usitatissimum) is an annual crop grows in cold climatic region, especially in northern Europe. Separate varieties are grown either for the fiber or for the seeds that are used in linseed oil production. In 3-4 months the plant grows to about 1 meter in height and has attractive pale blue flowers. The fibers are extracted by pulling out the whole plant once the flowers are bloomed. In the traditional process, the flax stems dried in bundles. When the stems are dry, they are hackled with a special rippling rake to remove the seed pods. The stems are then retted in a wet field for a couple of weeks, where they ret in the dew, or by leaving them in standing water for a few days.

The retted stems are rinsed and dried before breaking them with a flax-brake and cleaning them by scutching [74]. The fibers are then combed on hackles to produce long line fibers that can be spun, called line flax. The short fibers that are combed out are the hackle tow or flax tow and are carded and spun into coarse yarns and thread.

Cristiano et al. [79] engineered an experiment for evaluating mechanical and impact characteristics of flax/vinyl ester and basalt/vinyl ester composites. One knows that flax is one of the most durable natural fibers currently known. Flax composites showed tensile modulus of 8.15 GPa and a flexural modulus of 8.27 GPa. The energy absorbed during an impact of 3.90 kN is 33.69 J.

Kong et al. [80] designed and manufactured an automobile hood using Flax/PLA composite and concluded that this composite could withstand the structural requirements necessary for the hood of an automobile.

2.4.1.3 Hemp Fiber

The general name for the genus Cannabis plants is Hemp (from Old English hænep), but it is usually used to refer to the hemp fiber cultivated from cannabis strains and for another non-drug uses. Cannabis sativa is the variety grown for hemp fiber in Europe, Canada and elsewhere, while Cannabis Sativa Indica is used for drug production.

The principal difference between the two types is that Indica produces a large quantity of cannabinol and less and poor fiber, while Sativa gives good quality fiber and very less or poor cannabinol. Common hemp is an annual flowering herb, and wild hemp can grow up to 6 meters tall in a warm climate and as short as 30 cm in cold climates [74].

Hemp is used as construction materials and has a high load carrying tendency towards an extended period. According to Sair et al. [81], hemp/polyurethane composite has shown better thermal insulation compared to the conventional asbestos insulation and the tensile and bending modulus are higher. The water absorption is quite high compared to synthetic materials.

2.4.1.4 Sisal Fiber

Sisal (Agave Sisalana) is a hard fiber extracted from the leaves of sisal plants which are perennial succulents that grow best in hot and dry areas. Sisal is an environmentally friendly fiber as it is biodegradable and almost no pesticides or fertilizers are used in its cultivation. World production is about 300,000 tons per year.

Sisal plants grow fast and all year round. The first harvest can be made when the plants are about two years old, and they still are productive for 10 to 12 years. Each plant produces 180 to 240 leaves in a lifetime yielding 1 to 4 tons of fiber per hectare. Unlike synthetic fibers, sisal is 100 % biodegradable during its lifetime, and sisal strings and ropes can be recycled as paper. During processing, sisal produces only organic wastes, which can often be reused. In the past, 96 % of the leaf weight was discarded. Now, this is used as fertilizer, cattle feed and as fuel for biogas production [74].

The experiments carried out by Zuccarello et al. [82] on sisal fibers, to study the high-performance biocomposites and characterized the mechanical behavior, showed that the tensile modulus they achieved from optimized manufacturing method is 34.5 MPa. They concluded that higher fiber volume fractions increase the strength of the composite.

2.4.1.5 Abaca Fiber

Abaca is also called Manila hemp. Abaca is extracted from the leaf sheath around the trunk of the abaca plant (Musa textilis), a close relative of the banana, native to the Philippines and widely distributed in the humid tropics. Harvesting abaca is labor intensive as each stalk must be cut into strips which are scraped to remove the pulp. The fibers are then washed and dried.

Currently, abaca is being used as patching material for bolster and interior trim parts in the automotive industry. However, given its greater tensile strength, it can also be used for semi-structural and structural applications for exterior components as a substitute for glass fiber in reinforced plastic components.

Mercedes Benz has used a mixture of PP/abaca yarn composites in automobile body parts. Replacing glass fibers by natural fibers can reduce the weight of automotive parts and eases more environmentally friendly production and recycling [83].

Other fibers such as ramie, coir, and cotton are also an alternative for structural and nonstructural application, but there are few studies on those fibers. The food and agriculture organization of the United Nations published an article in 2016 on future fibers as an alternative for synthetic fibers in the field of automotive, aerospace and construction purpose. In that article, they mentioned these fibers. In the near future, there will be many experiments and studies for these fibers subjecting it to structural and nonstructural applications. A property summary of various natural fiber and glass fiber is shown in Table 6.

Table 6 Properties of glass and natural fibers [84]

Properties	**Fiber**								
	E-glass	**Flax**	**Hemp**	**Jute**	**Ramie**	**Coir**	**Sisal**	**Abaca**	**cotton**
Density (g/cc)	2.55	1.4	1.48	1.46	1.5	1.25	1.33	1.5	1.51
Tensile Strength (MPa)	2400	300-1500	550-900	400-800	500	220	600-700	980	400
E-Modulus (GPa)	73	24-80	70	10-30	44	6	38		12
Elongation at failure (%)	3	1.2-1.6	1.6	1.8	2	15-25	2-3		3-10
Moisture absorption (%)	-	7	8	12	12-17	10	11		8-25
Price/kg €, Raw (mat/fabric)	1.3 (1.7/3.8)	1.5 (2/4)	0.6-1.8 (2/4)	0.35	1.5-2.5	0.25-0.5	0.6-0.7	1.5-2.5	1.5-2.2

2.4.2 *Sustainable-matrix and additives for composites.*

The first and most important aim of this thesis was to create an Eco-friendly and sustainable composite bonnet system. To achieve this, both the matrix and the dispersed phase need to be sustainable. In this case, the dispersed phase will be a natural fiber, and the matrix will be either natural material or utterly recyclable system. Thus, it is needed to look for matrices and natural fibers able to comply with the necessary requirements.

2.4.2.1 Poly-Lactic Acid (PLA)

Polylactic acid (PLA) belongs to the family of aliphatic polyesters made from alpha-hydroxy acids, which include polyglycolic acid, and are considered biodegradable and compostable. PLA is a thermoplastic, high-strength, high-modulus polymer that can be made from annually renewable resources to yield articles for use either in the industrial packing field or the biocompatible and bioabsorbable medical device market. It can be efficiently processed on standard plastics equipment to yield molded parts, film or fibers. It is one of the few polymers in which the stereochemical structure can easily be modified by polymerizing a controlled mixture of the L- or D-isomers to yield high molecular-weight amorphous or crystalline polymers that can be used for food contact and are generally recognized as safe [85]. Figure 21 illustrates the polymerization of PLA.

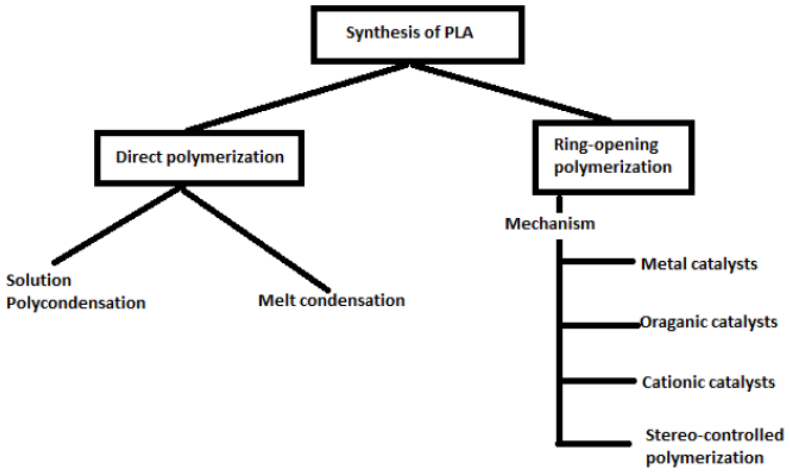

Figure 21 Polymerization reaction and mechanism [85]

Samples with three different fiber-mass proportions (10%, 20%, 30%) have been produced regarding the PLA/flax composite. The composites were pressed at a temperature of 170 °C and 18 MPa for 5 min. This composite shows excellent mechanical properties regarding the Charpy impact test (9.97, 10.45, 11.13 kJ/m^2), Young's modulus (3.90, 5.06, 6.31 GPa) and tensile tests (42.73, 49.23, 54.15 MPa). This shows that PLA and flax show excellent mechanical properties in general [86].

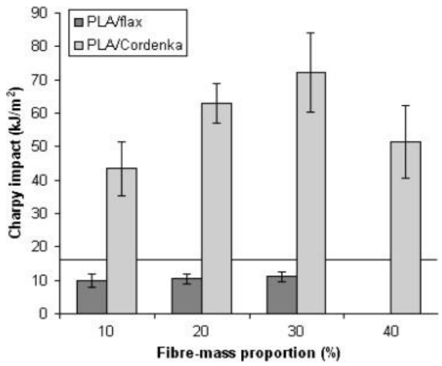

Figure 22 Impact strength of the composites versus their fiber-mass proportion [86]

The mechanical performance of industrial hemp fiber reinforced polylactic biocomposites is carried out with the fiber content ranges from 0 to 40 % and the rest is Polylactic biopolymer, which gives a tensile strength of 75.5 MPa, Young's modulus of 8.18 GPa and impact strength of 2.64 kJ/m^2. However, plane-strain fracture toughness and as the fiber content increases the strain energy release rate decreases. The alignment of long fiber in PLA/ALK composites has enhanced the mechanical properties [87].

The mechanical properties of two types of UD flax/PLA. One made with layers of aligned flax roving alone and the other having an added paper layer fabricated using papermaking techniques, were tested. The results showed that specific tensile properties of the flax/PLA (252 MPa·cm^3/g) and flax-paper/PLA (217 MPa·cm^3/g) composites are like those made using woven glass fabrics impregnated with epoxy (227–278 MPa·cm^3/g). Remarkably high impact strength (600 J/m) was also obtained for UD flax-paper composites compared to the unreinforced resin (15 J/m) [88].

2.4.2.2 Elium® Acrylic-based thermoplastic resins.

Acrylic resins are a group of related thermoplastic/thermosetting polymers derived from acrylic acid, methacrylic acid or other related compounds. Acrylic polymers are characterized by their elasticity, their resistance to rupture and their transparency. These resins are used as adhesives and widespread in the surface coating industry (paints) [89].

Acrylic-based resins are represented in the industry market by the polymethyl methacrylate polymer (PMMA). In 2014, Arkema presented on a commercial basis its new liquid thermoplastic resin named Elium®. Regarding chemistry, Elium® is considered an acrylic resin. Its development is a new source for more environmentally friendly production of composites. Besides being recyclable, this resin is time and cost effective. Indeed, it does not need either in-mold heating nor extra curing time. In addition to the acrylic monomer (MMA), the resin also has an accelerator agent used to activate the catalyst agent. The peroxide used as a catalyst is added before the injection of the resin starts [90].

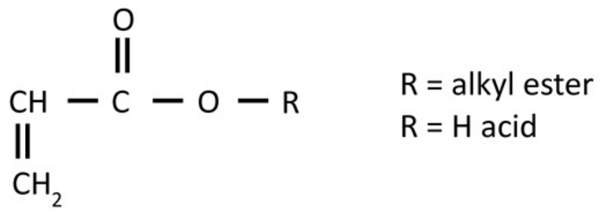

Figure 23 Acrylic-based resin molecular schema [89].

Elium® resins can be processed by RTM, infusion, and pultrusion, depending on the number of parts to be manufactured per day and the specifications of the part. Elium® resins are processed in similar equipment to those used today for thermoset composites, with similar polymerization cycle times and conditions.

Fiber-reinforced Elium® resin parts can be thermoformed with heat and pressure. This process needs the heating of the joint part at 180 – 200 °C for a few minutes, and the compression at a pressure between 5 and 20 bar depending on the reinforcement type and the thickness of the part. Fiber-reinforced composites made with Elium® resins can be assembled with adhesives. The SAF® 30 adhesive, from AEC Polymers, is recommended for structural bonding. A cohesive failure is obtained according to the EN-1465. To use the advantage of the thermoplastic behavior of Elium® resin in an assembly by welding is also possible. This process needs the heating of the two joint parts at 180 – 200 °C for a few minutes, followed by compression till it solidifies again [91].

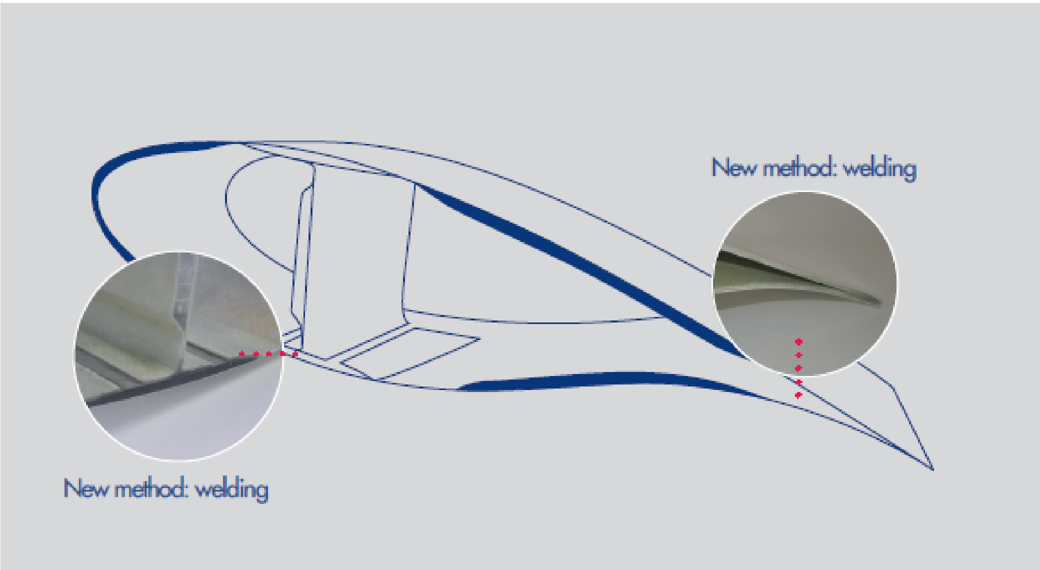

Figure 24 Welded wind blade section without adhesive [91]

The composite parts made from Elium® resin can be recycled after EOL in two different ways. The first one would involve grinding and compounding to use as chopped fiber compounding resin, and the second would be a thermolysis process which allows the recovery of fibers and the monomers by depolymerization.

The shelf life of the Elium® resins in the original sealed container is six months guaranteed at a temperature not higher than 25 °C [91].

2.4.2.3 Polyphenylene sulfide

Polyphenylene sulfide (PPS) is high-performance engineering thermoplastic. It consists of a crystalline polymer made of asymmetrical, rigid backbone of recurring p-substituted benzene rings and sulfur atoms.

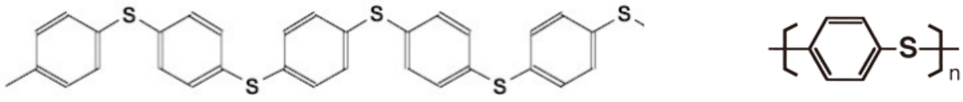

Figure 25 Molecular structure of PPS (left) and its repetitive sequence (right) [92]

Among PPS resins, two main polymer families can be found: chemically branched and linear polymers. The branched PPS shows high stiffness under elevated temperature conditions. It also delivers unique benefits associated with resistance to creep deformation, is based on a linear PPS polymer and has the desirable features associated with tensile elongation and impact resistance because of the linear polymer. Moreover, they show higher purity; it is less prone to absorbing moisture under high heat and humidity conditions, compared to another cross-linked polymer.

PPS may be polymerized by the polycondensation reaction of para-dichlorobenzene (p-DCB) and sodium sulfide (Na_2S) or sodium hydrosulfide (NaSH) in a polar solvent and under high temperature and pressure conditions. Furthermore, it shows an excellent balance of properties, such as high melting point and maximum temperature service (285 °C, 300 °C and 218 °C respectively). Also remarkable is its inherent flame retardancy ability and its corrosion resistance, which make it ideal for high-temperature electrical applications. PPS is widely used in diverse fields such as automotive, electrical or medical health-care, among others [93].

2.4.2.4 Polyether ether ketone (PEEK)

Polyether ether ketone (PEEK) is a colorless organic thermoplastic polymer in the polyaryletherketone (PAEK) family, used in engineering applications. Victrex PLC initially introduced it in the early 1980s. PEEK polymers are obtained by step-growth polymerization by the dialkylation of bisphenol salt which can be seen in Figure 26. Typical is the reaction of 4,4'-difluorobenzophenone with the disodium salt of hydroquinone, which is generated in situ by deprotonation with sodium carbonate. The reaction is conducted around 300 °C in polar aprotic solvents - such as diphenyl sulphone [92].

PEEK has a density of 1.320 g/cc with Young's modulus of 3.6 GPa, tensile strength of 90-100 MPa, and melting point of 343 °C. PEEK is a semi-crystalline thermoplastic with excellent mechanical and chemical resistance properties that are kept to high temperatures. The processing conditions used to mold PEEK influence the mechanical properties [94].

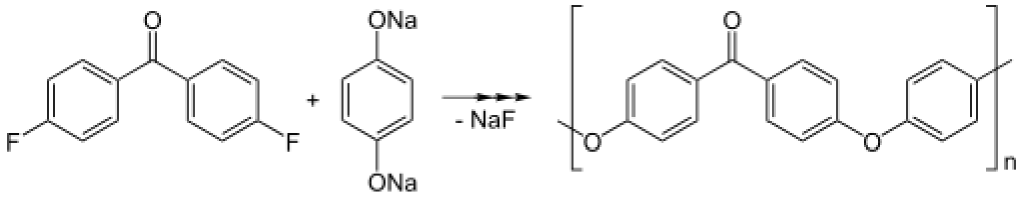

Figure 26 PEEK Chemical Structure Parker et al. [92].

Harry et al. [95] developed a cargo floor using graphite/PEEK composite for helicopter applications. They replaced aluminum with composite in one of a prototypes of their cargo-helicopter. Harry et al. [95] developed a composite drive shaft for the same helicopter application. David et al. [96] successfully perfected the manufacturing of thermoplastic composite pressure vessels for CNG and hydrogen storage for vehicles. There are many applications for the PEEK composites in structural applications. Roux et al. [97] defragmented a CFRP door hinge using electrodynamic fragmentation process, which can be seen in Figure 27.

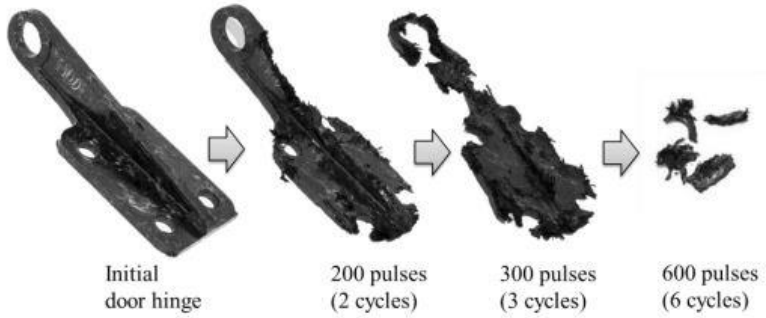

Figure 27. Evolution of the CFRP door hinge during electrodynamic fragmentation process [97]

The problem with PEEK composites is that it consumes more energy and effort to recycle, which increases the embodied energy of a product on a total scale.

2.4.2.5 Tamarind seed powder (TSP)

The tamarind plant is botanically known as Tamarindus Indica, habitually grows in the tropical regions and is highly appreciated for its ornamental qualities. Belonging to the large plant family Caesalpiniacae, Tamarind plant has marked a distinct identity of its own due to its many uses in food, medicine, and other areas. Though, it is for the sweet pulp of the ripened pod that tamarind has gained immense popularity. However, the plant bark and seeds are also used in various applications.

Today, as a commercial plant, tamarind is cultivated in different parts of the world like tropical America, Bermuda, and many Asian and African countries. In India, different tamarind orchards are producing 275,500 tons of tamarind annually [98].

Tamarind kernels are powdered and are used as a source for starch in the Indian textile industry. This proves to be a very cost-effective deal as the tamarind seed powder is 300 % more efficient than cornstarch and is extremely economical. The tamarind seed powder is also used in color printing of textiles, paper sizing, leather treating, glue for wood, as stabilizer in bricks, as binder in sawdust briquettes, and as thickener in some explosives, etc.

Figure 28 Tamarind tree [Self-elaborated]

The amber oil extracted from tamarind seeds is also used as an illuminant and varnishing agent. The leaves, flowers, seeds, and fruits of tamarind plant give good animal fodder, but can also be used for various foods. The tannin-rich seed coat of the seeds is used as an adhesive for plywood's and in dyeing and tanning, though it is of inferior quality and gives a red hue to leather [99]. The seed powder is also employed for various medicinal purposes, such as:

- The powdered tamarind seeds are transformed into a paste for drawing boils and are prescribed for chronic diarrhea and dysentery;
- These prove highly effective in curing fever, intestinal diseases, and diarrhea;
- Tamarind seed has its natural stiffness property which is helpful in treating fractured bones in ancient Indian medicinal technique called SIDDHA [100].

2.4.3 *NFRP composite manufacturing process*

Fabricating the natural fiber composites is similar to the manufacturing of synthetic fiber composites or plastics. However, in manufacturing the natural fibers, one has to more cautious in selecting the process. According to [101], selecting the right manufacturing process is one of the critical factors in making NFRP composite parts. The best processes for manufacturing NFRP composites are listed below [102].

- Injection molding;
- Compression molding;
- Hot pressing;
- Resin transfer molding;
- Vacuum bag sealing or vacuum injection molding;
- Hand lay-up method.

2.4.3.1 Injection Molding

Injection molding (Figure 29) of composites is a process that forces a measured amount of mixture which has molten polymer and fiber into mold cavities. Many studies have been made on the potential of using natural fibers as reinforcement for renewable polymers to make a composite through injection molding. The first thermoplastic polymer used by this process was designed for plastic pellets. For fiber reinforced composites, the pellets with chopped fibers are fed individually through a funnel-shaped feed hopper into a heated compression barrel with a rotating screw (''screws'' for twin-screw extruder). The purpose of heating the barrel is to transform the solid pellets into a viscous liquid, which can be driven through the sprue nozzle and finally forced into the matched-metal closed mold cavities. The mold is tightly clamped against injection pressure where the polymer solidifies, freezing the orientation and distribution of fibers. The composite is then removed from the closed mold after it is sufficiently cooled to be ejected to form a part of the desired shape. As the mixture must move toward to the sprue nozzle, the polymer is pressurized because of the screw mechanism.

In injection molding (and extrusion compounding) of fiber-reinforced polymers, the mechanical action of the screws causes significant damage to the fibers [101]. Changes in fiber size and shape distribution arise from the interaction of the fibers with each other, with the polymer and with the machine. Moigne et al. [103] performed a statistical analysis of natural (flax, sisal or wheat straw) fibers in polypropylene. Disaggregation of the fibers led to the presence of particles in all the studied composites. A major factor controlling the heterogeneity of the composites, and the following rheological and mechanical behavior, was the origin of the fibers.

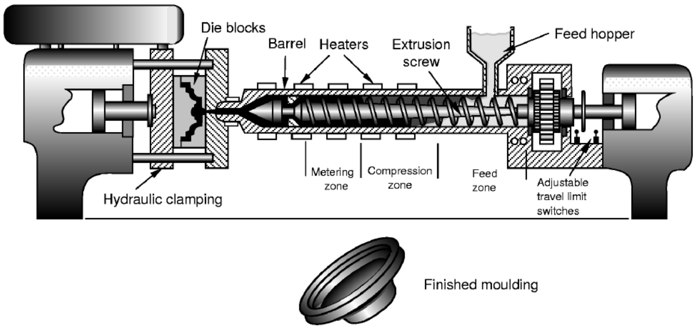

Figure 29 Injection molding process [102]

2.4.3.2 Compression Molding

Compression molding is a well-known technique to develop the type of composite product. It is a closed molding method with air mass application. During this methodology, as shown in Figure 30, matched metal molds are used to fabricate the composite product. In compression molding, the base plate is stationary while the top plate is movable. Reinforcement and matrix square measure placed within the aluminous mold and therefore the whole assembly is unbroken in between the compression molder. Heat and pressure are applied as per the necessity of composite for a particular amount of time. The fabric placed in between the molding plates flows due to the application of pressure, heat, and acquires the form of the mold cavity with high dimensional accuracy, which depends upon mold style. In theory, a compression molding machine may be a press that is bound vertically with two molding halves (top and bottom halves). Generally, a hydraulic mechanism is employed for pressure application in compression molding. The dominant parameters in compression molding methodology to develop superior and desired properties of the composite square measure are pressure, temperature and time of application. All the three dimensions (pressure, temperature and time) for the process need to be optimized effectively to produce the tailored composite part as each dimension is equally vital to other. If applied pressure is not spare, it will result in poor surface adhesion of fiber and matrix. If the pressure is just too high, it should cause fiber breakage and the expulsion of enough organic compound from the composite system. If the temperature is naturally too high, properties of fibers and matrix might get modified. If the temperature is lower than desired, fibers might not get adequately wetted thanks to the high consistency of polymers, particularly for thermoplastics. If the time of application of those factors (pressure and temperature) is not spare (high or low), it will cause any of defects related to depleted pressure or temperature. The different producing factors like mold wall heating, closing rate of two matched plates of the plates and de-molding time additionally have an effect on the assembly method.

2.4.3.3 Hot Pressing

This process is also called hot compression molding of thermoplastic prepregs, or the matched die technique. This process is like the sheet metal forming process. In this process, thermoplastic prepregs are stacked together and then placed between heated molds (Figure 31). Unlike GMT, the prepregs, in this case, are made with unidirectional continuous fibers. The fiber volume fraction is higher than 60%. A typical hot pressing is illustrated in Figure 31.

Molds for this process are made of stainless steel or aluminum. Because most flat laminates are made using this technique, the molds are quite simple. In-mold design, both part shrinkage, and mold expansion and contraction are taken into consideration. It is desirable to have the same coefficient of thermal expansion between the composite and tooling materials when contoured surfaces are made. The mold design for this process is much simpler than for injection molding or RTM [104].

Figure 30 Compression Molding Machine

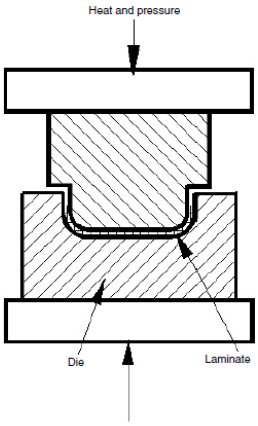

Figure 31 Hot Pressing [104]

2.4.3.4 Resin Transfer Molding

Liquid composite molding processes encompass RTM, VARTM, S-RIM, CIRTM and other subsets, where the basic approach is to separately inject the liquid resin into a bed of stationary preforms. The RTM process has become a popular composite manufacturing process due to its capability for high volume production and cost-effectiveness. In the RTM process, dry fiber preforms (impregnating) or porous fibrous preform are placed into the mold cavity. Two equal mold halves are clamped tightly to avoid leakage of the resin during the injection process. Then, using dispensing equipment, pressurized molten plastic is injected into the heated mold using single or multiple inlet ports in the mold, depending on the complexity of the shape of a final product until the mold is filled with resin. After cooling, the part is then removed from the mold. Post-curing is typically needed to ensure the resin is fully cured (chemically reacted between the resin and its catalyst).

For natural fiber composites, small clearances may exist between the fiber preform and mold edges because of loose edge fiber bundles, poor fitting size, or deformation of the fiber preform in the RTM process. The clearance results in a preferential resin flow path during the mold filling stage [101].

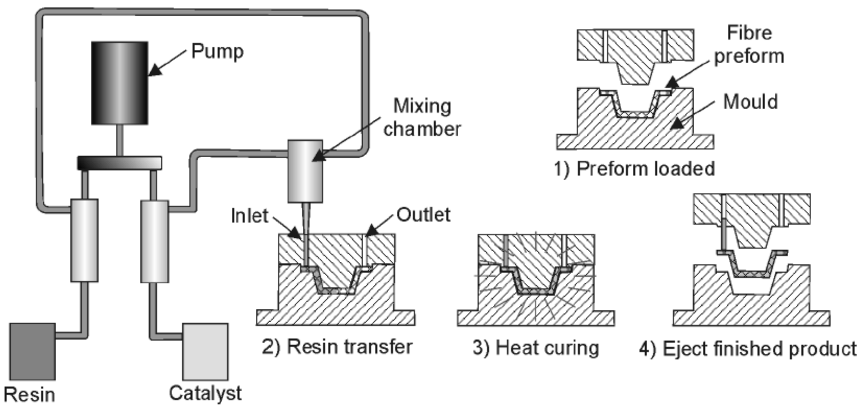

Figure 32 Resin Transfer molding process [102]

2.4.3.5 Vacuum Bag Sealing or Vacuum Injection Molding

This process is like Injection molding, but the resin is injected, and the composite is cured in the presence of a vacuum. The VARTM manufacturing process uses a vacuum to remove gas or air from the preform and the light mold due to low press injection. The VARTM method is slightly different from the RTM, which consists of solid stiff molds. It uses a solid stiff mold for one side and a flexible mold with vacuum for the other side. By using both the positive pressure and vacuum pressure, the resin filling time can be shortened to less than the gelling time, as well as the fiber volume fraction is improved by reducing voids in the preform. Therefore, the VARTM process is an advanced composite manufacturing method that allows much higher quality product than the hand lay-up process, and less manufacturing costs compared to the RTM and the autoclave method [105].

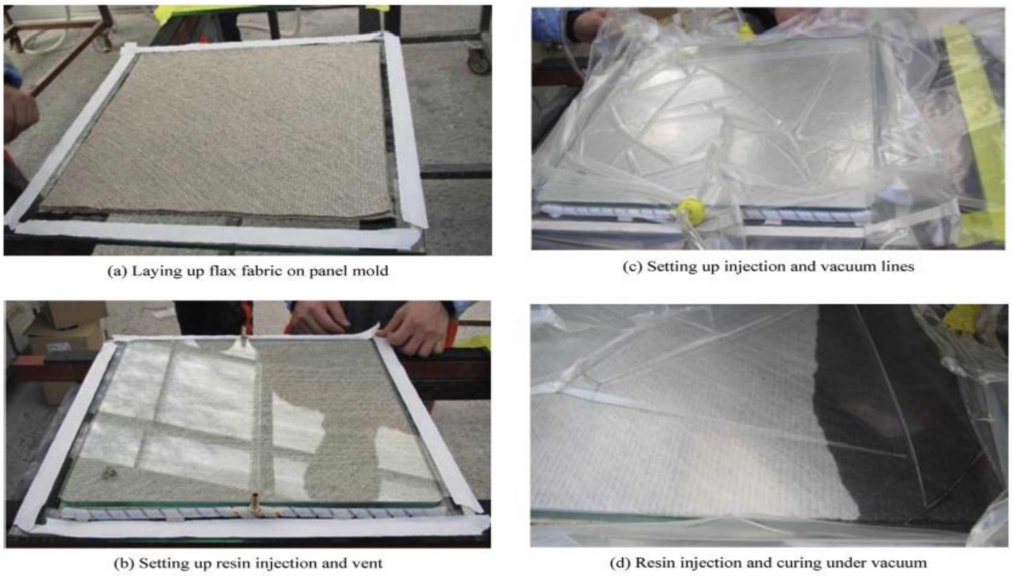

Figure 33 Manufacturing process of flax/vinyl ester panel using VARTM [105].

2.4.3.6 Hand lay-up method

Hand lay-up technique is that the most straightforward method of composite process. The infrastructural demand for this method is additionally marginal. The process steps are quite comfortable. First, an unharness gel is sprayed on the mold surface to avoid the sticking of the composite to the surface. Thin plastic sheets are used at the highest and bottom of the mold plate to urge the superb surface end of the merchandise. Cut-type carpet reinforcements are cut according to the size of the mold and placed on the surface of the mold. Then a suitable hardener is mixed proportionally with the thermoset compound applied onto the surface of the mat already placed within the mold. The compound is uniformly unfolded with the aid of a brush, and the next layers are stacked over that following the same procedure, and a roller is captive with a gentle pressure on the mat-polymer layer to get rid of any air retained in excess in the compound. The method is perennial for every layer of compound, and mat till the specified layers are stacked. The mold is then covered with plastic sheet and allowed to cure.

After curing either at room temperature or inside an oven, the mold is opened, and the developed composite part is de-molded and processed. The schematic of hand lay-up is shown in Figure 34. The time of curing depends on the type of polymer used for composite processing. For example, for the isophthalic based system, the usual curing time at room temperature is 24 - 48 hours. This method is suitable for thermosetting polymer-based composites. A typical hand lay-up method can be seen in Figure 34.

Hand lay-up molding is used to produce parts of any dimensions such as technical parts with a surface area of a few square feet, as well as swimming pools as large as 150 m² (1600 square feet approx.). However, this method is limited to the manufacture of parts with simple shapes that need only one face to have a smooth appearance. It is recommended for small and medium volumes needing minimal investment in molds and equipment.

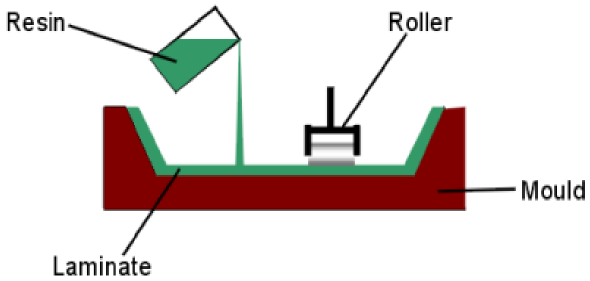

Figure 34 Hand Lay-Up Method [102]

2.4.4 *Bench Marking Non-Metal Bonnets*

The composite material is a material that still is new and unused in the automotive industry in parts with many requirements and demands. This is due to the nonlinear properties of the materials, as the metallic materials have. These properties make it hard to predict how the material will deform or behave in different load cases or impacts. However, it exists vast knowledge on how different composite materials behave in easy cases like tensile tests or compression tests in axial and transverse direction. However, in more complex examples like dynamic loads or large and fast deformations, it is still hard to predict the behavior of the materials. Because of the harder environmental requirements in the automotive industry regarding emissions and fuel consumption, the trend is moving towards lighter cars. Due to this, composite materials become more interesting [106]. Some companies have introduced plastic or composite materials in the hood or some parts of the hood. Very few of them are mass production cars, and some are more exclusive sports cars, which are listed below.

A2mac1 is a tool provided with benchmarking services for the automotive industries. The tool is used here to gain an understanding of what is developed in automobiles when it comes to bonnet material solutions. Features used in the tool are “AutoVision” from “Global shows” and “AutoReverse” from “Teardown.”. “AutoVision” is a feature giving a visual insight of automotive products just being released on global shows. Teardown is a feature giving a technical insight into automotive products. Cars have been dismantled, part by part, and analyzed to give information about, weight, material used, etc. One feature called Show Coverage displays pictures of cars shown in various angles from large motor shows around the world. It is possible to see how new cars look here without going to the show oneself.

2.4.4.1 BMW i3

The BMW i3 has a hood made of the polymer polypropylene and has a mass of 8.053 kg. The BMW i3 with polymer bonnet can be seen in Figure 35.

Figure 35 BMW i3 [107]

2.4.4.2 Renault Twingo

The Renault Twingo has a hood made of Polyethylene and has a mass of 2.518 kg. Renault Twingo with polyethylene bonnet is shown in Figure 36.

Figure 36 Renault Twingo [107]

2.4.4.3 Aston Martin V12 Vanquish

The inner hood of the Aston Martin Vanquish is shown in Figure 37, where one can see that it is made in a cross shape out of carbon fiber because of the pattern in the inner hood material. This inner hood looks entirely different in comparison to other hood used in cars. This may be due to the low series production of the Aston Martin car; this means that Aston Martin car does not have the demands from EuroNCAP and do not need to make a hood that has as good pedestrian protection properties.

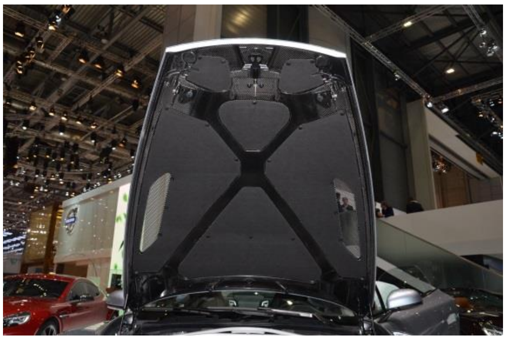

Figure 37 Aston Martin V12 Vanquish inner CFRP hood [107]

2.4.4.4 Porsche 911 R

The new Porsche 911 R has a hood in carbon fiber; this can be seen in Figure 38. There is no information about the mass of the hood, but it is a fact that the whole car is 50 kg lighter in comparison to its predecessor, the Porsche GT3. However, then it is not just the hood that is made of carbon fiber [108].

Figure 38 Porsche 911 R Carbon hood [107]

2.4.4.5 Ford Focus

Initial tests performed by Ford suggest that carbon fiber reinforced polymer components such as the prototype hood on the Ford Focus will meet Ford's high standards for stiffness, dent resistance, and crash performance. The prototype hood has also performed well in pedestrian protection head-impact tests. It is said that a hood made in this type of material will reduce the weight of the hood with 50% [109]. Foam cored CFRP bonnet form Ford Focus can be seen in Figure 39.

Figure 39 Foam core material sandwiched between two layers of carbon fiber reinforced polymer [107]

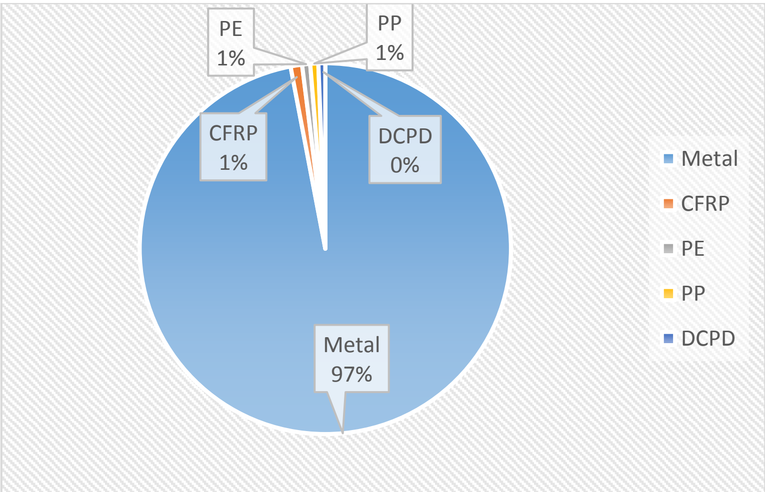

Figure 40 Car Bonnet Material Usage [Self Elaborated]

According to this benchmarking tool, only 0.8% of cars have a plastic bonnet which is shown in Figure 40.Two of them were BMW i3 and Renault Twingo, using PP (polypropylene) and PE (polyethylene), respectively, as bonnet material. These two cars are classed as small family cars, which means that the area of the bonnets is small. According to EuroNCAP pedestrian safety results, these two cars scored weak in comparison to Volvo XC90s aluminum bonnet. It was therefore not relevant to compare these small cars with an SUV car such as Volvo XC90 due to the area and design of the hoods are different. Those two factors are highly dominant when speaking of impact resistance. It is not an only material selection that determines the scoring in pedestrian safety aspects. The scorings of BMW i3, Renault Twingo and Volvo XC90 are presented in Figure 41, Figure 42, and Figure 43, respectively.

Figure 41 Pedestrian safety results from EuroNCAP BMW i3 [107]

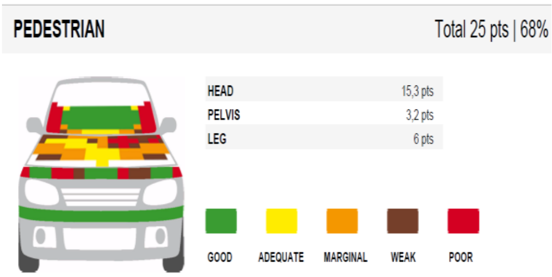

Figure 42 Pedestrian safety results from EuroNCAP Renault Twingo [107]

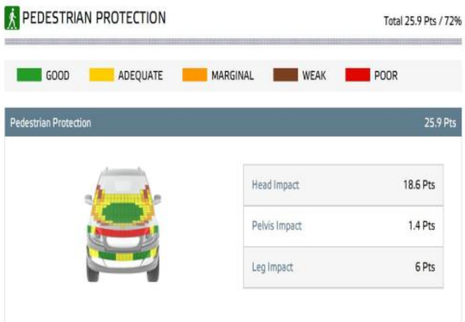

Figure 43 Pedestrian safety results from EuroNCAP Volvo XC90 [107]

To summarize the benchmarking from A2mac1, the reason a few cars have a bonnet made of another material than steel and aluminum is that the behavior of composite materials is challenging to predict through simulation software, which is severely hampering the development of making use of composite materials in the automotive industries.

The BMW and the Renault hoods are made of different polymers and have a lower mass than Volvo's hood; these are also series production cars and therefore, must be tested and meet the pedestrian requirements from EuroNCAP.

As shown in Figure 41 and Figure 42, these plastic hoods are not a good choice as hood material. Figure 41 shows that the Renault Twingo has a good score in points, but parts that get good values are not in the hood region but the front fender and the windscreen.

Moreover, Volvo Cars have good results in the A zone and adequate or marginal in zone B on the hood. The zones A and B is shown in Figure 96.

The EuroNCAP does not test the composite hoods in the Aston Martin and the Porsche, because of the low number of cars that are made of this type. Due to the low series production of these cars, they do not have the same rules as the Volvo cars, and this is why no data about the pedestrian safety of these hoods are presented.

Ford focus composite hood is still in the development stage. Because of that Ford has not released any data about what kind of materials it has and how well it performs in a pedestrian head impact test.

Because of the low number of composites or polymer materials in the car hoods and little information about them, the benchmarking gave little help and valuable information to the research about a new and lighter material to a hood. The only information that was taken from this stage of the investigation was that a solid plastic material might not suitable in a car hood.

2.5 *Composite recycling*

Composite materials are most well-liked for several engineering applications owing to their sturdiness and superior strength. Correct waste disposal and use at the top of the useful lifetime of composite materials is critical. Several current and future waste management and environmental legislation can mandate engineering materials to be recovered and recycled, from merchandise like vehicles, wind turbines, and craft that have lived their practical life. Though several technologies are developed like mechanical use, thermal use, and chemical recycling; they are on the brink of being utterly commercial. Intensive analysis and development are being done to develop more utile composites and use technologies for composite materials. This may contribute to the property development of the composites industry.

Composite materials are hard to recycle due to the complex hybrid structure. Mechanical, thermal and chemical methods could be applied to materials. There are no commercial operations for recycling composites economically. Composite materials need to be designed sustainably for the better future. More R&D is needed for sustainable composites and efficient separation technologies [110]. The problem in the recycling of thermoset plastic reinforced composites is that most of the technology is commercialized and the energy which is consuming for recycling process is remarkably high. In some cases, the energy matches the embodiment energy of the composite [111]. The recycling process of thermoset plastics can be seen in Figure 44 and various composite recycling technologies for different types of composites is tabulated in Table 7.

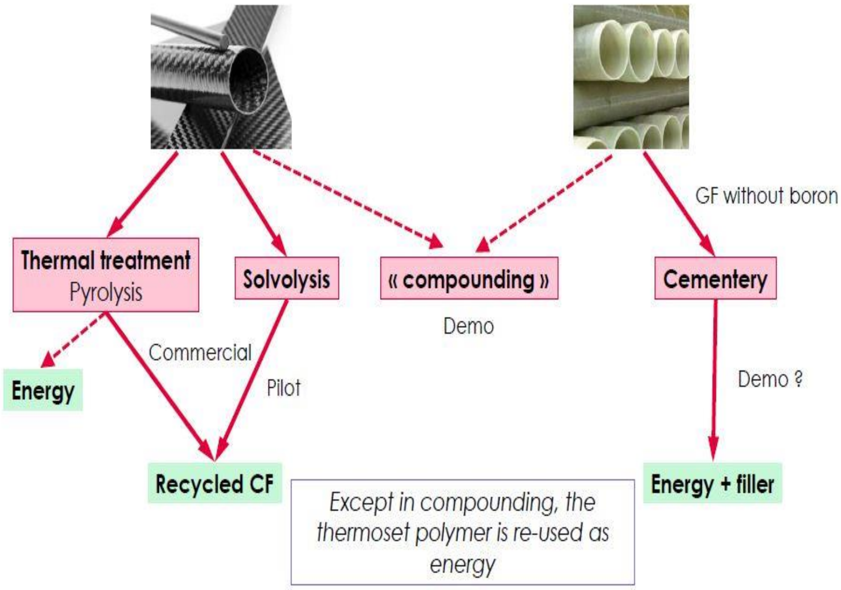

Figure 44 Thermoset Recycling [91]

Table 7 Composite recycling technologies

	Recycling methods	Technology features	Status of the technology
Thermoplastic–matrix composites [110]	Re-melting and re-molding	No separation of the matrix from the fiber	***More studied for the manufacturing or process scrap***
		• Regrinding–compression or injection Molding /extrusion • Product as pellets or flakes for molding • Fiber breakage – property degradation	***Commercial operation unknown***
	Chemical recycling	Dissolution of matrix Fiber breakage – property degradation	***Not much studied***
	Thermal processing	Combustion or incineration for energy recovery	***Not much studied or published***
Thermoset–matrix composites [111]**.**	Mechanical Recycling	Comminution – grinding – milling	***Commercial operation***
		Products: fibers and fillers	***ERCOM (Germany)***
		Degradation of fiber properties	***Phoenix Fiberglass (Canada)***
	Chemical recycling	Chemical dissolution of the matrix	***Only laboratory studies***
		Solvolysis (supercritical organic solvent)/hydrolysis	
		The product of high-quality fibers, potential recovery of resin	
		The inflexibility of solvent and potential pollution	
	Thermal Recycling	Combustion/incineration with energy	***Hindered by the***

		recovery	***market for recycled fibers***
		Fluidized-bed thermal process for fiber recovery	
		Pyrolysis for fiber and matrix recovery	
Metal–matrix composites [112]	Re-melting - casting	Die-cast scrap: direct re-melting - casting	***MMC is much more expensive than the alloys or reinforcements***
		Foundry scrap: direct re-melting with (dry Ar) cleaning	
		Foundry scrap: direct re-melting with (dry Ar) cleaning	
		Very dirty scrap: metal recovery only – re-smelting and refining to separate reinforcement from Al (alloy)	

Sustainability and requirement for a healthy environment is the reason behind recycling. In the past 50 years, the usage of non-biodegradable plastics increased exponentially and found a new application every day. Due to this increase in usage, the production also arose, simultaneously. The problem is that these plastics take age to decompose, while it is costing very less to produce. Because of this ratio, the world is facing a crisis on how to manage these plastic wastes. This crisis is termed as *Plastic Invasion.*

In recent studies carried out by ACS Publications-Environmental Science and Tech department around the world, some shocking facts were revealed, such as microplastics have been found in seas all over the world. The microplastics content was 550–681 particles/kg in sea salts, 43–364 particles/kg in lake salts, and 7–204 particles/kg in rock/well salts. The abundance of microplastics in sea salts was significantly higher than that of lake salts and rock/well salts. This result shows that sea products, such as sea salts, are contaminated by microplastics. The sea salt contamination percentage is shown in Figure 45. An article published in CNN on March 2018 said that there is a garbage patch in the Pacific Ocean that is three times the size of France.

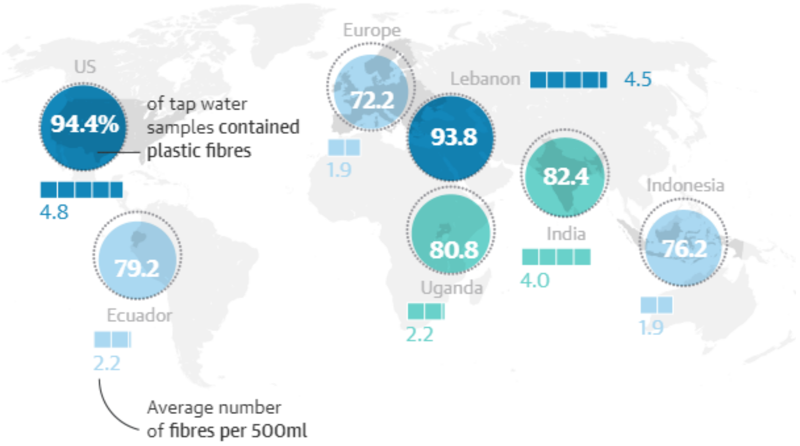

Figure 45 Tap water contamination

2.6 *CAE*

Most engineers and scientists studying physical phenomena are involved with two major tasks;

- Mathematical formulation of the physical process;
- Numerical analysis of the mathematical model.

The mathematical formulation of a physical process requires background in related subjects such as physics and most often certain mathematical tools. The formulation results in mathematical statements, often differential equations, relating quantities of interest in the design of the physical process. Development of the mathematical model of a process is achieved through assumptions concerning how the process works. In a numerical simulation, one must use a numerical method through computers to evaluate the mathematical model and estimate the characteristics of the process.

In computer aided engineering (CAE) the first step is to create a 3D CAD model. The commercial software used was CATIA™ V5. In this part of the work is important to establish all the dimensions of the parts.

After the CAD geometry is created, it is necessary to discretize the domain to allow the calculation software to use this node. For this job, Altair® HyperMesh® was used. The software can generate a mesh automatically but is possible for the user to check the quality of the generated mesh and edit it to satisfy the needed criteria.

When a good quality mesh is obtained, it is necessary to perform the test setup. This setup can be done in HyperMesh® but Altair has another pre-processing software that is more indicated for crash analysis. The software is called HyperCrash™ and allow the user to setup different materials, properties, connections between materials, velocities, forces and other relevant parameters to obtain the best resemblance of the simulation to the test.

The last steps are to run the calculations and post-process the results. For the calculations, RADIOSS™ was used. RADIOSS™ is a solver software capable of performing explicit as well as implicit non-linear analysis. The analysis setup file is the input and the outputs are a series of files that have all the information about the crash test simulation. The results are analyzed in HyperView® and HyperGraph®. HyperView® let the user see an animation of the test and observe any major problems with the structure. HyperGraph® compiles the relevant information in graphs and allows a treatment of the output data, defined in the crash setup phase.

2.6.1 *HyperMesh*

HyperMesh presents users with an advanced suite of easy-to-use tools to build and edit CAE models. For 2D and 3D model creation, users have access to a variety of mesh-generation capabilities, as well as HyperMesh's powerful automeshing module.

High Fidelity Meshing

- Surface meshing
- Solid map hexa meshing
- Tetra meshing
- CFD meshing
- SPH meshing

Mesh Morphing:

HyperMorph is powerful solution for interactively and parametrically changing the shape of a finite element model. Its unique approach enables rapid shape variations on the finite element mesh without sacrificing mesh quality. During the morphing process, HyperMorph also allows the creation of shape variables, which can be used for subsequent design optimization studies.

Batch Meshing:

Using Altair® BatchMesher™ is the fastest way to automatically generate high-quality finite element meshes for large assemblies. By minimizing manual meshing tasks, this auto-meshing technology provides more time for value-added engineering simulation activities. BatchMesher provides user-specified control over meshing criteria and geometry clean-up parameters as well as the ability to output to customized model file formats.

CAD Interoperability:

HyperMesh provides import and export support for industry-leading CAD data formats. Moreover, HyperMesh has robust tools to clean up imported geometry to allow for the efficient generation of high-quality meshes. Boundary conditions can also be applied directly to geometry for automatic mapping to underlying elements.

- CATIA and CATIA Composite Link
- FiberSim
- IGES (import and export)
- Intergraph
- JT (import and export)
- Parasolid (import and export)
- ProE and CREO
- SolidWorks
- STEP (import and export)
- Tribon
- UG

Connectors:

Connectors are geometric entities used to connect geometry or FE entities. They are used to create spot- and seamwelds, adhesives, bolts or masses. Connectors can be realized from geometric entities into various solver specific FE representations. It is possible to unrealize them to change the representation to a different type or solver profile on the next realization. Connectors contain their location, linking partners, connection rules and realization types. They can be created manually, absorbed from FE existing FE connections or imported and generated from text files.

Composites:

HyperMesh holds strong features for modeling highly complex composites structures. Ply entities allow defining the shape of individual layers based on geometry or elements. The laminate entity defines the stacking order of a composite part. The composites definition is generic and can be realized into many solver profiles.

For review purposes composites structures can be visualized in 3D, individual layers isolated and ply orientations visualized graphically.

For a highly efficient workflow the CATIA reader has been enhanced to read composite definitions, such as ply shapes, material and ply orientations, directly from the geometry file. Fibersim drape data can be imported in a very similar way. HyperMesh offers sophisticated mapping algorithms to transfer the geometric input data to an FE mesh and associated properties.

2.6.2 *Radioss*

RADIOSS' advanced multi-processor versions (Hybrid Massively Parallel Processing) have enabled the best scalability in the industry for large, highly nonlinear structural simulation. The use of Advanced Mass Scaling and single precision option speeds up orders of magnitudes while retaining the same accurate results. Detailed and accurate analysis can also be achieved without decreasing the global time step or increasing overall simulation time. Speed-up solutions like Multi-Domain, Submodeling are unique solutions to bring the right answer in the right time delay. Special provisions in the implementation guarantee full repeatability of results regardless of the number of computer cores, nodes or threads used in parallel computation. This unique advantage allows to take advantages of the clusters and to apply in a short time optimization technique. Numerical scattering of results is highly minimized due to the quality of the software.

Here are some of the key advantages of Altair RADIOSS:

- RADIOSS provides one of the most comprehensive material and rupture libraries in the industry. The material laws and rupture criteria span across definitions for concrete, foam, rubber, steel, composites, biomaterials, and more. The coupling with MDS (Multiscale Design Systems) opens the door to précised and advanced behaviors.

- RADIOSS is tightly integrated with OptiStruct and HyperStudy. Design optimization and robustness studies can be performed easily to improve design performance.
- RADIOSS support is very responsive in reacting to user input. A rigorous quality assurance regime makes it possible to implement new features quickly and without regression in quality.
- PBS Professional is a powerful workload management software. RADIOSS jobs can be efficiently managed and monitored on sever infrastructures to minimize job turn-around-time.

RADIOSS' application areas include crash safety, drop testing, blast and hydrodynamic impact, terminal ballistic fluid structural interaction, forming and composite mapping.

A complete set of elements, connectors, and boundary conditions are available. Contacts are managed thru different algorithms to allow accuracy and robustness assuming all contact conditions and some assembling ones. Materials laws including composite, concrete and soils, …,, failure models (Johnson-Cook, Extended Mohr-Coulomb ….) are provided in RADIOSS thru libraries. Any rupture criteria can be used with any of the material laws. These combinations bring more than 300 materials. Advanced composites modeling and simulation are leading the industry.

Innovative element formulations provide accuracy, speed and robust solutions. Dozens of boundary condition types are supported, for both simple and advanced load cases and constraint setups.

Solution types include:

- Nonlinear explicit dynamic structural analysis
- Nonlinear implicit structural analysis
- Explicit Computational Fluid Dynamics (CFD)
- Euler, Lagrange and Arbitrary Euler-Lagrangian (ALE) formulations
- Smoothed-Particle Hydrodynamics (SPH)
- Finite Volume Method (FVM) based airbag simulation. Unique solution for accurate airbag deployment. Pure CFD solution with full coupling with structures.
- XFEM for crack propagation in multi-layer shells. High interest in pedestrian impact for windshield rupture prediction (Energy absorption) as well screen behavior under impacts for electronic industry, wash machine cover deck behavior under impacts, …
- Multi-Domain to manage models with fine meshed components needed to "zoom" for rupture prediction. This feature is fully compatible with FSI (Fluid Structure Analysis)
- Advanced Mass Scaling for quasi-static problems, drop and impact tests, … to increase the time step and by the way reduce the elapse time significantly without degradation of the accuracy.
- Sub-Modeling for local design of components or sub-structures.

Occupant Safety

For vehicle occupant safety, simulation RADIOSS has access to a large library of dummies, barriers, and impactors. RADIOSS provides the most comprehensive toolset in the industry through partnerships with Humanetics and CellBond. Coupling with Madymo (TASS) is also possible. In addition, the HyperCrash and HyperMesh modeling environment provides outstanding support for automotive crash and safety simulation.

THESIS DEVELOPMENT

3 THESIS DEVELOPMENT

In this chapter, the practical and experimental work will be presented, and the results are discussed, which include the study of the part, test development regarding the produced samples, mechanical tests, creating a CAD geometry for a bonnet in CATIA and performing CAE simulations for the bonnet using the software HyperMesh/HyperCrash and Radioss

3.1 *CEIIA*

CEIIA - Centre of Engineering, and Product Development is a nonprofit organization founded in the year of 1999 and situated in Matosinhos, Portugal. CEIIA is one of the ten largest research and development centers in Portugal that designs, develops and produce innovative products in many sectors, namely the automotive sector, urban mobility, aeronautics, and ocean and space. CEIIA is also the representative for the mobility sector of the United Nations Global Compact's Breakthrough innovative global platform. Apart from mobility and sustainability approach, CEIIA is globally known for its extraordinary skills in structural engineering. CEiiA's vision is to determine Portugal as a reference within the transportation and mobility industries, significantly within the development of technologies, product and systems envisaged, industrialized and operated from Portugal [113].

Figure 46 CEIIA Nerve center [113].

In the automobile and mobility, CEIIA develops new concepts of mobility that involve new devices, new mobility services, and new business models, more sustainable for the cities.

- **Mobi.me** – it is an agnostic mobility management platform for cities, which integrates all kinds of real-time mobility objects, enabling the management and operation of various shared mobility and on-demand services (public transport, automobiles, bikes, and motorbikes) in an integrated urban way public transport. It is present in more than 70 cities around the world with 400,000 users and with customers such as

UBER and Cooltra, the most extensive European network of scooter sharing. It is also the first one that allows to account in real time the emissions of CO_2 saved and recognized by the United Nations (UN). In the face of work on sustainable mobility, the United Nations Global Compact has invited CEIIA to be one of the world's entities to coordinate the Breakthrough innovation initiative.

- **Be** – it is an interactive vehicle with autonomous functions designed to be an aggregator of mobility services, is being developed by CEIIA, in partnership with TMG Automotive, and various companies and universities. The "Be" prototype is shown in Figure 47.
- **Buddy** – it is a 100% electric motor vehicle and one of the smallest in the world (and therefore chosen as an example of sustainability in the Hollywood movie *DOWNSIZING*, featuring Matt Damon released in February 2018). The new generation Buddy was developed at CEiiA in 2009 for the ElbilNorge of Norway and counted with 30000 hours of Portuguese engineering.

Figure 47 The Be Car-Prototype [113].

3.2 *Main goals*

In this section, the main goals of this work are discussed:

- Study and benchmark various natural fibers, sustainable matrix, and Bonnet system;
- Sustainable material selection;
- Designing a Bonnet system CAD part;
- Successfully design and manufacture a sustainable composite;

- Validate the physical strength of the composite by both experimentally and numerically;
- Validate some essential safety requirements that the bonnet must satisfy using CAE software (HIC and Crash);
- Successfully recycle the composite and reuse it without consuming much energy.

The overall goal is to complete the primary step in new product development (developing a sustainable bonnet) for the *"Be"* car.

3.3 *Brainstorming*

A brainstorming session is conducted with the mobility team in CEIIA to understand about "Be" car. From the first discussions, it is understood that the "Be" will be an autonomous electric vehicle and we must focus on sustainability and environmental impacts to produce a more sustainable car, which results in reducing the carbon footprints and greenhouse effect. The session is conducted in the presence of Head of Product Development-Mobility Unit, Head of the Manufacturing Division and the rest of the Product Development Team-Mobility Unit.

The session began with a discussion on selecting any one part from the car and analyzing the feasibility and viability of using the natural and eco-friendly material on to it. Since the approach is new in the field of the automotive industry, a semi-structural part will be the best choice. There are many semi-structural parts in a car, but the bonnet section and the fenders stood out during the discussion since these two parts are more connected to the appearance of the car. The bonnet section was chosen as the part to be studied by the end of the session, and its requirements were discussed.

In the next session of brainstorming, based on the bonnet's requirement, various material and manufacturing process were suggested and put into the discussion. The team members raised numerous questions about manufacturing feasibility sustainability and the strength of the composite, and many suggestions were given to achieve the goals. By the end of the session, along with the team members, an optimum solution was sorted to proceed with this work.

3.4 *Bonnet*

The bonnet system is an access panel to the engine compartment to enable maintenance of powertrain, drive belts, battery, fluid levels, and lamp units. The conventional bonnet system consists of a bonnet (inner and outer), striker, opening system, and latch and, in some cases, a pedestrian safety system. The primary functions of the bonnet are to protect the under-bonnet system and work for pedestrian safety. The system should allow inspection of the engine and service of the under-bonnet systems such as filling fluids. Together with the latch system and opening system, the bonnet should fulfill the demands in ergonomics concerning opening and closing forces and opening geometry. It should be robust enough not to be damaged by the average daily use of the car. It usually weighs about 10 kg. This weight is considered too high, and the potential for improvement by weight reduction is expected to be worked out. The most significant potential areas for weight reduction are material changes and redesign of the inner bonnet. The essential requirement to consider is that the bonnet should reduce the pedestrian head injury criterion (HIC) value.

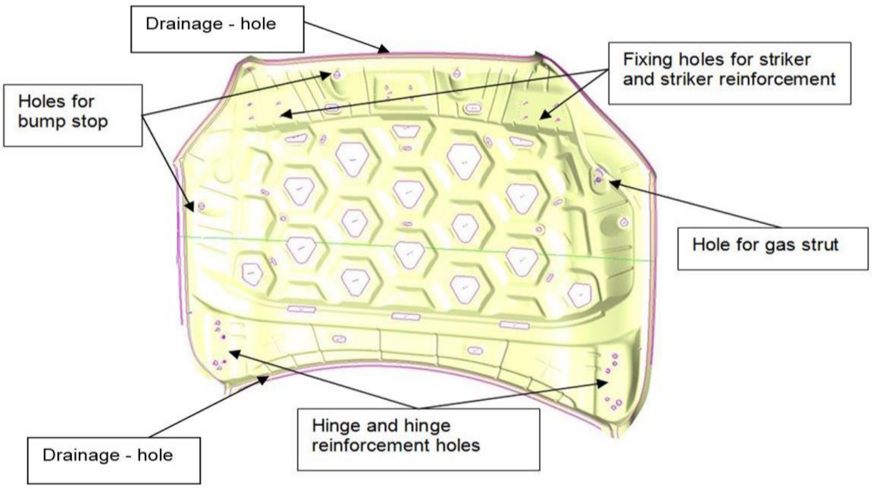

Figure 48 Inner bonnet structure of V526 [106]

3.4.1 *Requirements on the bonnet*

There are a lot of essential requirements influencing the bonnet due to pedestrian safety, drivers, engine protection, etc. The demands on the bonnet also differ to some extent between the environment and the purpose regarding the car type. For instance, car brands like Lamborghini or Ferrari do not have the same requirements as Toyota, Hyundai or Ford, due to their lower production volume. The scope of this work was to study the possibilities of using natural fiber reinforced eco-friendly composites. The demands which were taken into consideration here were:

- Pedestrian safety (energy absorption);
- Stiffness requirements.

Some issues, not dealt in this study, still need to consider when a complete bonnet is taken into consideration, such as:

- Passive safety (at 0^{o} & 35 km/h the front attachment must break or open);
- Hinges and latches system safety;
- Open/close endurance of bonnet;
- Over opening strength of bonnet.

The boundary conditions for designing a bonnet can be seen in Figure 49. The boundary conditions are prioritized based on the necessary properties for a particular condition which can be seen in Table 8.

Pedestrian safety

- *Child head impact criterion (1)*
- *Adult head impact criterion (2)*
- *Bonnet leading edge geometry (3)*

Vehicle quality

- *Torsional stiffness (4)*
- *Flutter resistance (bending stiffness) (5)*
- *Dent resistance (palm print) (6)*
- *Dent resistance (hail stone and stone chip) (7)*
- *Corrosion resistance (8)*
- *Low mass (ease of opening) (9)*
- *Low mass weight distribution (10)*
- *Low mass vehicle centre of gravity (11)*
- *Noise attenuation (12)*

Occupant Safety

- *Frontal crash collapse (13)*
- *Frontal crash maintain integrity with hinges etc. (14)*
- *Frontal crash retention of loosed component (15)*

Styling

- *Tight radii on hemmed panel edges (16)*
- *Excellent painted surface quality (17)*
- *Stretch flanges (18)*
- *Good shape: low strain doubly curved surfaces (19)*

Manufacturing

- *Paint drain features (20)*
- *Outer panel dent resistance during assembly (21)*
- *Outer panel clean sheared edges (22)*
- *Outer panel no Lüder lines or other visual defects resulting from stretch forming (23)*
- *Inner panel gauling resistance (24)*

Figure 49 Design boundary conditions for Bonnet

Concerning the design boundary conditions, the prioritization matrix is constructed by listing all candidate materials properties and characteristics in columns. The functional requirements are obtained from the affinity.

Table 8 Prioritization matrix for bonnet requirement

Bonnet system		Elastic Modulus (E)	Tensile Yield Strength (σy)	Ultimate Tensile Strength (UTS)	Uniform Tensile Elongation	Total Tensile Elongation	N-Value	R- Value	Density	DBTT	Strain Rate Sensitivity	Corrosion Resistance	Flexural Strength	Bondability	Ease of Manufacturing
Functional needs		GPa	MPa	MPa	%	%			kg/m³		S^{-1}		MPa		
Pedestrian safety	1		Maximum	Maximum	Maximum		Minimum	Maximum	Minimum	Minimum	Maximum			Maximum	Maximum
	2		Maximum	Maximum	Maximum		Minimum	Maximum	Minimum	Minimum	Maximum			Maximum	Maximum
	3		Minimum		Maximum		Maximum	Maximum		Minimum	Minimum				Maximum
Vehicle Quality	4	Maximum					Maximum	Maximum					Maximum	Maximum	Maximum
	5	Maximum						Maximum	Minimum				Maximum	Maximum	Maximum
	6	Minimum	Maximum				Minimum						Maximum	Maximum	
	7	Minimum	Maximum				Minimum				Maximum	Maximum	Maximum		
	8											Maximum			
	9		Maximum				Maximum	Maximum	Minimum					Maximum	Maximum
	10		Maximum				Maximum	Maximum	Minimum					Maximum	Maximum
	11		Maximum				Maximum	Maximum	Minimum					Maximum	Maximum
	12													Maximum	Maximum
Occupant Safety	13				Maximum	Maximum				Minimum	Minimum				Maximum
	14		Maximum	Maximum	Maximum	Maximum				Minimum		Maximum			Maximum
	15			Maximum	Maximum	Maximum				Minimum		Maximum			Maximum
Styling	16		Minimum		Maximum		Maximum								
	17											Maximum			
	18		Minimum	Maximum	Maximum	Maximum	Maximum								
	19	Maximum	Minimum	Maximum			Maximum	Maximum							
Manufacturing	20				Maximum	Maximum	Maximum	Maximum							
	21		Maximum				Minimum								
	22		Maximum	Maximum			Minimum								
	23							Maximum				Maximum			
	24		Maximum				Minimum								

** *Maximum* *Minimum* *For the corresponding 1,2, 3,……, 24 data refer* Figure 49.

Most cases DBTT (Ductile to Brittle Transition Temperature) can be a severe problem for individual grades of steel undergoing large deformation at low temperature. Since the focus here is on designing with NFRP, one can ignore this column. The resistivity is not considered in this case since natural fibers are nonconductors by nature. The judgment (or result of experience/analysis or test) shows that this property does not apply for the load cases or product requirements. Blank columns may be collapsed to enable possible alternative conclusions.

3.4.1.1 Pedestrian safety test

Euro NCAP is a division working with safety aspect tests of cars in the form of pedestrian protection since about 7000 pedestrians per year are killed by a traffic accident in the European Union [114]. About 14 % of all road unexpected events in Europe are with pedestrians. Most accidents occur within city areas where the speeds are moderate. In these tests, the potential risk of injuries to the pedestrian head, pelvis, upper and lower leg are assessed. To estimate the potential risk of head injury when a vehicle is striking an adult or a child, a series of impact tests are carried out at 40 km/h using a head-shaped impact mass (4,8 kg). Impact testing for pedestrian protection is done as illustrated in Figure 50.

The test consists of three stages:

- The impact of the head-shaped mass onto the vehicle bonnet
  - To estimate the potential risk of head injury when a vehicle is striking an adult or a child, a series of impact tests are carried out at 40 km/h using an adult or child head form impact mass.
- The impact of a leg-shaped mass on the front bonnet
  - To estimate the potential risk of the pelvis and upper leg injuries in case of a vehicle striking an adult, a series of impact tests are carried out at 40 km/h using an adult upper leg form impact mass.
- The impact of an upper leg-shaped mass to the leading edge of the bonnet.
  - To estimate the potential risk of leg injuries in case of a vehicle striking an adult, a series of impact tests are carried out at 40 km/h using an adult leg form impact mass.

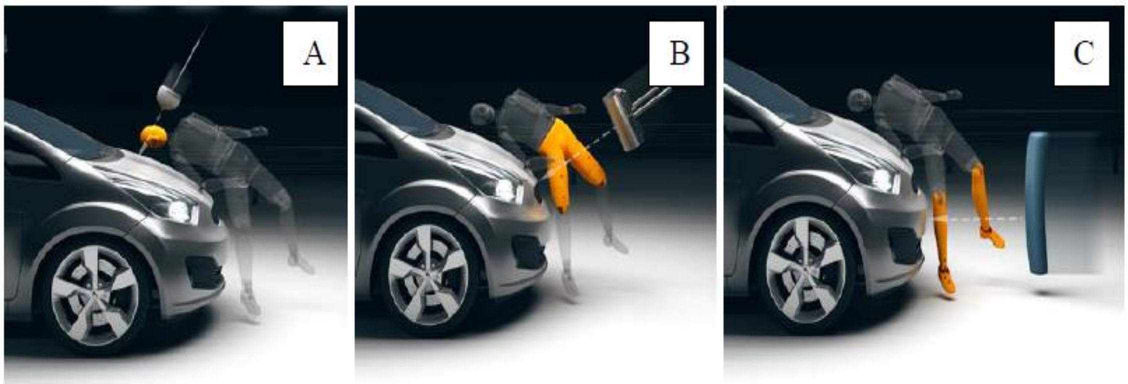

Figure 50 Crash impact testing of Car Bonnet at 40 km/h, A is a head impact, B is leg impact, and C is lower leg impact testing [Source 4 Institut für Kraftfahrzeuge, RWTH Aachen University, Dr. J Bovenkerk]

Head Injury Criteria (HIC)

HIC shows the potential risk of pedestrians getting injured following a collision with a vehicle. The value depends on the design of the bonnet, the type of material chosen, the type of impact and structure. HIC is calculated by Equation 3.1.

$$HIC = \left[\frac{1}{T_2 - T_1}\int_{T_1}^{T_2} A_v dt\right]^{2.5} (T2 - T1) \qquad \textbf{3.1}$$

Av is the resultant acceleration m/s²

T1 and T2: two times instants (in seconds), which define the beginning and end time of the recording when HIC is at maximum.

The experiment should be carried out within 15 ms. The other conditions (more than 15 ms) are ignored because the time is enough to gain maximum HIC value and this will gradually decrease in the following time range. According to the EEVC/WG (European Enhanced Vehicle-Safety Committee/Pedestrian Safety) standard, the highest value of HIC must not exceed more than 1000 [114].

3.4.1.2 Stiffness Requirements

Among several requirements, it was found that many were related to stiffness. Those requirements are listed as:

- Stiffness and Strength/Stiffness of the Bonnet:
  - Vertical Stiffness;
  - Flexural Stiffness.
- Resistance to dents:
  - Static resistance to dents;
  - Dynamic resistance to dents.

As mentioned, many requirements listed previously are related to stiffness. Vertical stiffness is a requirement that the bonnet must be sufficiently stiff to resist vibrations at any speed up to the maximum. Flexural stiffness is a requirement of the bonnet to be sufficiently stiff to resist flutter at high speed. Also, the bonnet has to be stiff enough for static loads, meaning no damage on the “class A” surface when applying a load. This requirement can be related with a person placing his hand on the bonnet and leaning on it without being deformed. There is also another test related to stiffness called “vertical robustness” test. This is when a bonnet is subjected to a person sitting on it without being deformed.

Static and dynamic resistance to dents are also requirements related to the global stiffness of the bonnet, meaning that the bonnet should be able to withstand static and dynamic loading conditions. Those requirements can be evaluated throughout a three-point bending test.

3.4.1.3 Other tests

The other tests, which include tensile tests, impact tests, moisture absorption tests, SEM study of the fracture zone and degradability of the composite, which are necessary to categories the material properties and its application. In this case, the application of the material is a car bonnet. Thus, the tensile and impact test helps in studying the behavior of the composite under tensile loading and during sudden impacts. Since the fiber used in this study is a natural fiber which tends to absorb moisture from the atmosphere, it is necessary to study the moisture absorption tendency of the composite. The test to find the degradation rate of the part is essential for the knowledge of understanding the life cycle and decomposition of the part after the life cycle. The higher the degradation rate, the smaller is the impact on the environment.

3.5 Design and Manufacturing

3.5.1 Material selection process

3.5.1.1 Fiber Selection

The very first step in designing any product or a part is setting the needs and requirements. Then the material selection matrix is made based on the needs and requirements. The first step in every material selection process is to define the performance index or material index. The performance index (P) is an empirical representation of parameters such as functional requirements, geometric parameters, and "material performance index" [39].

$$P = [f(F)\, f(G)\, f(M)] \qquad \textbf{3.2}$$

F- Functional requirements, G- Geometrical parameters, M- Material properties

In this study, the designed product is an eco-friendly car bonnet. The main functional requirements are biodegradability and stiffness. In order to design the bonnet, some assumptions need to be made. They are:

- The bonnet is flat, as a rectangular plate with a/b greater than 1;
- The boundary conditions of the plate are clamped at least two corner points;
- No ribs are present.

The bonnet system to be designed must abide by the parameters such as eco-friendly, and the stiffness performance index must be improved. To improve this parameter, it is needed to consider some equations:

$$m = \rho * a * b * t \qquad \textbf{3.3}$$

$$\delta = (\alpha * P * a^2)/12D_2 \quad \textbf{3.4}$$

$$\alpha = 3EI\left(\frac{b}{a^2}\right)\left(\frac{D_2}{T}\right)C \quad \textbf{3.5}$$

$$I_z = \frac{m}{12}(a^2 + b^2) \quad \textbf{3.6}$$

m- mass kg, P- Load applied in N. D_2 and T are flexural and torsional stiffness in Nm^3, E-Young's Modulus for respective a, b and t values refer to Figure 51

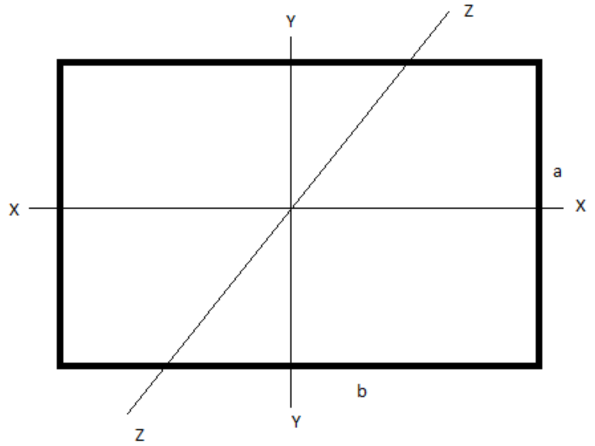

Figure 51 Bonnet considered as a flat plate

$$M = \left(\frac{C}{12\alpha\, a^2}\right)^{\frac{1}{3}} b^2 \left(\frac{E^{\frac{1}{3}}}{\rho}\right) \quad \textbf{3.7}$$

By substituting these three equations (m, δ, I_z) in Equation 3.2 and eliminating the free variables such as stiffness, length, width, and thickness, the material index will be:

$$M = \frac{E^{\frac{1}{3}}}{\rho} \quad \textbf{3.8}$$

E- Young's modulus N/m^2, ρ- density in kg/m^3

The resultant value is crosschecked with the general value from [115] (Table A1 - Stiffness limited design at minimum mass (cost, energy, eco-impact)) and it matches the results. Ashby chart illustrating tensile strength vs E can be seen in Figure 52. The chart is just to visualize how materials are categorized based on their properties. Where, the based on derived material index the possible material region can be seen in Figure 53.

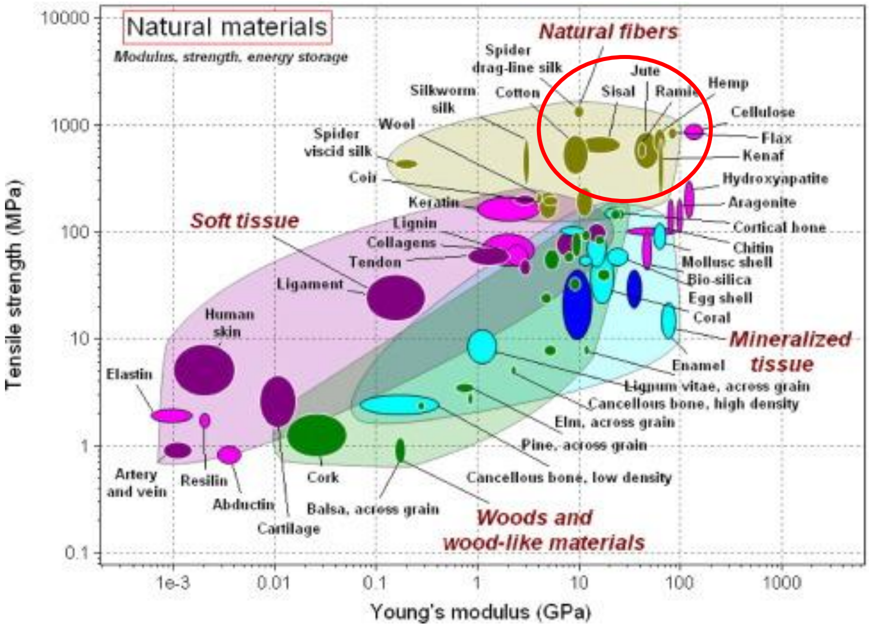

Figure 52. Ashby plot is illustrating Young's modulus and tensile strength of traditional engineering materials and natural materials on the same axis [115].

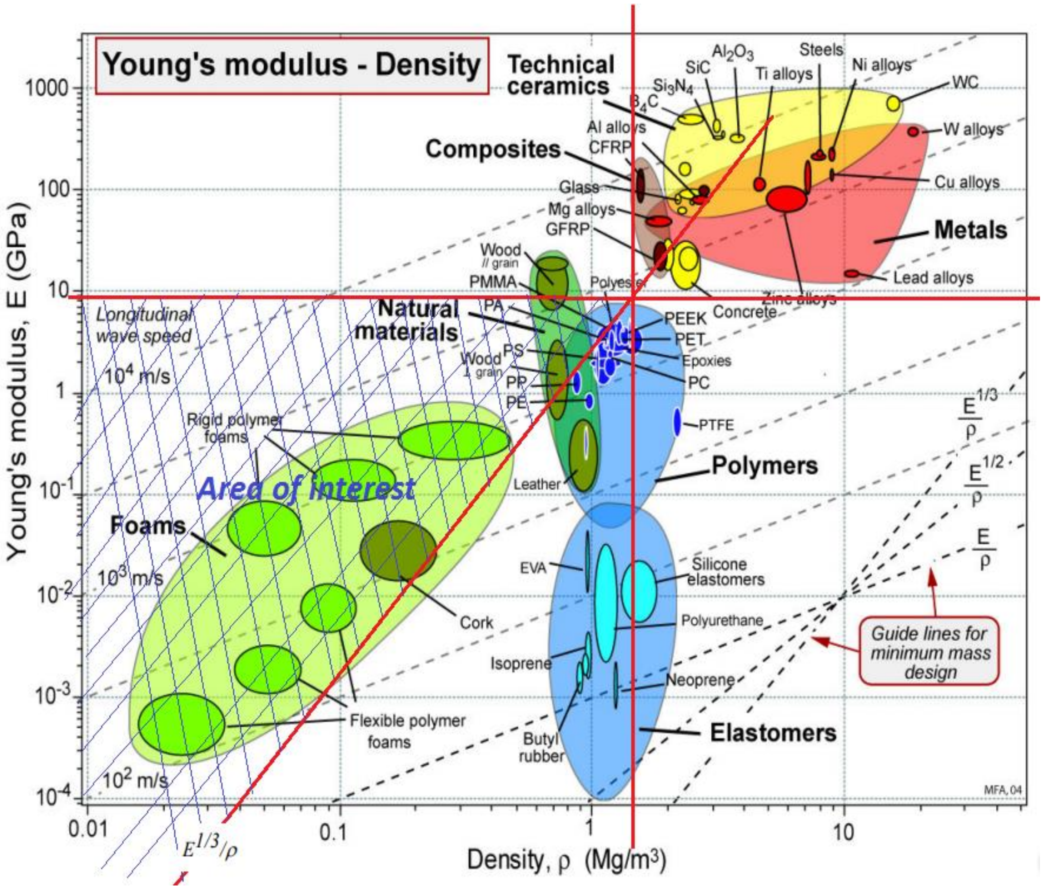

Figure 53 Ashby chart is representing the area of interest concerning the Material index [115].

From Figure 53, the most suggestive materials are Flax, Hemp, and Jute. The next step is to narrow it to a single material with the help of a decision matrix.

Step1 - Determination of the importance of the properties (ω_i)

Table 9 Property importance table for fiber (ω_i)

S. No	Properties	(1/2)	(1/3)	(1/4)		Importance	Required State
1	σ_{UT}/ρ [MPa/kg/m^3]	55	55	60	1.00	***0.3028***	***High***
2	Eco-friendly (Embodied energy) [MJ/kg]	45			0.8182	***0.2477***	***Low***
3	Tensile failure strain ε_U [%]		45		0.8182	***0.2477***	***High***
4	Cost			40	0.6667	***0.2018***	***Low***
				Total	***3.3031***	***1.000***	

Detailed calculation of Table 9 can be seen in Annex 6.2.1.

Step 2 - Creating the selection matrix

Table 10 Material selection matrix for fiber

MATERIAL			σ_{UT}/ρ [MPa/kg/m^3]		Eco-friendly (Embodied energy) [MJ/kg]		Tensile failure strain ε_U [%]		Cost [€/kg]		γ
			ω_1=0.3028 ↑		ω_2=0.2477↓		ω_3=0.2477↑		ω_4=0.2018↓		∑(C_i)
Flax	***A***	***C***	0.7137	30.28	15	19.81	3.2	24.77	1.5	4.708	**79.57**
	B		100		80		100		23.33		
Hemp	***A***	***C***	0.6202	26.33	14	21.23	2.1	16.25	1.8	3.923	67.74
	B		86.95		85.71		65.62		19.44		
Jute	***A***	***C***	0.574	24.35	12	24.77	1.8	13.93	0.35	20.18	83.23
	B		80.42		100		56.25		100		

Calculation for flax:

Property 1 – σ_{UT}/ρ [MPa/kg/m^3]

A:

$$\frac{\sigma_{UT}}{\rho} = \frac{1035}{1450} = \mathbf{0.7137}$$

B:

$$\frac{Numerical\ value\ of\ property}{Maximum\ Value\ in\ the\ list} * 100 = \frac{0.713}{0.713} * 100 = \mathbf{100}$$

C:

$$C = \omega_1 * B = 0.3028 * 100 = \mathbf{30.28}$$

Property 2 – Embodied energy [MJ/kg]

***A*:**

$$E = \mathbf{15\ MJ/kg}$$

B:

$$\frac{Minimum\ value\ in\ the\ list}{Numerical\ value\ of\ the\ property} * 100 = \frac{12}{15} * 100 = \mathbf{80}$$

C:

$$C = \omega_2 * B = 0.2477 * 80 = \mathbf{19.81}$$

Property 3 – ε_U [%]

A:

$$\varepsilon_u = \mathbf{3.2}\%$$

B:

$$\frac{Numerical\ value\ of\ property}{Maximum\ Value\ in\ the\ list} * 100 = \frac{3.2}{3.2} * 100 = \mathbf{100}$$

C:

$$C = \omega_3 * B = 0.247 * 100 = \mathbf{24.77}$$

Property 4 – Cost [€/kg]

A:

$$Cost = \mathbf{1.5\ €/kg}$$

B:

$$\frac{Minimum\ value\ in\ the\ list}{Numerical\ value\ of\ the\ property} * 100 = \frac{0.35}{1.5} * 100 = \mathbf{23.33}$$

C:

$$C = \omega_4 * B = 0.201 * 23.33 = \mathbf{4.70}$$

Performance index for Flax:

$$\Upsilon = \sum \boldsymbol{C_i} = 30.28 + 19.81 + 24.77 + 4.70 = \mathbf{79.57 \sim 80}$$

**for the values of σ_{UT} and ρ refer Table 6 [84].

Step 3 - Justification for the choice

From Table 10, the performance index of jute is higher compared to hemp and flax but, regarding mechanical behavior, flax presents a higher value compared to jute. Also, the performance index of jute is better because of the cost criteria. However, the importance of cost is marginally lower than the importance of $\sigma_{UT/}\rho$ and ε_U. In such a situation as an engineer, the decision must be made according to the 'importance criteria.' Therefore, flax will be the chosen material for this desired purpose.

3.5.1.2 Matrix selection

Unlike the composite reinforcement, the matrix selection will be pretty simple, since there is only a handful of the matrix which obeys the criteria of this study. The first and the most important criterion for this study is that both the matrix and the reinforcement must be sustainable and eco-friendly, and the embodied energy should be less compared to conventional materials, without compromising a lot on strength. As discussed in section 2.4.2, three matrices stood in front, which are PLA, Elium® and PEEK.

The properties which are essential for this sole purpose are sustainability, tensile strength over density, ease of manufacturing and cost.

Step1 - Determination of the importance of the properties (ω_i)

Table 11 Property importance table resin (ω_i)

S. No	Properties	(1/2)	(1/3)	(1/4)		Importance	Needed State
1	**Sustainability [Ease of recycling]**	55	55	60	1.00	***0.3028***	***High***
2	**σ_T/ρ [MPa/kg/m^3]**	45			0.8182	***0.2477***	***High***
3	**Young's Modulus [GPa]**		45		0.8182	***0.2477***	***High***
4	**Cost**			40	0.6667	***0.2018***	***Low***
				Total	***3.3031***	***1.000***	

Detailed calculation of Table 11 can be seen in Annex 6.2.1.

Here the sustainability is rated in between 1-10 based on the type of recycling, ease of recycling, the energy needed to recycle, ease of manufacturing, and cost to recycle.

From various sources mentioned in section 2.4.2, the values of the corresponding matrix are listed below.

- *PLA-5/10*, recycling PLA needs more energy and the strength of the recycled product is marginally low, and the recycling techniques for PLA are limited;
- *Elium®-7.5/10*, since it is a liquid thermoplastic in nature, it is easy to recycle either by the mechanical, chemical or thermal process. Depolymerization is remarkably simple;
- *PEEK-6.5/10* is also limited in the recycling process. Indeed, to recycle PEEK in an efficient way, it needs more energy pulses to break the chains at the molecular level.

Step 2 - Creating the selection matrix

Table 12 Material selection matrix for resin

MATERIAL			Sustainability		σ_{UT}/ρ [MPa/kg/m³]		Young's Modulus [GPa]		Cost [€/kg]		γ
			ω₁=0.3028↑		*ω₂=0.2477↑*		*ω₃=0.2477↑*		*ω₄=0.2018↓*		*Σ(Cᵢ)*
PLA	***A***	***C***	5	20.18	0.0323	1.43	3.5	3.21	17.5	20.18	45.01
	B		66.67		5.809		12.96		100		
Elium®	***A***	***C***	7.5	30.28	0.556	24.77	27	24.77	21	16.81	**96.63**
	B		100		100		100		83.33		
PEEK	***A***	***C***	6.5	26.24	0.075	3.37	3.6	3.30	35	10.09	43.00
	B		86.67		13.615		13.33		50		

Step 3 - Justification for the choice

From Table 12, it is seen that the performance of Elium is higher compared to the other two choices, although it costs a bit higher than PLA. However, about sustainability and strength, Elium proves to be superior. Thus, Elium will be the best choice for making this composite.

Calculation for Elium®:

Property 1 – Sustainability

A:

$$\text{Sustainability value} = \mathbf{7.5}$$

B:

$$\frac{Numerical\ value\ of\ property}{Maximum\ Value\ in\ the\ list} * 100 = \frac{7.5}{7.5} * 100 = \mathbf{100}$$

C:

$$C = w_1 * B = 0.3028 * 100 = \mathbf{30.28}$$

Property 2 – σ_{UT}/ρ [MPa/kg/m³]

***A*:**

$$\frac{\sigma_{UT}}{\rho} = \frac{557}{1001} = \mathbf{0.556}$$

B:

$$\frac{Numerical\ value\ of\ property}{Maximum\ Value\ in\ the\ list} * 100 = \frac{0.556}{0.556} * 100 = \mathbf{100}$$

C:

$$C = w_2 * B = 0.2477 * 100 = \mathbf{24.77}$$

Property 3 – Young's Modulus [GPa]

A:

$$\mathrm{E} = \mathbf{27\ GPa}$$

B:

$$\frac{Numerical\ value\ of\ property}{Maximum\ Value\ in\ the\ list} * 100 = \frac{27}{27} * 100 = \mathbf{100}$$

C:

$$C = w_3 * B = 0.247 * 100 = \mathbf{24.77}$$

Property 4 – Cost [€/kg]

A:

$$Cost = \mathbf{21}\ €/\boldsymbol{kg}$$

B:

$$\frac{Minimum\ value\ in\ the\ list}{Numerical\ value\ of\ the\ property} * 100 = \frac{17.5}{21} * 100 = \mathbf{83.33}$$

C:

$$C = w_4 * B = 0.201 * 83.33 = \mathbf{16.81}$$

Performance index for Elium®:

$$\Upsilon = \sum \boldsymbol{C_i} = 30.28 + 24.77 + 24.77 + 16.81 = \mathbf{96.63}$$

For values such as ρ, σ, and E refer to section 2.4.2.

3.5.1.3 Development of the additives

The natural additive used in this study is Tamarind seed powder (TSP) detailly explained in chapter 2.4.2.5. The production of TSP is a simple process which is explained in the following steps:

1. The seeds are extracted from the Tamarind fruits;
2. The seeds are then washed with clean water to get rid of the waxy layer present around it;
3. The extracted seeds are then dried under the sunlight to get rid of the moisture;
4. The dried seed is then inspected for any foul seeds or damaged seeds;
5. After careful inspection, the seeds are fed into a flour mill machine to get the fine powder;
6. The ground powder is then stored in a dry container to keep it away from moisture.

In this study, the required quantity of the powder is very small. Therefore, a home appliance mixer is used to grind the seeds. The seed and the seed powder can be seen in Figure 54.

Figure 54 A-Tamarind seeds, B-Seed powder

3.5.2 *Composite design*

Designing any part in composite is different from designing a part using metals since the properties of composites depends on various factors such as type of fiber, fiber orientation, volume or mass fraction between matrix and fiber (rule of mixtures), bonding between the matrix and fiber and, thus, it is hard to predict a defined result. Trial and error are one of the ways to find out the best solution. However, the problem with trial and error is that it consumes time, wastage of materials and it results in high cost. The best possible way is to use Micromechanics and Classical laminate theory (CLT) to mathematically define an approximate solution and the failure mechanism of the composite.

The fiber used in this study is a biaxial (-45 deg) untreated fabric made of 20 Âµu diameter flax thread. The fabric is woven in such a way that two layers of the thread which are aligned at (-45 deg) and are mutually perpendicular to each other. This results in showing even properties in all directions. It is necessary to calculate the ply properties of a composite material to model and analyze in simulation software. The ply properties are calculated for three different configurations, which are *45%, 50%, 55%* mass fraction of fiber. The best value is taken into consideration for numerical simulation. To adequately model a composite in the FEA program, six composite properties are needed: E_1, E_2, V_{12}, G_{12}, G_{13}, and G_{23}. However, the values such as G_{13} and G_{23} are automatically calculated by the numerical solvers, since that software have built-in composite equation solver.

The axial stiffness E_1 is derived from the well-known rule of mixtures:

$$E_1 = E_f V_f + E_m(1 - V_f) \qquad \textbf{3.9}$$

For transverse stiffness, E_2:

$$E_2 = \frac{E_f E_m}{E_f(1-V_f)+E_m V_f} \qquad \textbf{3.10}$$

Poisson's ratio in ν_{12}: ν_{12} describes the contraction in the 2nd direction when a stress is applied in the first direction, the 12 Poisson's ratio can be found from a rule of mixtures.

$$\nu_1 = \nu_f V_f + \nu_m(1 - V_f) \qquad \textbf{3.11}$$

The shear modulus, G_{12}, shows the ratio of shear stress (acting in the direction1 on the plane with a normal in the direction2) and shear strain (is the rotation towards the direction1 of the two axes). It should be noted that, since the composite body is not rotating, $G_{ij} = G_{ji}$ and since in for aligned fiber composites, the 2- and 3-directions are equivalent, there are only two shear moduli as, $G_{12}=G_{21}=G_{13}=G_{31}\neq G_{23}=G_{32}$ [116] [117].

$$G_{12} = \frac{G_f G_m}{G_f(1 - V_f) + G_m V_f} \tag{3.12}$$

$$V_f = \frac{\frac{M_f}{\rho_f}}{\frac{M_f}{\rho_f} + \frac{(1 - M_f)}{\rho_m}} \tag{3.13}$$

The data for the material properties from various sources are tabulated in Table 13.

Table 13 Material properties for composites fiber and the resin

Material property	Value	Unit	Source
	Flax Fiber		
Young's modulus, E	30	GPa	Table 6
Poisson's ratio, v	0.45-0.5		[118]
**The above values are for chemically treated flax fiber. The fiber used in this study is an untreated fiber.			
	Elium® Resin		
Young's modulus, E	27	GPa	Arkema
Poisson's ratio, v	0.51		Arkema

Using properties from Table 13, and Equation 3.9, Equation 3.10, Equation 3.11, Equation 3.12, and Equation 3.13, the properties needed to model a composite in the FEA program are found for three different mass fractions. The properties for three different mass fraction (45%, 50% and 55%) can be seen in Table 14,Table 15 and Table 16 respectively.

Table 14 Composite properties values for 45% mass fraction of fiber

Property	Calculated Value	Correction factor	Corrected value	Units
Volume fraction	35.52			%
E_1	28.07	0.25 [119]	7.02	GPa
E_2	27.99		6.99	GPa
ν_{12}	0.50			
G_{12}	9.33		2.33	GPa

Table 15 Composite properties values for 50% mass fraction of fiber

Property	Calculated Value	Correction factor	Corrected value	Units
Volume fraction	40.24			%
E_1	28.21	0.25 [119]	7.05	GPa
E_2	28.13		7.03	GPa
ν_{12}	0.50			
G_{12}	9.38		2.34	GPa

Table 16 Composite properties values for 55% mass fraction of fiber

Property	Calculated Value	Correction factor	Corrected value	Units
Volume fraction	45.14			%
E_1	28.36	0.25 [119]	7.09	GPa
E_2	28.28		7.07	GPa
ν_{12}	0.50			
G_{12}	9.43		2.36	GPa

One can see that the values E_1, E_2, and G_{12} are increasing as the mass of the fiber increases. This is because the strength of the reinforcement is comparatively higher than the matrix. However, this is possible on paper, but in a real scenario in case of natural fiber, the ratio must be kept at 45 ± 10% because the natural fibers tend to absorb the matrix more than synthetic fiber and, under loading, insufficient matrix can induce inter laminar shear [120]. The numerical simulation of the composite can be seen in section 3.6. From Equation 2.1 one knows about the stiffness matrix and A, B, and CLT matrices. Using CLT, one can find the stress, coupling and bending stiffness matrix of a composite layer by layer.

$$[A] = \sum_{k=1}^{N} (\bar{Q})_k (Z_k - Z_{k-1}) = \sum_{k=1}^{N} (\bar{Q})_k (t_k) \quad \textbf{3.14}$$

$(\bar{Q})_k$- stiffness of the k^{th} layer and t_k-thickness of the k^{th} layer

$$[B] = \frac{1}{2} \sum_{k=1}^{N} (\bar{Q})_k (Z_k^2 - Z_{k-1}^2) = \frac{1}{2} \sum_{k=1}^{N} (\bar{Q})_k t_k \bar{Z}_k \quad \textbf{3.15}$$

$\bar{Z}$-distance from the mid-plan to the centroid of the k^{th} layer

$$[C] = \frac{1}{3} \sum_{k=1}^{N} (\bar{Q})_k (Z_k^3 - Z_{k-1}^3) = \frac{1}{3} \sum_{k=1}^{N} (\bar{Q})_k t_k \bar{Z}_k \quad \textbf{3.16}$$

$$[A] = \begin{bmatrix} 234.8 & 117.1 & 0 \\ 117.1 & 234.8 & 0 \\ 0 & 0 & 60.80 \end{bmatrix} \frac{GPa}{mm} \quad \textbf{3.17}$$

$$[B] = \begin{bmatrix} 0 & 0 & 0 \\ 0 & 0 & 0 \\ 0 & 0 & 0 \end{bmatrix} \frac{GPa}{mm^2} \quad \textbf{3.18}$$

$$[D] = \begin{bmatrix} 1.223x10^4 & 6100 & 0 \\ 6100 & 1.223x10^4 & 0 \\ 0 & 0 & 3167 \end{bmatrix} \frac{GPa}{mm^3} \quad \textbf{3.19}$$

3.5.3 *Modeling the CAD part*

The CAD geometry for the bonnet is created using CATIA V5.

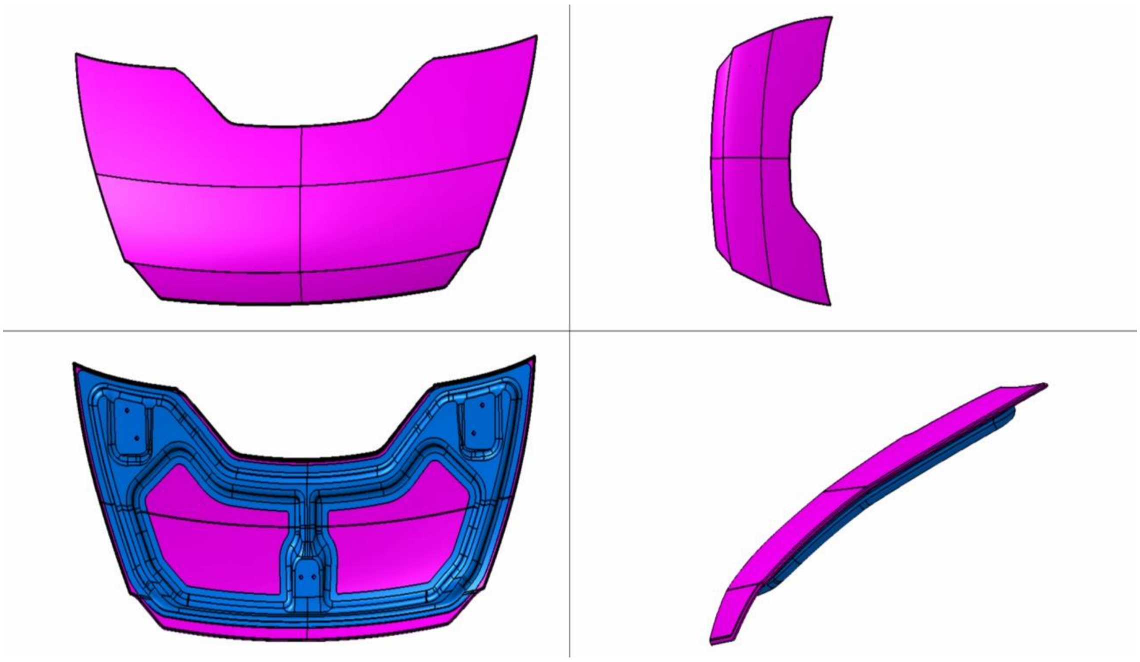

Figure 55 Bonnet geometry

Few design modifications were made on the earlier prototype's CAD geometry considering a composite bonnet surface. The thickness of the bonnet was increased from 3 mm to 5 mm, and a little tolerance towards the inside of the bonnet section for adhesive bonding was also considered. The new bonnet design can be seen in Figure 55.

3.5.4 *Manufacturing the composite*

Two different composite laminates are manufactured. One of the laminates presents matrix and reinforcement, and another laminate has been made with Elium® matrix, flax fiber reinforcement, and a natural additive called tamarind seed powder to study the changes in stiffness properties of the composite.

The fiber is in the form of woven (-45 Biaxial) fabric. Biaxial reinforcement offers mechanical performance advantages over traditional woven reinforcements because of the straight, flat path in which the fiber bundles are stitched. Unlike a woven cloth, where the intersecting weft and warp fibers go over-under-over-under, biaxial reinforcements are two layers of unidirectional fiber aligned at 90° to each other. Because these unidirectional fibers take a much more direct line (rather than being woven up and down), when the laminate is stressed the fibers cannot try to 'straighten-out' as they do with woven cloth, resulting in significant improvements in the tensile strength of the laminate.

Figure 56 Flax fiber (-45 Biaxial)

Elium®150 is an infusion grade liquid *thermoplastic resin,* a product of Arkema technologies, which can be processed and cured at room temperature. Since it is a thermoplastic resin, it can be recycled. Tamarind seed powder is a natural additive, which is supposed to act as filler and must enhance the mechanical properties of the composites.

The laminates are manufactured using vacuum bag infusion process as it is explained in the earlier steps. First laminate is manufactured with just matrix and the reinforcement. The reinforcement fiber is first dried in the oven for around 30 minutes at 50 ^{o}C without the presence on any humidity, i.e., the relative humidity is 0%. This is to remove the moisture present in the fiber. Once the fiber is dried, the fabric is cut into layers to stack inside the mold.

The matrix is Elium®150, which is a liquid thermoplastic resin at room temperature. The matrix is stable at room temperature, and there will be no chemical reaction. Perkadox® CH-50X is Dibenzoyl Peroxide with 50% dicyclohexyl phthalate. 3-5% of peroxide is added to start the hardening process of the resin as instructed by the supplier. The structure of the peroxide is quite open and straightforward, in such a way that it releases the oxygen molecule and form a strong bond with Elium®. This bonding formation takes time to complete. The mixture has the pot time of 20-60 min concerning the temperature. At room temperature (25-27 °C) the pot time is around 40 minutes. The chemical structure of the peroxide which is used to initiate the chemical reaction can be seen in Figure 57.

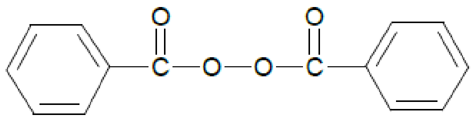

Figure 57 Structure of Perkadox CH-50X [118]

This mixture is then used to infuse the reinforcement. The time taken to infuse the total reinforcement is directly proportional to the inner surface area of the mold or bagging and the suction pressure. The pressure used in this experiment was 1 bar and the time taken for the total infusion was about 20 minutes. An exothermic reaction takes place once the flow of resin is cut-off. The peak exothermic time of the mixture is about 33-35 min, which is the cure time of the laminate. Demolding is done after 10-15 minutes of the peak exothermic time. The entire process is completed within 90 minutes, and the laminate is ready.

The manufacturing process adopted here to produce the specimens is the vacuum infusion technique. This method is one of the most effective and efficient ways of manufacturing composites under low manufacturing cost. The principle of vacuum infusion technique is quite simple. The fluid flows from high pressure to low pressure region. Here, a vacuum medium is created inside an insulating bag, using a vacuum pump which sucks the resin inside the insulation bag. The manufacturing process is explained in following steps:

1. The glass surface or the mold is first cleaned with distilled water then drained utterly and wiped out with a clean cotton gauge;
2. Then, the mold is thoroughly cleaned with cleaning alcohol, and a layer of PVA release agent is applied;
3. The boundary for the mold region is created by double-sided sealant tape on the glass table;
4. The required number of fiber layers are cut and laid inside the created boundary;
5. A layer of peel ply is laid over the fiber. The peel ply is nylon® fabric which helps in releasing the composite from the outer layers, such as infusion mesh and the vacuum bag;
6. The next layer is the infusion mesh, which is a plastic mesh that helps the matrix to flow over the reinforcement;
7. Then two layers of breather cloth are laid over the infusion mesh. This breather helps in absorbing the excess matrix which is flowing over the reinforcement;

8. An inlet piping is created at one end of the bagging to allow the mesh to enter. The inlet piping is made of a T-Junction and a spiral coil, which helps in resin flow over the flow mesh;
9. At the other end of the bagging, the outlet piping is formed using a single way valve;
10. The single valve is connected to the resin infusion catch-pot which is directly connected to the vacuum machine;
11. As for the last part of the setup the vacuum bag is placed and sealed using the sealant tape, and the gaps are closed using the sealant tapes as shown in (Figure 58);

Figure 58 Setting up vacuum bagging

12. The vacuum pump is started to create a vacuum inside the boundary;
13. The matrix is mixed to a right proportion and is placed in reach of the inlet piping;
14. As we know from gas law the fluid flow from high pressure to low pressure, the resin flows inside the bagging. The pressure inside the bagging is lower than the atmospheric pressure. Resin flow can be seen in Figure 59;
15. The air inside the bagging is completely sucked out, and the resin started to flow towards the Catch-pot via outlet piping;
16. Once the resin reached the other end and the reinforcement is infused both the ends are clamped using C-clamps, and the vacuum supply and resin supply are cut off;
17. Then, the bagging is left untouched to cure for the best time;
18. Once it is fully cured, the sealing is opened, and the laminate is separated from the other auxiliary layers such as peel ply infusion mesh, etc. (Figure 60);
19. The surfaces are cleaned with a dry cloth to make sure that no moisture is present;

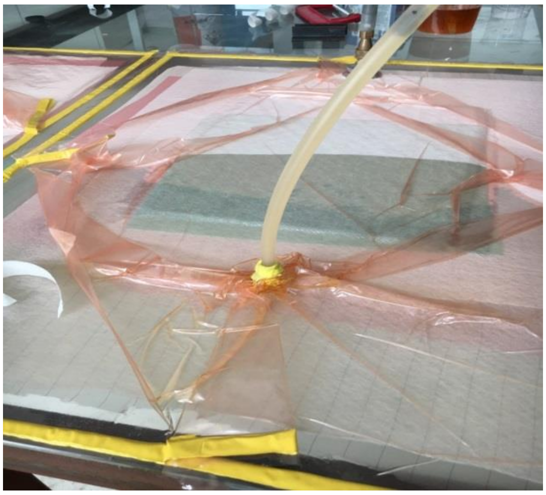

Figure 59 Infusion flow

Figure 60 Fabricated laminate

20. The edges are trimmed, and the samples are cut by the ASTM standards for testing (tensile, flexural, impact, moisture absorption) (Figure 61).

Figure 61 Peel ply, flow mesh, vacuum bag, breather cloth

The various components and accessories used during manufacturing process can be seen in Figure 62, Figure 63 and Figure 64.

T-Junction

Infusion Spiral Coil

Figure 62 T-junction and spiral coil

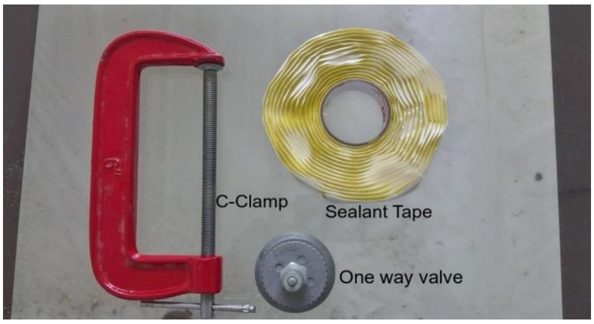

Figure 63 Clamp, sealant tape, and valve

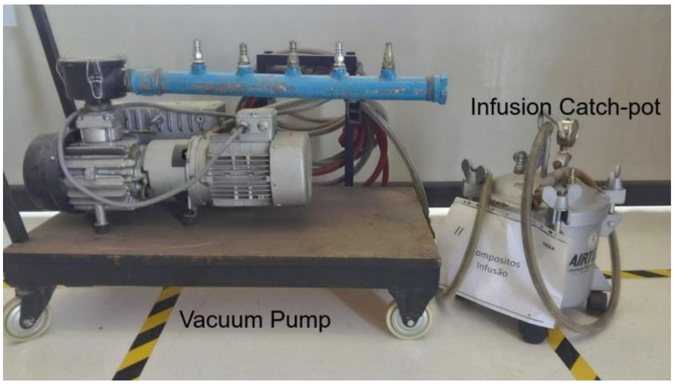

Figure 64 Vacuum pump and catch pot

3.5.4.1 Sample set 1

The laminate (Figure 65) without any additives was manufactured, and the edges were trimmed for a better look and to remove the matrix and reinforcement excess. The trimmed laminate presented the dimensions of 320 x 320 x 4.2 mm^3. The configuration of the manufactured sample set 1 can be seen in Table 17.

Table 17 Sample set 1 manufacturing data table

Laminate 1 manufacturing			
Material	Flax	**Density**	1.50 g/cc
No of layers	4		
The dimension of a single layer	360 x 360 x 0.9 mm^3		
Total wt. of fiber layers	380 g		
Matrix	Elium®150	**Density**	1.01 g/cc
Matrix consumed	1200 g		
Peroxide	Perkadox® CH-50X	**Density**	1.23 g/cc
Peroxide consumed	40 g		
Additives	Nil	**Density**	Nil
Infusion time	20 min		
Cure time	40 min		
Demolding time	5 min		
Laminate thickness	4.2 mm		
Laminate weight	~700 g		

Figure 65 Sample set 1

3.5.4.2 Sample set 2

The second laminate (Figure 66) is like the first, but this time a natural additive was added to the matrix enhancing the material stiffness. The edges were trimmed for a better look and to remove the matrix and reinforcement excess. The trimmed laminate presented the dimensions of 320 x 320 x 4.2 mm^3. The configuration of the manufactured sample set 2 can be seen in Table 18.

Figure 66 Sample set 2

Table 18 Sample set 2 manufacturing data table

Laminate 2 manufacturing			
Material	Flax	**Density**	1.5 g/cc
No of layers	4		
The dimension of a single layer	360 x 360 x 0.9 mm^3		
Total Wt. of Fiber layers	385 g		
Matrix	Elium®150	**Density**	1.01 g/cc
Matrix consumed	1250 g		
Peroxide	Perkadox® CH-50X	**Density**	1.230 g/cc
Peroxide consumed	40 g		
Additives	TSP	**Density**	0.481 g/cc
Infusion time	20 min		
Cure time	40 min		
Demolding Time	5 min		
Laminate thickness	4.2 mm		
Laminate weight	~710 g		

The specimens of these two laminates were prepared for mechanical testing. The samples for the following tests were cut from the manufactured laminates:

1. Tensile tests;
2. Flexural tests;
3. Impact test (Drop);
4. Moisture absorption tests;
5. Chemical and Mechanical recycle process.

The samples were cut using a vertical ax-saw cutting machine with the blade thickness of 2 mm, which is powered by a 1 hp and 3450 rpm electric motor.

Figure 67 Vertical ax-saw machine

The samples were cut using the ax-saw machine since the unavailability of wire cut EDM or water jet cutting machine. These are the conventional way for cutting composite materials.

3.6 *Testing, Results, and Discussion*

The abundant availability and accessibility of natural fibers are the primary reasons for an emerging new interest in sustainable technology. Natural fibers, as reinforcement, have recently attracted the attention of researchers because of their advantages over other established materials. They are environmentally-friendly, fully biodegradable, abundantly available, non-toxic, non-abrasive, renewable, cheap, and have low-density [122].

3.6.1 *Tensile testing*

3.6.1.1 Mechanical Tensile test

To evaluate the mechanical properties of this natural fiber composite, tensile tests were performed. Tests used rectangular specimens of 250 x 25 x 4 mm^3 as per ASTM Standard D3039 [123] manufactured using natural fibers. Tests were performed at CEIIA Test Lab facilities. The specimen references are:

- AT (AT003, AT004, AT005, AT006);
- T (T001, T002, T003, T005)

AT- Samples with the additive material, T-Samples without additive material.

For each composite plate of T and AT characteristic, five specimens were cut as shown in Figure 68 and Figure 69 respectively. Some specimens were used to adjust the equipment, and the results were not considered in the final report. Specimens presented a very irregular geometry and cutting surfaces (general dimensions and thickness) and had to be measured at its initial state. The tensile testing specimen for both the samples can be seen can be seen in Table 19.

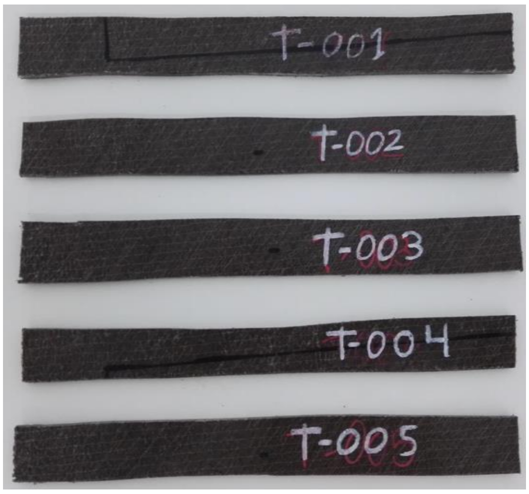

Figure 68 Initial state of specimen reference T

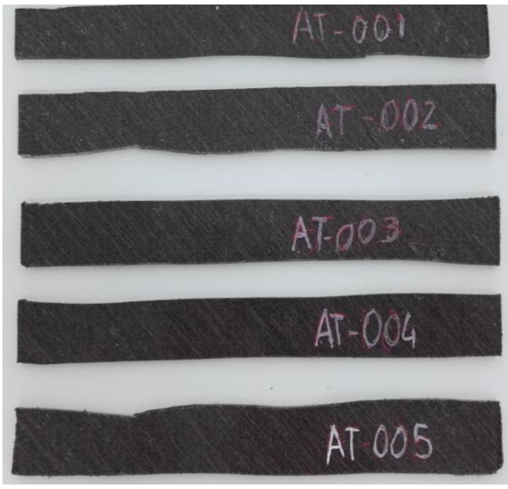

Figure 69 Initial state of specimen reference AT

Table 19 Tensile testing specifications

Specimen Characteristics		Test Parameters	
Material	*Flax/Elium Composite*	**Test velocity [mm/min]**	*1.00*
Specimen geometry	*Rectangular*	**Wedge distance [mm]**	*150*
Test condition	*24 °C*	**Gauge length [mm]**	*25*
Test Standard	*ASTM D3039*	**Test Equipment**	*The servo-hydraulic 100 kN load cell*

Figure 70 Tensile testing

Two different sets of samples are prepared and measured to perform the test. The testing conditions and parameters are given in Table 19. The test results are tabulated in Table 20 and Table 21. The samples after the testing are shown in Figure 72 and Figure 74.

Table 20 Results for specimen AT

Specimen No.	Area [mm²]		Modulus of elasticity (E) [GPa]	Poisson Coefficient
AT 003	W=27.38 / T=4.370	119.65	4.39	0.56
AT 004	W=25.26 / T=4.6	116.20	4.20	0.56
AT 005	W=28.41 / T=4.271	121.31	4.69	0.55
AT 006	W=30.07 / T=4.6	138.32	4.13	0.58
Average			***4.35 ± 0.22***	***0.56***

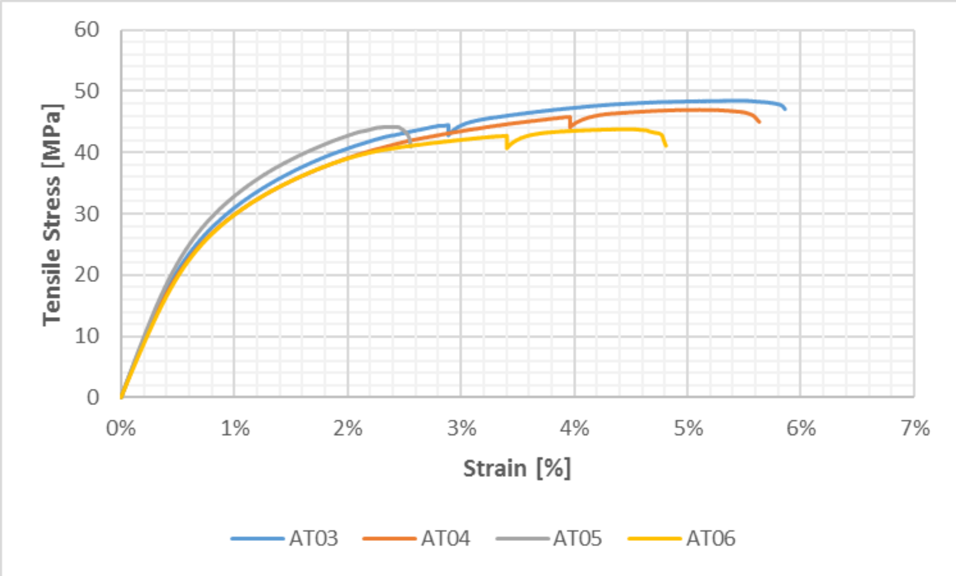

Figure 71 Stress strain graph for specimen AT

The stress drop presented in results graphs was induced by a necessary pause of the test while the bi-axial extensometer was removed.

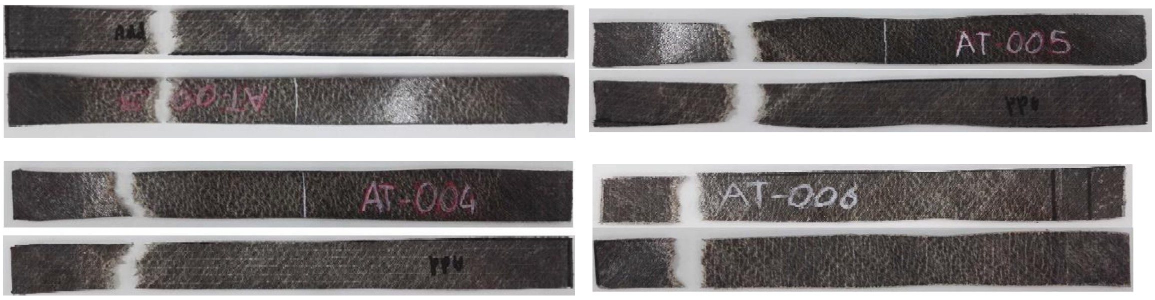

Figure 72 Specimen AT after testing

Table 21 Results for specimen T

Specimen No.	Area [mm²]		Modulus of elasticity (E) [GPa]	Poisson Coefficient
T 001	W=27.16 / T=4.66	126.57	4.03	0.54
T 002	W=27.48 / T=4.33	118.99	4.11	0.53
T 003	W=27.27 / T=4.720	128.71	3.76	0.55
T 005	W=27.31 / T=4.420	120.71	3.90	0.53
Average			**3.95 ± 0.13**	**0.54**

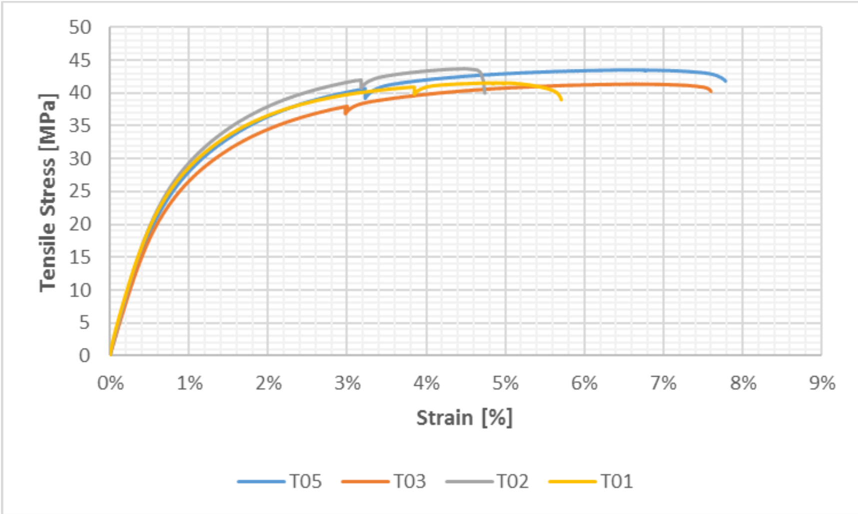

Figure 73 Stress strain graph for specimen T

The stress drop presented in results graphs was induced by a necessary pause of the test while the bi-axial extensometer was removed.

Figure 74 Specimen T after testing

From the tensile testing, it is clear that the additive influences the strength of the specimen. The E of the average specimen 'AT' is 4.35 GPa whereas the E of sample T is around 3.95 GPa which is a marginal difference. Thus, the 'TSP' plays an important role in this composite's strength. The added additive helped in enhancing the strength of the composite remarkably by ***10%***. The tensile curves for individual specimens with Rp0.2 offset can be seen in Annex 6.2.2.

3.6.1.2 Software simulated tensile test

The tensile test was also simulated in HyperMesh/Radioss to compare with the experimental value and the value which was obtained from the micromechanics calculation. A specimen size of 250 x 25 x 5 mm^3 was designed in CATIA V5 software (Figure 75) and imported into HyperMesh and solved by Radioss.

The imported 3D model is converted into the 2D surface to perform the analysis. The model meshes with the size of 10 mm (Figure 76) and the material for the specimen is created using the *M25_COMPSH* an orthotropic material card and the property is assigned using the

P10_SH_COMP card. The load and boundary conditions have been applied by creating the 1D rigid element on both ends of the specimen, respectively (Figure 76). The fixed end is constrained in all 6 DOF's. The velocity of 2 mm/min was applied on the other end by imposed velocity load card.

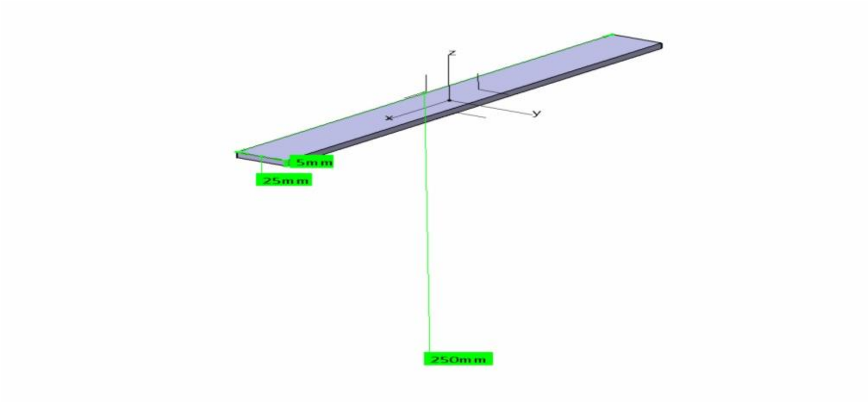

Figure 75 Tensile Simulation Specimen

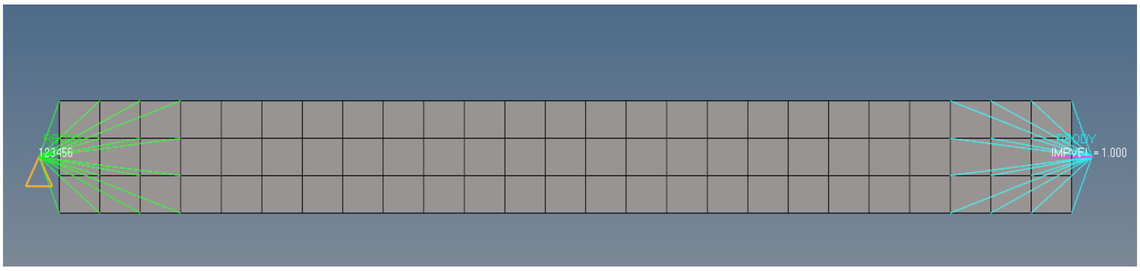

Figure 76 Finite element modeling of tensile test

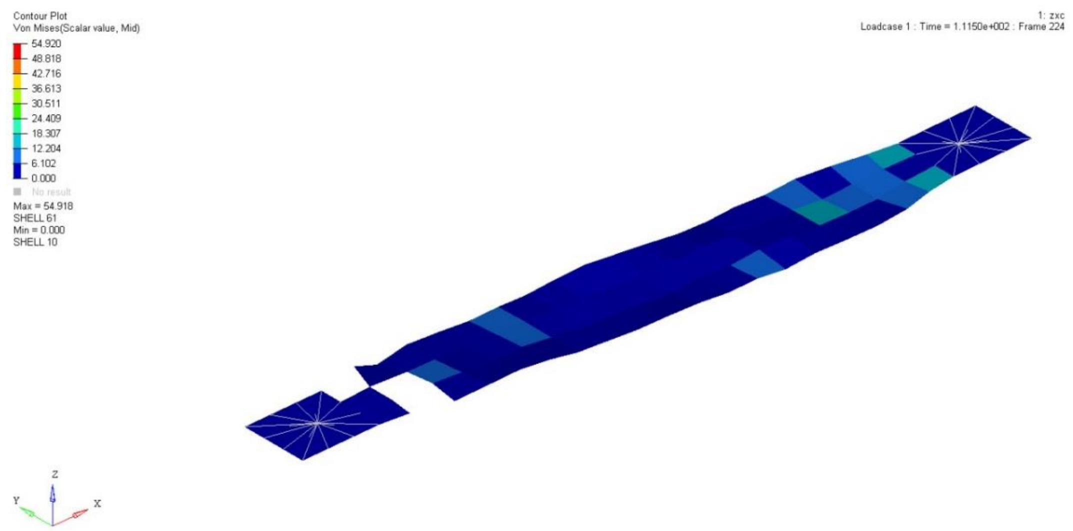

Figure 77 Fracture view of the tensile simulation

The sample reached the ultimate stress of 54.92 MPa which can be seen in Figure 77. The obtained stress value is similar to the stress obtained from mechanical testing. The values of the stress-strain are then exported to an excel sheet to plot stress vs. strain graph. The stress vs strain graph for the numerical simulation is placed along with experimental values which can be seen in Figure 78.

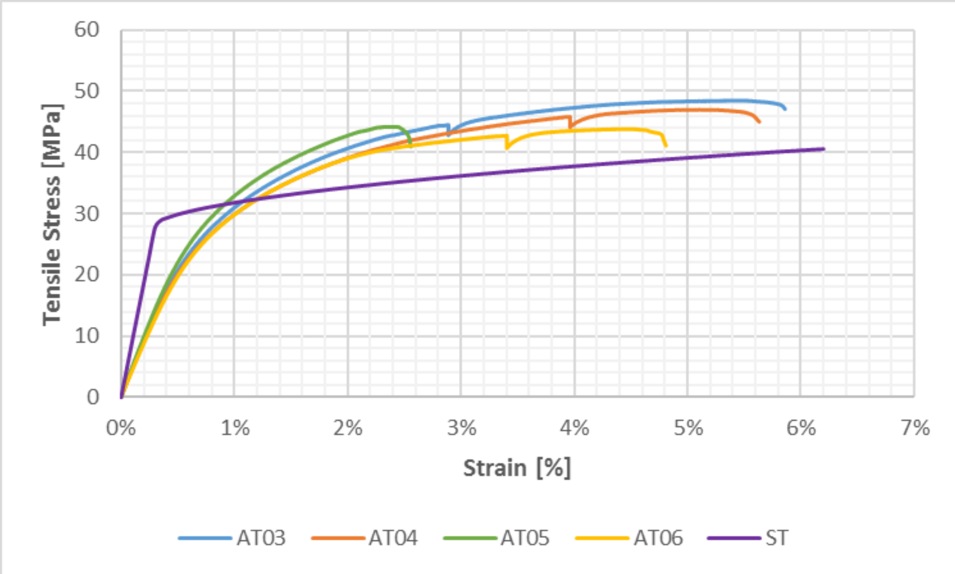

Figure 78 Stress vs. Strain comparison (Experimental vs. Simulation)

ST stands for simulated tensile test

From the numerical simulation, the obtained Young's modulus is around 6.67 GPa. This modulus is similar to the modulus obtained from mechanical testing because the material for the simulation is designed with the theoretical values obtained by the micromechanics calculation.

3.6.2 *Flexural Testing*

The flexural test measures the force needed to bend a beam under *three-point loading* conditions. The data is often used to select materials for parts that will support loads without flexing. Flexural modulus is used as a sign of a material's stiffness when flexed. Since the physical properties of many materials (especially thermoplastics) can vary depending on the ambient temperature, it is sometimes proper to test materials at temperatures that simulate the intended end use environment. Most commonly the specimen lies on a support span, and the load is applied to the center by the loading nose producing three-point bending at a specified rate.

The parameters for this test are the support span and the speed of the loading. Flexural strength, also known as modulus of rupture, bend strength, or fracture strength a mechanical parameter for brittle material, is defined as a material's ability to resist deformation under load. The transverse bending test is most often employed, in which a specimen having either a circular or rectangular cross-section is bent until fracture or yielding using a three-point flexural test technique [124]. The flexural strength stands for the highest stress experienced within the material at its moment of rupture. The general flexural stress equation can be seen in Equation 3.20.

$$\sigma_f = \frac{3FL}{2bh^2} \qquad 3.20$$

σ_f=flexural stress in megapascal, F=force applied in newton, L=span in mm, b=width of the specimen in mm, h=thickness of the specimen in mm and d=deflection in mm.

There is no expression for flexural strain, but a method for calculating the flexural modulus is given in Equation 3.21. This is the ratio of flexural stress to flexural strain in the material and is found from [122].

$$E_f = \frac{FL^3}{48Id} \qquad 3.21$$

E_f=modulus in megapascal, L=span between the supports in mm, b=width of the specimen in mm, h=thickness of the specimen, in mm, F=force, in newton and d=deflection in mm.

The short-beam strength equation from [125] can be seen in Equation 3.22.

$$Beam\ shear\ strength = \frac{3P_m}{2bh} \qquad 3.22$$

P_m – maximum load, applied in N, b=width of the specimen in mm, h=thickness of the specimen in mm

3.6.2.1 Mechanical bending test

To analyze the short-beam strength and failure mode of this natural fiber composite, short beam test is conducted as per the ASTM standard D2344 40 x 12 x 5 mm^3 [125]. Short Beam Shear is used to define the interlaminar shear strength of parallel fibers. It applies to all types of parallel fiber reinforced plastics and composites. For each composite plate of A and AB characteristic, five specimens were cut. Some specimens were used to adjust the equipment, and these preliminary results were not considered in the final report.

Specimens presented a very irregular geometry (general dimensions and thickness) and had to be measured at its initial state. The same span was used (17,7 mm) to compare the properties of two different set of specimens, and the tests were performed at CEIIA Test Lab facilities. The specimen references are:

- A (A002, A003, A004, A005);
- AB (AB002, AB003, AB004, AB005)

AB is the samples manufactured with additives, and A samples are without additives.

The short beam bending is illustrated in Figure 79 and the test parameters are given in Table 22.

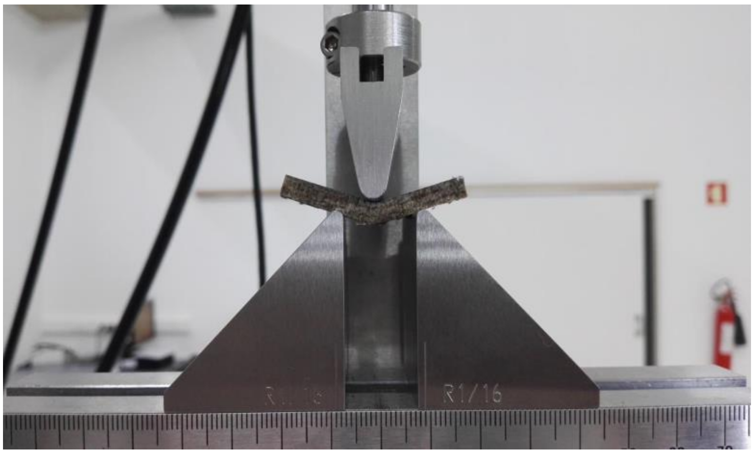

Figure 79 Short-Beam Bending test

Table 22 Bending test specification

Specimen Characteristics		Test Parameters	
Material	*Flax/Elium Composite*	**Test Velocity[mm/min]**	*1.00*
Specimen Geometry	*Rectangular*	**Span[mm]**	*17.70*
Test Condition	*24 °C*		
Test Standard	*ASTM D2344*	**Test Equipment**	*The servo-hydraulic 100 kN load cell*

The short-beam strength is calculated using Equation 3.22 which can be seen in Table 23, Table 24 and in Figure 80 and Figure 83. The detailed calculation of beam strength can be seen in Annex 6.2.2.

Table 23 Results for specimen A

Specimen No.	Maximum Load [N]	Maximum Displacement [mm]	Beam strength [MPa]	Failure mode
A 003	1456.89	2.72	19.37	***Flexure Tension / Interlaminar Shear***
A 004	1573.15	1.87	20.92	***Flexure Tension / Interlaminar Shear***
A 005	1460.40	2.11	19.42	***Flexure Tension / Interlaminar Shear***
Average	**1496.81**	***2.23***	**19.90 ± 0.76**	

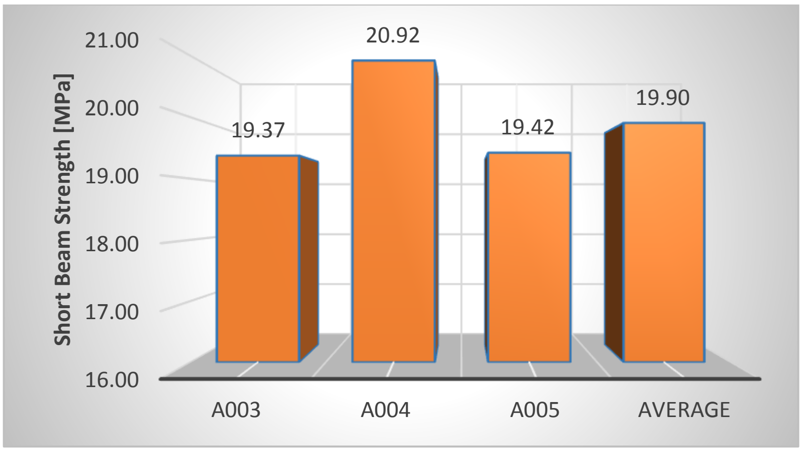

Figure 80 Beam strength for specimen A

Figure 81 Failure mode view of specimen A

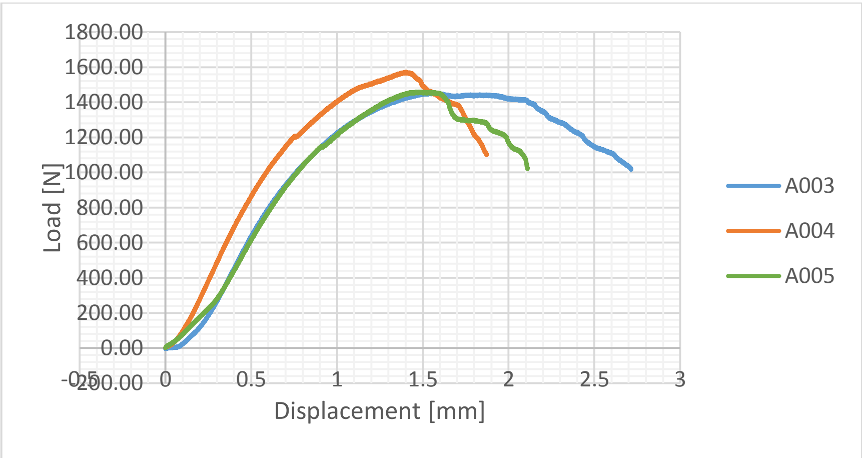

Figure 82 Load vs. Displacement curve (Specimen A)

The failure mode view of specimen A and AB can be seen in Figure 81 and Figure 84 respectively.

Table 24 Results for Specimens AB

Specimen No.	Maximum Load [N]	Maximum Displacement [mm]	Beam strength [MPa]	Failure mode
AB 002	1520.80	1.83	21.12	***Flexure Tension Failure/ Interlaminar Shear***
AB 003	1595.22	1.79	22.16	***Flexure Tension Failure/ Interlaminar Shear***
AB 004	1714.82	1.90	23.82	***Flexure Tension Failure/ Interlaminar Shear***
AB 005	1297.39	2.28	18.02	***Flexure Tension Failure/ Interlaminar Shear***
Average	**1532.06**	***1.95***	**21.28 ± 0.68**	

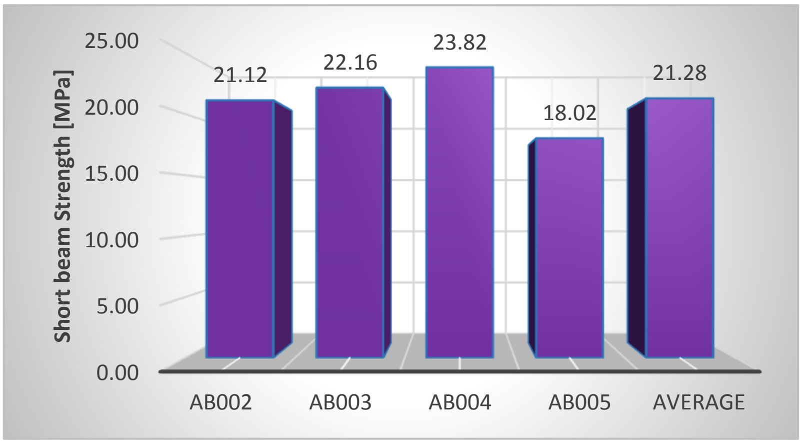

Figure 83 Beam strength for specimen AB

Figure 84 Failure mode view of specimen AB

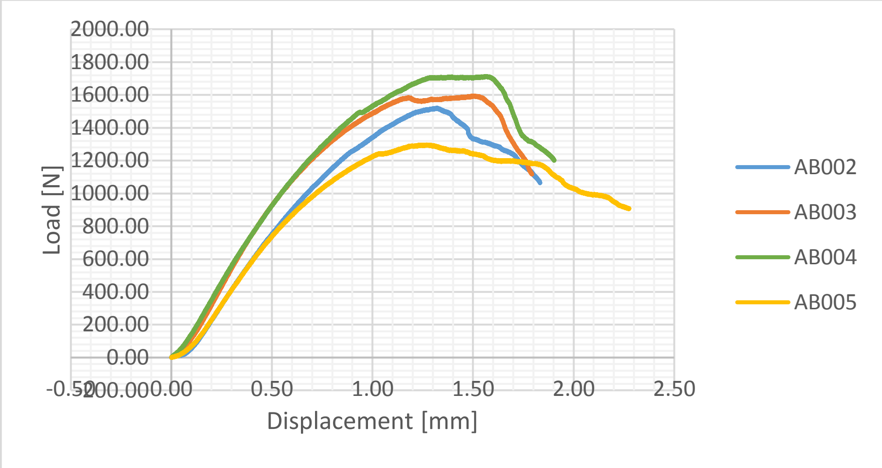

Figure 85 Load vs. Displacement Curve (Specimen AB)

The standard mode of failure seen in this composite with the short beam testing method is an Interlaminar shear failure.

Regarding the comparison in terms of strength between two different specimen's A and AB, the average strength of the specimen AB (specimens with additives) is higher than that of the specimen A, which shows that the natural additive added to the composite helped in increasing the strength of the composite part. The average shear strength of A series is ***19.90 MPa*** whereas for specimen series AB it is ***21.28 MPa***. The bending strength is enhanced up to **7%** by the addition of the additives. Further proper studies on the composite and the additive will help in improving its characteristics for future development.

3.6.3 *Impact test/Drop test*

3.6.3.1 Mechanical drop test

The impact test is performed to figure out the energy absorbed/energy needed to fracture a unit under test (UUT) or to describe the infliction impact damage of the specimen for the applied energy. Under controlled laboratory conditions, impact test may be used to validate designs on prototype or OEM components to ensure they meet product durability and safety requirements. Several safety-critical components, such as automotive bumpers, protective sports equipment, and head form impact testing for hard hats or helmets must meet various SAE, MIL, ANSI or ASTM test specifications.

The test is performed on a rectangular specimen(Figure 87) with the dimension 155 x 178 x 4 mm^3 at CEIIA test equipment (Figure 86) (the zone where the plate was fixed) was adopted.

Figure 86 Drop-Height impact test machine

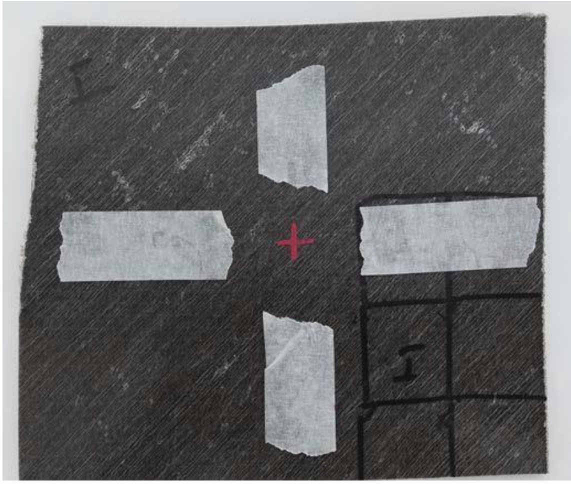

Figure 87 Centre marking for striking

To achieve a single shot in the center of the specimen, the initial position was marked. The testing machine has a mechanism which limits the striker to strike only once. There will not be any rebound from the impact. The test specification can be seen in Table 25.

Table 25 Impact test specification

Energy [J]	Striker diameter [mm]	Total mass [kg]	Drop Height [mm]
60.0 ± 1.50	25.4	15.0 ± 0.10	410 ± 3.00

The energy is calculated by considering the head impact on a bonnet. According to NCAP during accidents the head is impacted on the bonnet at a velocity of 40-60 km/h, and the average diameter of the human head is 152,4 mm (6 inches), and the energy will be around 236 J. Since the diameter of the impactor used here is 25.4 mm, which is 4-6 times different from the actual head diameter, the energy of the impactor is reduced to $1/4^{th}$ of the original energy.

In the case of head impact test, the surface area of the impactor is large, and the energy is absorbed over the surface. In this case, the surface area of the impactor is comparatively small to the head, and such high energy on a small surface area will result in more significant damage, and it could easily penetrate the specimen. With all these considerations kept in mind, the energy of the impact is reduced.

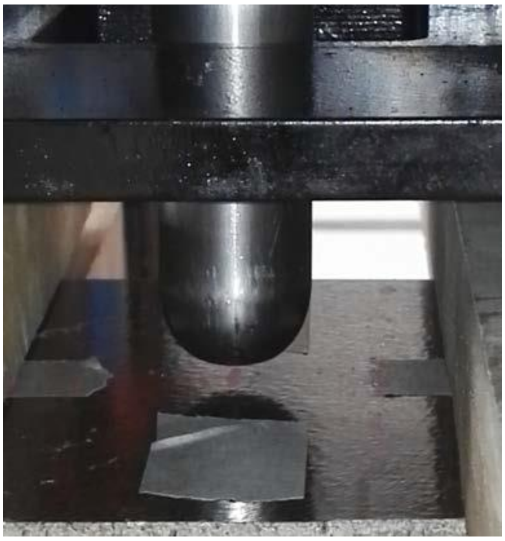

Figure 88 Striker positioning

The striker strikes at the velocity of 10 km/h and the time to impact from 0.4 meters is 145 milliseconds. After the impact, the damage infliction was visible in an area of 70 x 60 mm^2, and the indentation caused by the impact is equal to 2.17 mm.

Figure 89 Impact indentation measurement

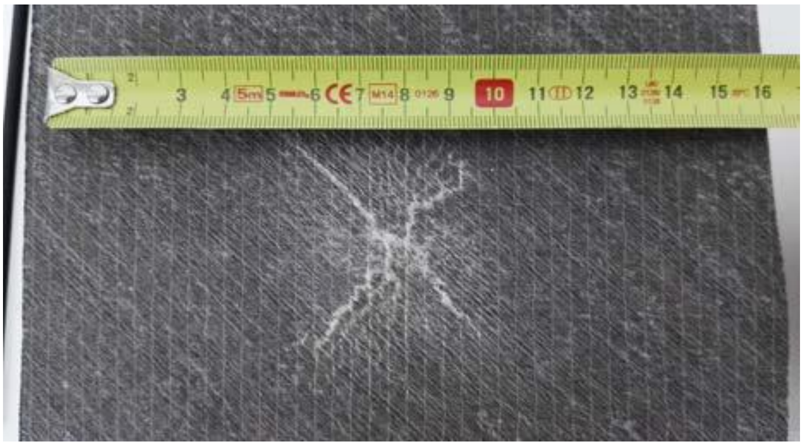

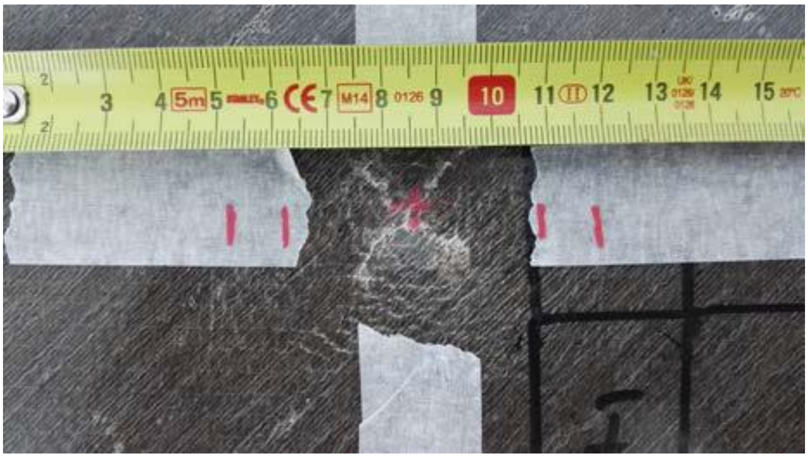

Figure 90 Visible damaged area after impact

From the test, one can see only the damage visible to the human eye. To study the damage inside the laminate at a microscopic level, the sample must be viewed under a Scanning Electron Microscope.

3.6.3.2 Software simulated test

The drop test is designed in HyperWorks and solved using Radioss solver. Composite modeling is a complicated process in most of the numerical analysis solver. In Hyperworks/Radioss interface, the composite is modeled using MAT/LAW25 (COMPSH) card to create the material, and PROP/TYPE 10 property card is used to define the orthotropic shell for the material. The simulation parameters can be seen in Table 26.

Table 26 Drop test parameters

Specification	
Specimen element type	Shell elements-Size 10 quad elements
Impactor element type	Rigid element
Boundary conditions	Plate - Fixed in all DOF's at its boundary
	Rigid is fixed in % DOF's except T_Z at Node 1
Contact type	Type 7 contact with a friction coefficient of 0.2
Min gap between striker and plate	1 mm
Load type	IMPVEL (Imposed Velocity) at Node 1

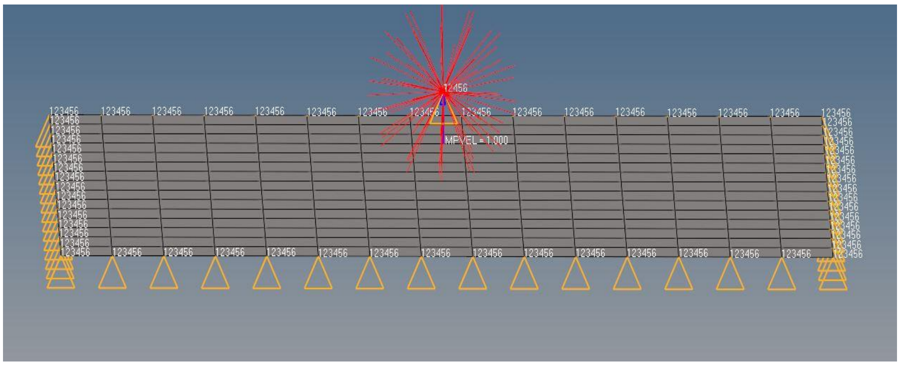

Figure 91 Drop test design in Hyperworks

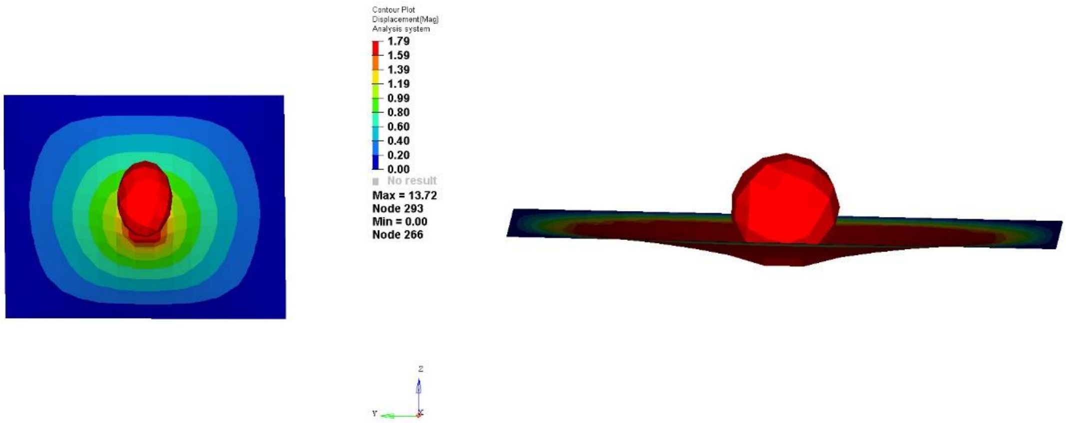

Figure 92 Impact indentation

The indentation created here is about 1.8 mm (Figure 92) approximately, and the value which is obtained during physical tests is 2 mm. The affected visible area is more or less equal to the physical test.

3.6.4 *Moisture absorption Test*

Moisture Absorption of Matrix Composites (ASTM D5229) is a gravimetric test method that checks change over time of moisture content by measuring the total mass change of a coupon that is exposed to a specified environment [126]. The composite is subjected to extreme condition testing compared to its intended application in this case. The specimens are placed in an atmosphere of 85°C at 90% humidity over a period of 120 hours. The coupons are weighted to know the initial weight, and then for every 24 hours, to figure out the absorbed moisture content. The average change in mass is seen which is necessary to conclude the absorbed mass in total.

Two sets of samples were tested. One is the samples with additives, and one is without additives. The test is conducted in the testing laboratory of CEiiA. The mass loss and the average effective moisture equilibrium is calculated by using Equation 3.23 and Equation 3.24:

$$Mass\ lost, \% = \frac{W_{ab} - W_p}{W_{ab}} * 100 \quad 3.23$$

$$EWE = |M_i - M_{i-1}| < 0.020\ \% \quad 3.24$$

W_{eb} - Initial weight, W_p-Present weight, M- Average Moisture content

i- Value at the current time, i-1 = Value at a previous time, EWE- Effective moisture equilibrium change

Table 27 Moisture absorption for AW sample

Specimens	Days	Average mass Absorption (%)	Average Effective Moisture Content (%)	Abs. Effective Moisture Equilibrium Change (%)
AW	0	0.0000	0.0000	0.0000
	1	1.4432	1.4432	1.4432
	2	0.2722	-1.1710	1.1710
	3	0.0474	-0.2247	0.2247
	4	0.0293	-0.0181	0.0181

From Table 27, the moisture absorbed on day one is marginally high, and on further days the coupons started losing the mass, as can be understood from Figure 93.

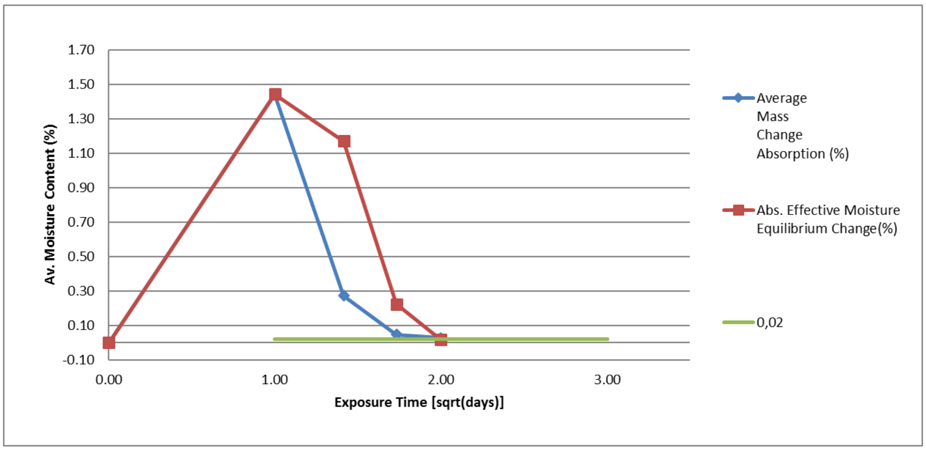

Figure 93 Moisture absorption for AW samples

The moisture absorption and equilibrium change for ‘W’ samples are given in Table 28 and in Figure 94.

Table 28 Moisture absorption for W samples

Specimens	Days	Average mass Absorption (%)	Average Effective Moisture Content (%)	Abs. Effective Moisture Equilibrium Change (%)
W	0	0.0000	0.0000	0.0000
	1	1.3398	1.3398	1.3398
	2	0.0849	-1.2549	1.2549
	3	0.0596	-0.0253	0.0253
	4	-0.0601	-0.1197	0.1197

As it can be seen in Table 28, the adsorption equilibrium is high during the first 24 hours, gaining mass and started losing the mass for the next consecutive hours, which implies that, like any other natural fiber, flax also absorbs moisture to its weight.

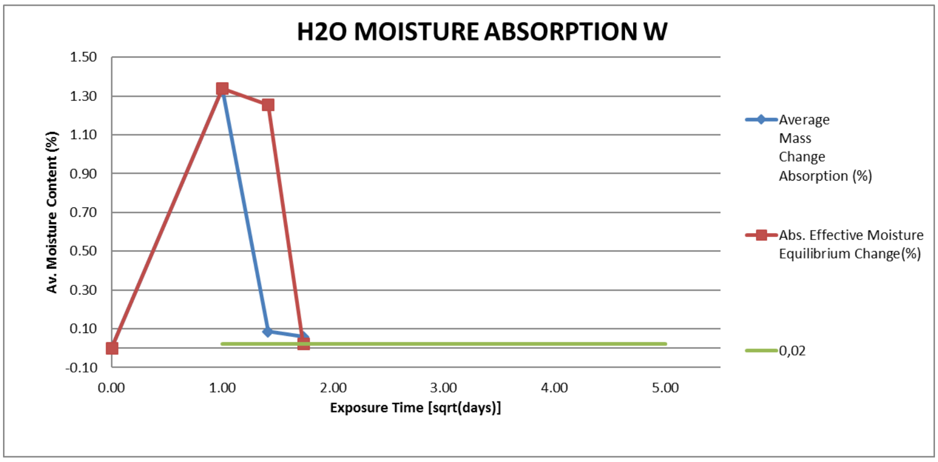

Figure 94 Moisture absorption for W samples

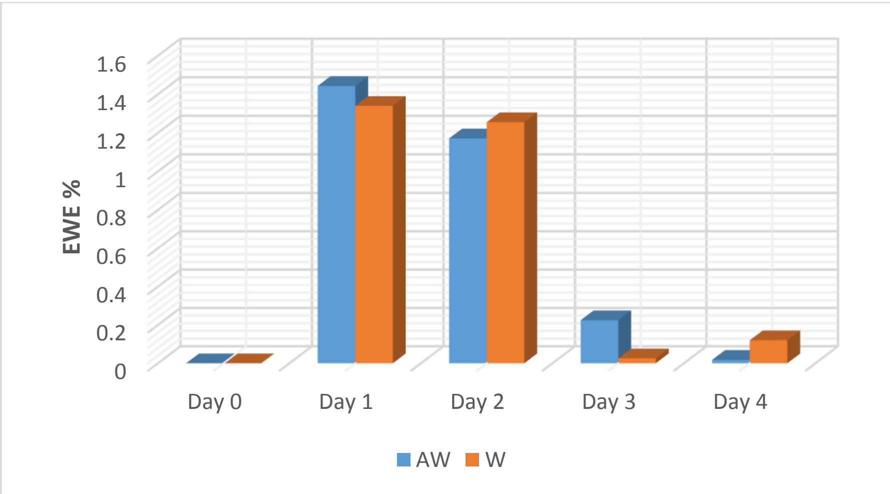

Figure 95 EWE comparison

From Figure 95 it can be seen that the coupons AW with additives absorb more moisture and loses less weight compared to the W coupons without additives. Since the TSP additive is a natural extract by nature itself, it tends to absorb moisture. This tendency also must be considered while designing a part using this composite. Moisture absorption is an essential factor which is inversely proportional to the mechanical properties of natural fiber composites, because if the composite absorbs more moisture the strength is decreased.

3.6.5 *Head Impact Test*

The head impact test is numerically simulated in Hyperworks/Radioss with the corresponding mechanical properties obtained in previous topics. The head injury criteria (HIC) is a variable calculated from head impact test using Equation 3.1, and it is a measure of the likelihood of head injury arising during impact. Based on the guidelines from [127] head injury risk is evaluated based on HIC. A value of 700 is a marginally acceptable value among the automobile sector. At HIC of 1000, there is 18 %probability of severe head injury, 55% probability of severe injury and 90% chance of moderate head injury. Lower the HIC, lesser is the risk of getting injured badly. The index 2.5 is chosen for the head, based on experiments [128].

$$HIC = \left[\frac{1}{T_2 - T_1}\int_{T_1}^{T_2} A_v dt\right]^{2.5} (T2 - T1) \qquad \textbf{3.25}$$

$$HIC = [A]^{2.5}(T2 - T1) \qquad \textbf{3.26}$$

Av-resultant acceleration m/s^2, A-Average value of acceleration at over the time interval T1 to T2.

T1 and T2: two times instants (in Milliseconds), which define the beginning and end of the recording when HIC is at maximum.

The time interval T2-T1 is limited to a maximum value of 36 ms but usually, 15 ms is used in common, since the interval is inversely proportional to HIC. 15 ms is to indicate the worst-case scenario. In general, the HIC is termed as HIC 15 showing that it is calculated for 15 ms.

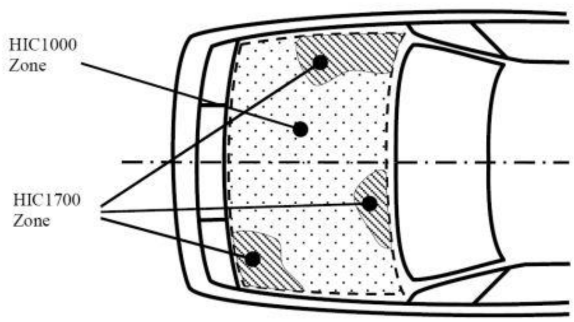

Figure 96 HIC zones [129]

According to [129], the HIC values for various zones are defined (Figure 96). The zones which are reinforced or the zones which are supported by other parts will have high acceptance value. In this study, the simulations are done only for adult head impacts. The head-shaped impactor is modeled in HyperWorks with the material properties of a human bone [130]. The acceleration and the energy absorbed is extracted from RADIOSS output file with an accelerometer sensor.

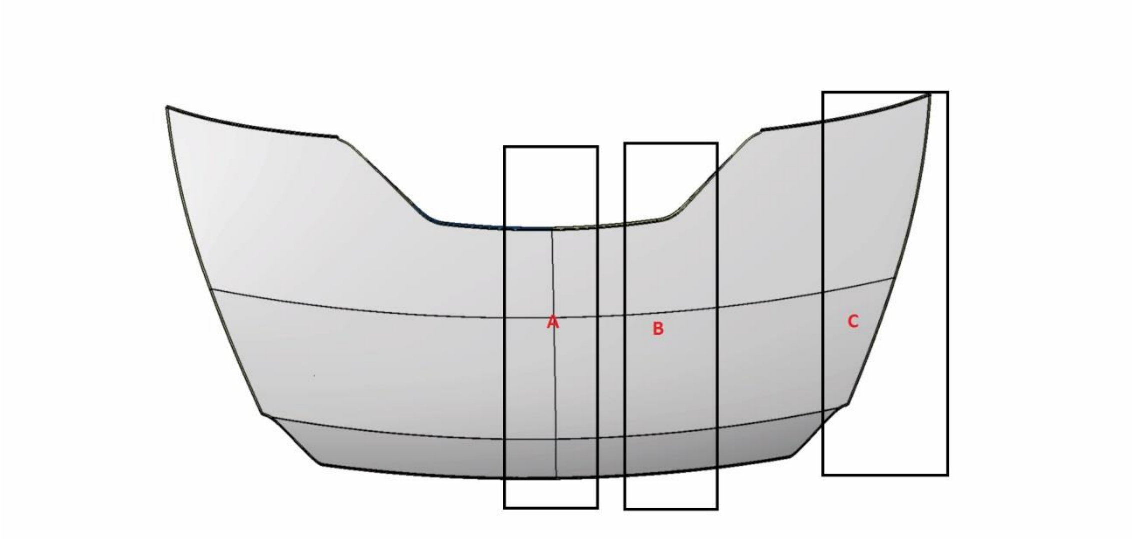

Figure 97 Head Impact Test location

A- Middle of the bonnet geometry which is supported by the frame, B- Just bonnet surface, C- Bonnet is supported by the frame and is rested over the fenders.

The impact is simulated on three different regions on the bonnet surface as shown in Figure 97. The simulation parameters are listed in Table 29.

Table 29 Head Impact Simulation Parameters

Part	Material	Property	Mesh type	Constraints
Bonnet	M25_COMPSH	P9_SH_ORTH	SHELL3N/SHELL4N	Glued with reinforcement
Reinforcement	M2_PLAS_JOHNS_ZERIL	P1-SHELL	SHELL3N/SHELL4N	Fixed in 6DOF's and Glued with Bonnet
Head	M2_PLAS_JOHNS_ZERIL	P1-SHELL	SHELL3N/SHELL4N	Constrained in All DOF'S except Z T_Z
Accelerometer sensor			1D-RBE3	Connected to Head part nodes
Adhesive	M59 Connect	P43_connect	HEXA8N	Connector

RBE3 Element is not a rigid element. The motion at the ‘dependent’ node is a weighted average of the motion at the ‘independent’ nodes. Thus, they are used in place of sensors and other load transmitting places. The modeling of the bonnet analysis system is shown below.

A mass of 5.5 kg is applied to the subordinate node of the RBE3 element using ‘admas’ card. *A velocity of 11.12 mm/ms* (40 km/h) was applied to the head elements. The test is run for 15 ms, and the results were exported to HyperView for post-processing.

Fixing the reinforcement section

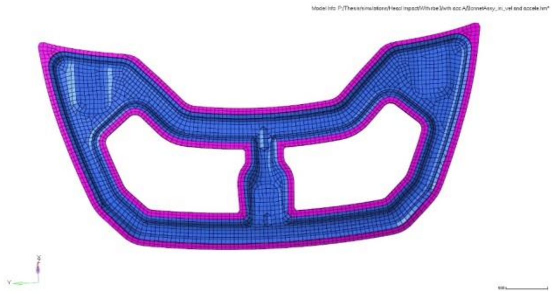

An adhesive which binds bonnet and the reinforcement

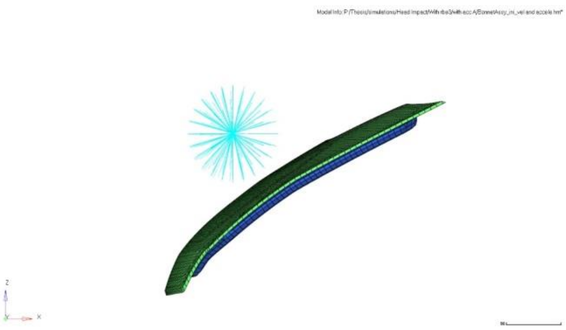

Sensor modeling

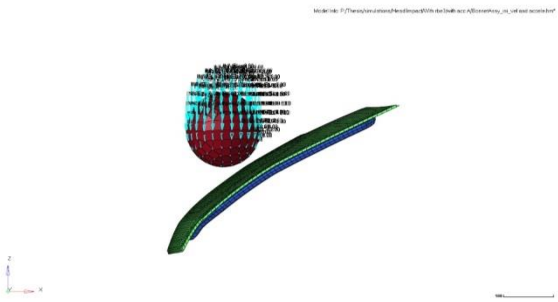

Applied Velocity for the head mass

Figure 98 Head impact numerical model

3.6.5.1 HIC at Zone A

In position A (Figure 99), the allowable HIC is 1000. Here the attained acceleration was converted into “A” according to Equation 3.26 using a script file for HyperWorks/Radioss developed by Centre for Automotive Safety Research - The University of Adelaide. This script helps in extracting the results of A at every individual time steps. The ‘A’ value obtained at zone *A* is 53,54.

Head positioning at A region

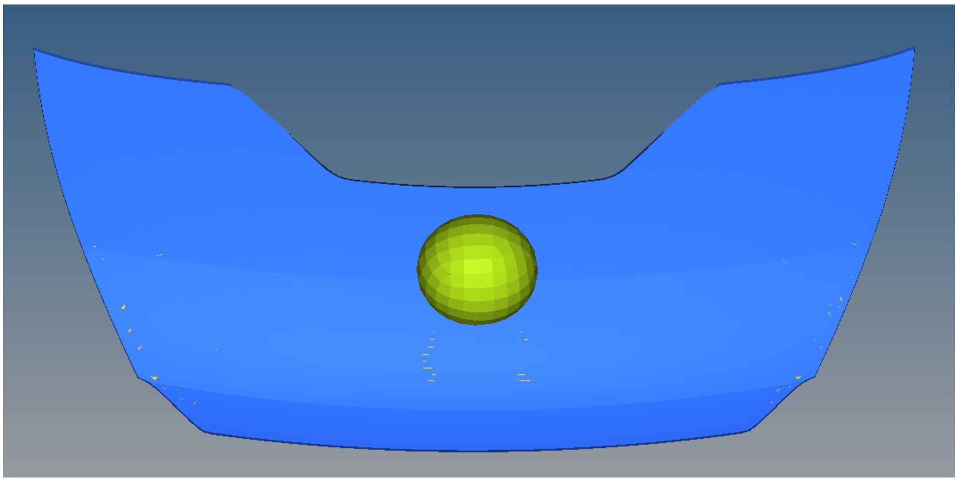

Acceleration reached in position A

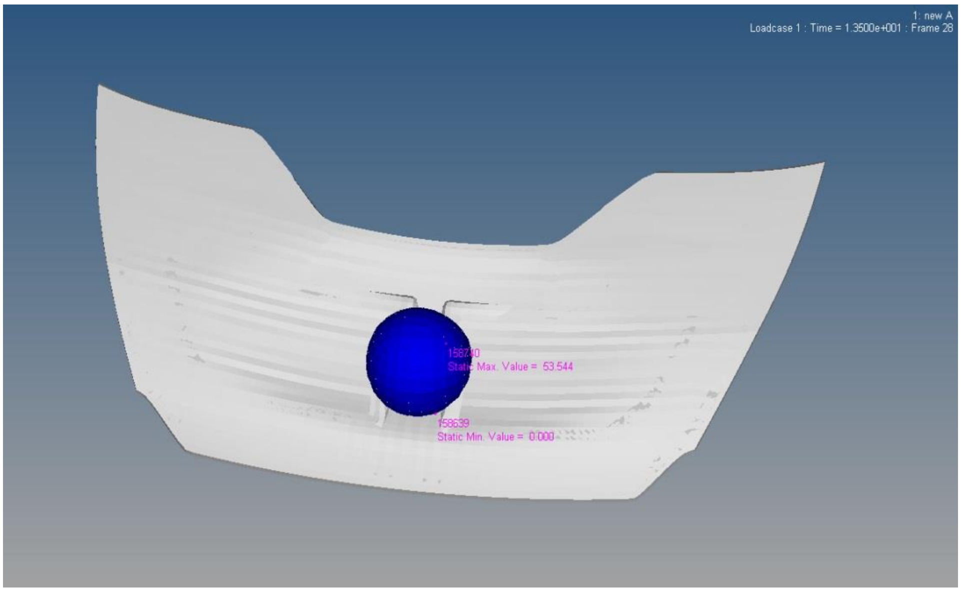

Figure 99 Head impact at zone A

$$HIC_{15(A)} = \{[53.54]^{2.5}(0.015)\} = \ 314{,}62$$

The calculated HIC_{15} at zone A is 314,62. Even though the HyperWorks script calculated the A, the HIC is calculated manually in Annex 6.2.4 using Equation 3.25.

3.6.5.2 HIC at Zone B

Zone B (Figure 100) is critical since there is no support or any reinforced metallic parts. This part of the bonnet is entirely designed using composites and has less resistance to impact force, thus offering higher deformation. The ‘A’ value obtained at zone B is 52,026.

Head Positioning at B region

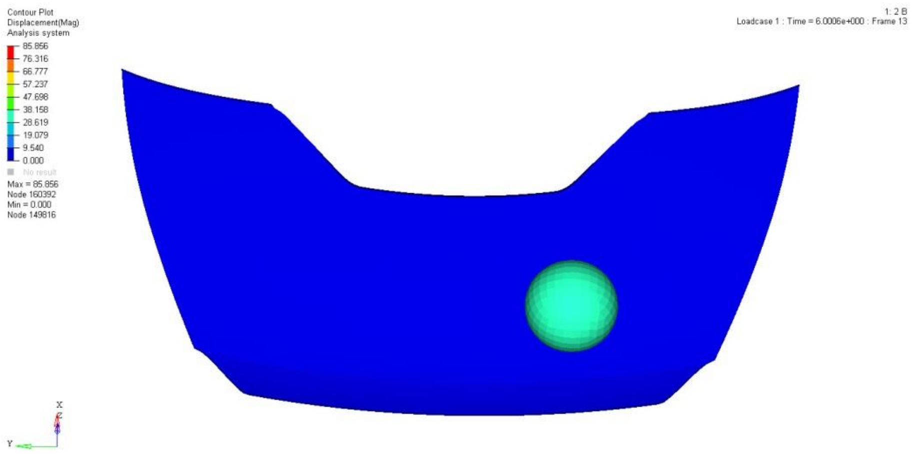

Acceleration reached in position B

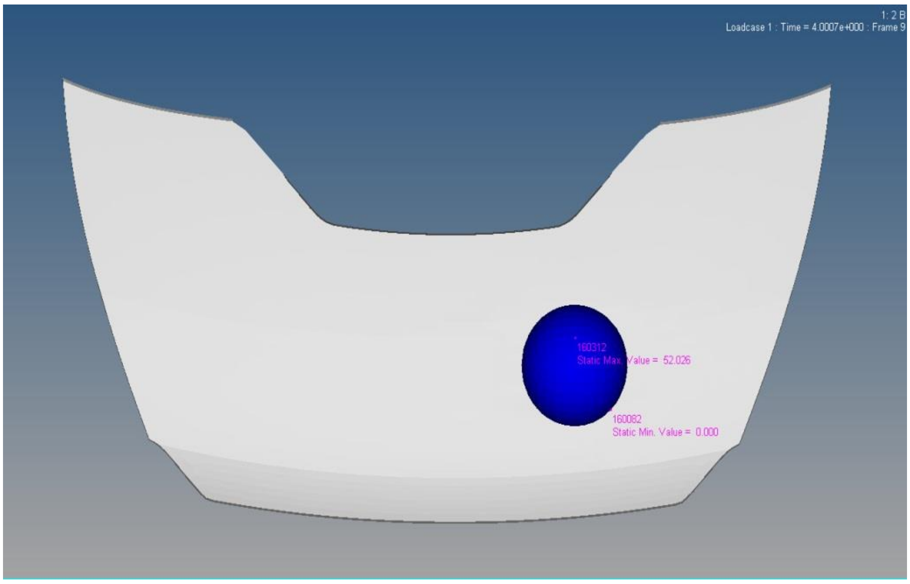

Figure 100 Head impact at Zone B

$$HIC_{15(B)} = \{[52.026]^{2.5}(0.015)\} = 292,84$$

The calculated HIC_{15} at zone A is 292,84.

3.6.5.3 HIC at Zone C

The zone C (Figure 101) is the zone where fender supports the bonnet. The HIC calculated in this zone is known as Relaxation HIC, whereas in other zones it is called normal HIC. In these zones, the HIC limit is set to 1700. The ‘A’ value obtained at zone C is 78,008.

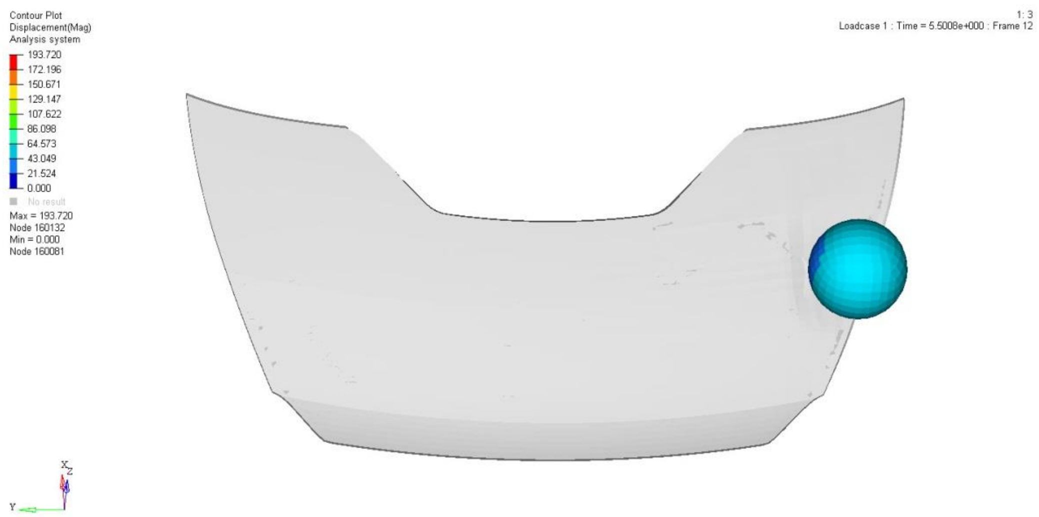

Head positioning at C region

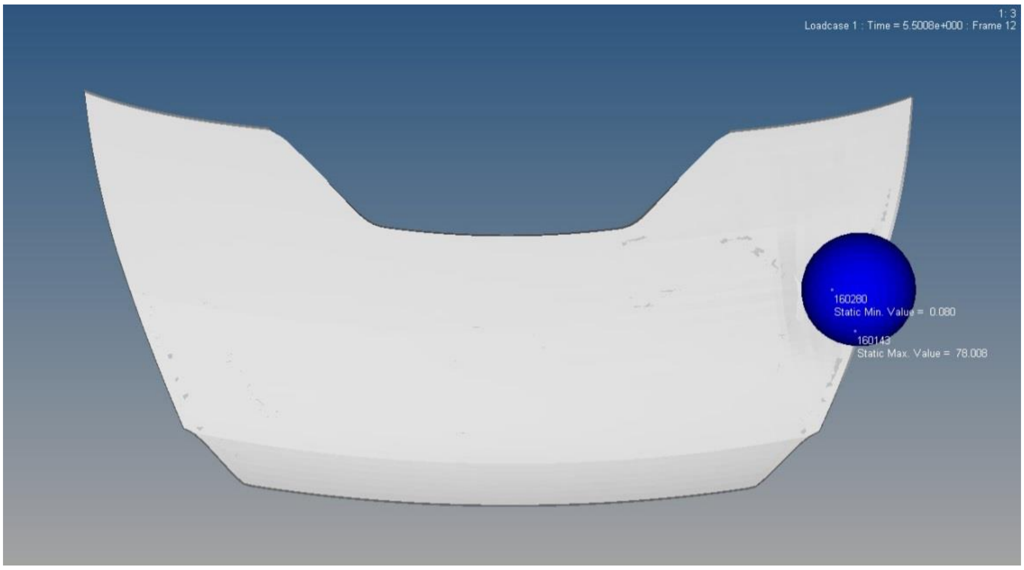

Acceleration reached in position C

Figure 101 Head Impact at zone C

$$HIC_{15(C)} = \{[78.008]^{2.5}(0.015)\} = \ 806{,}193$$

The calculated HIC_{15} at zone C is 806,193.

The HIC values calculated at various zones is compared with the allowable at that particular zone can be seen in Table 30.

Table 30 HIC values compared with allowable

Zone	Description	HIC Type	Allowable Value	Simulated Value
A	Over center support	Relaxation	HIC<1700	314,62
B	Just Bonnet section	Normal	HIC<1000	292,84
C	Over fenders	Relaxation	HIC<1700	806,193

The values which are obtained from the simulations are an approximation of the actual head impact tests. These numerical values were compared with the actual Injury Parameter Cutoff Values to predict the severity of the impact and the design considerations.

Table 31 HIC conclusion

Parameter	Good Acceptable	Acceptable Marginal	Marginal Poor	Obtained value	Review
HIC-15 [127]	623 [127]	779 [127]	935 [127]	314.62	The obtained value satisfied the acceptable value by a marginal difference.
				292.84	The obtained value satisfied the acceptable value by a marginal difference.
				806.193	The obtained value lies in a poor marginal scale. To be conservative and avoid fatal injuries redesign must be considered for that zone.

From the Table 31, the bonnet satisfies the HIC-15 criteria in two of three cases, which implies that the bonnet design is safe to use and in case of any accidents there will not be any fatal injury. However, in zone C (relaxation zone) the obtained HIC value is remarkably high. To avoid fatal injuries and to be conservative, redesign or reinforcement is recommended. However, overall, the bonnet satisfies the HIC criteria framed by IIHS [127].

3.6.6 *Car Pole crash test*

The front-end pole crash test is performed to analyze chest injury criteria for the passengers during the damage caused to the parts such as the bonnet, fenders, and bumper, during crash over a pole, a street lamp post or a tree. According to EURONCAP [128], the vehicle is made to crash on a rigid pole at 60 km/h. Here the simulation is done to analyze the damage caused just for the bonnet section.

For this study, a simple car model is created and used for the analysis. The windshield and the side glass are designed with a glass material, the tires are modeled with rubber material, the body of the car is modeled with steel, and the bonnet is modeled with flax/Elium composite. The car is made to crash onto a rigid pole at 60 km/h. The bumper of the car is made of steel, which absorbs more energy during the impact and transmits quite less to the significant parts of the car.

Table 32 Pole impact analysis specification

Parts	Material	Material card	Property Card	Mesh type
Windshield	Tempered glass	M2_Plas_Johns_Zeril	P1_SHELL	2D
Tires	Rubber	M2_Plas_Johns_Zeril	P1_SHELL	2D
Bonnet	Flax/Elium composite	M25_COMPSH	P10_SH_COMP	2D
Car Body	Steel	M2_Plas_Johns_Zeril	P1_SHELL	2D
Chassis, and support beams	Steel	M2_Plas_Johns_Zeril	P2_TRUSS	1D

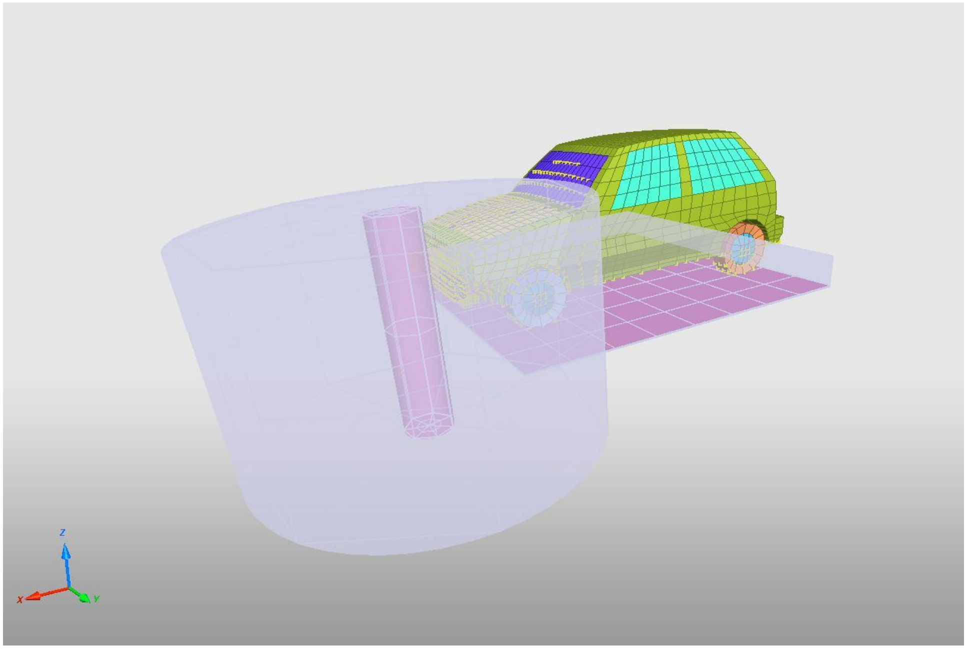

Figure 102 Pole impact modeling

On crashing the car towards a rigid pole, maximum stress occurred on the bonnet is 203.3 MPa, which is comparatively high than the yield strength of the composite, and it will cause *unrepairable damage* on the bonnet. Also, the absorbed energy during impact is exceedingly high proving that the bonnet will fail during the crash.

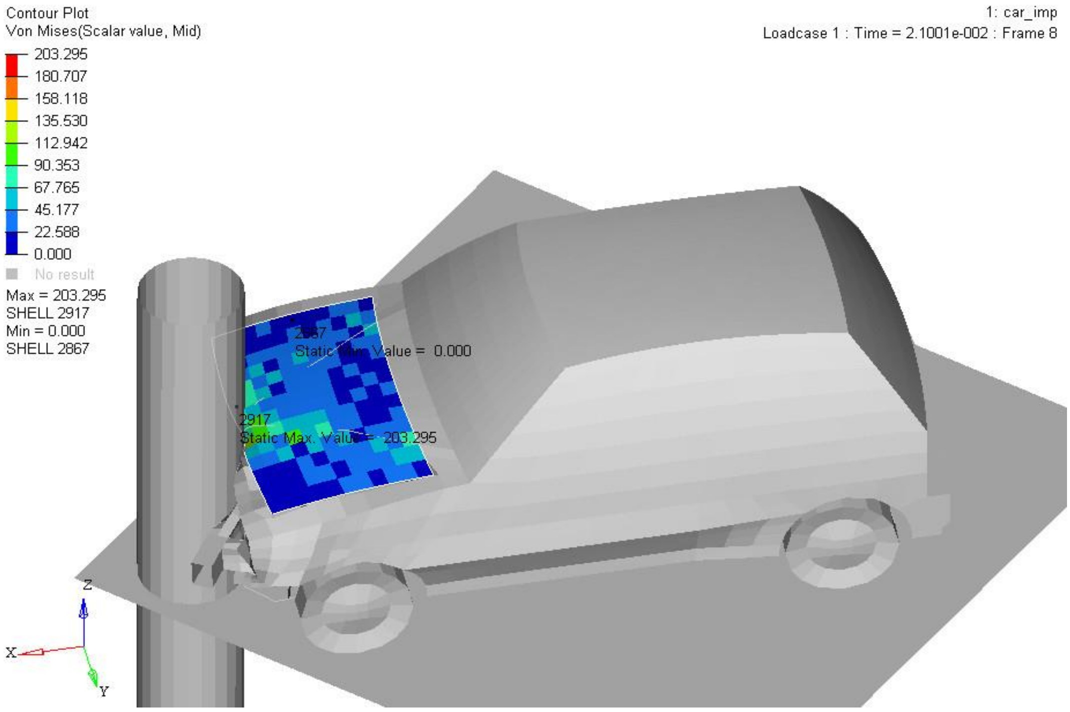

Figure 103 Pole Impact Simulation

3.7 *Recycling of the composite*

Recycling is one of the primary keys to sustainability. This composite is considered as an eco-friendly and sustainable composite because the reinforcement is a natural material and the matrix is a thermoplastic which can be recycled very easily. The recycling of Flax/Elium® is remarkably simple and very efficient. The recycling process of thermoplastics is discussed in Table 7. In this study, only the chemical and mechanical recycling process are considered and done successfully.

3.7.1 *Mechanical recycling*

Mechanical recycling is the conventional way of recycling any product. It is one of the easily understandable and executable processes. There are different methods for mechanical recycling. The method applied in this study was hot-press compression molding. The process can be understood through the following steps:

1. The part which is to be recycled is first ground or shredded (Figure 104) into small pieces. In this study, a leftover specimen is used for the recycling process;

Before Shredding — After shredding

Figure 104 Specimen preparation for molding

2. The shredded specimen is then analyzed visually to ensure the samples are free from any impurities or foreign materials. If so, it is removed and clean;
3. Then, the shredded pieces are mixed with Elium®150/ Perkadox® CH-50X mixture. The mixture weights 15-25% of the shredded part weight to start the recycling process;
4. The mixture is then placed in a mold;

5. The mold is then placed inside the hot plate compression molding machine. The working temperature is 180-220 ^{o}C, and a pressure of 5-20 bar is applied for 3-10 minutes, based on the part thickness.

Figure 105 Oven used in the process

6. Then, it can cool for 60 minutes to room temperature or inside the oven itself.

In this study, since the unavailability of the actual hot-plate compression molding machine, it was replaced by two aluminum plates. Those plates are heated to 180 ^{o}C for 30 minutes inside the oven (Figure 105), then the shredded mixture was placed between those plates, and a load of 50 kg was applied using a solid cast iron block, and the rest of the process was carried out in the usual way.

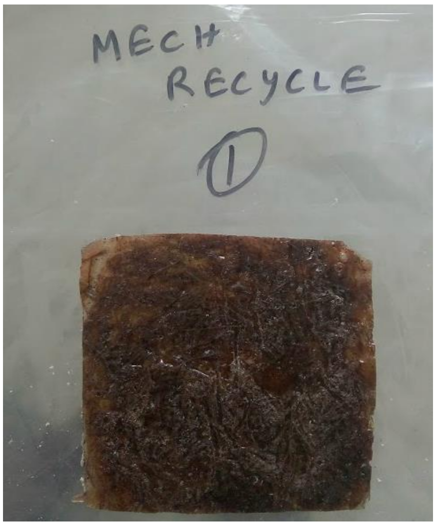

Figure 106 Mechanically recycled specimen

The dimension of the recycled specimen is 106 x 95 x 2 mm^3 (Figure 106). Since the way of manufacturing is entirely different from the conventional hot-press molding, one can see improper curing and lack of surface finish. The proper recycling can be achieved by following the above steps and with proper equipment setup effectively at low cost.

3.7.2 *Depolymerization*

Chemical recycling is one of the primary ways to recycle composites. In chemical recycling, the composite is immersed in a solvent, which dissolute the matrix. According to Yanga et al. [110]. this way of recycling was only done in laboratory studies so far.

Arkema, the manufacturer of Elium®150 liquid thermoplastic resin declared that their resin could be depolymerized using certain solvents, but they never recycled the composite by chemical depolymerization. However, Arkema successfully recycled a composite part by thermal depolymerization and showed it in JEC Composites tradeshow 2017, Paris [89].

In this study, chemical depolymerization is achieved by using a universal solvent based on the idea of chemical depolymerization from Arkema. The solvent used here is Toluene-Methyl Ethyl Ketone (MEK) a general organic solvent, which is used in the surface coating industry in the manufacture of smokeless powder, in colorless synthetic resins and to dissolve paint.

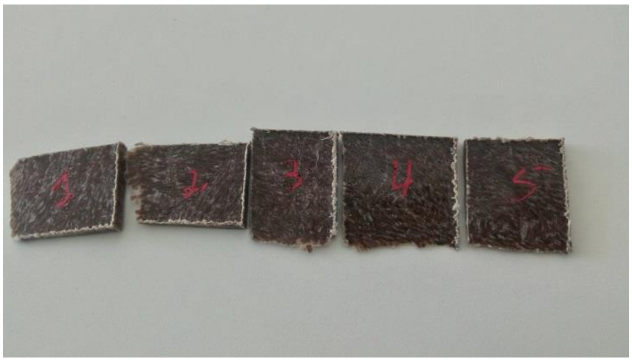

Figure 107 Specimens for Chemical Recycling

The chemical depolymerization is achieved from the following steps:

1) The samples are individually weighed in a weighing machine (Figure 108);

Figure 108 Weighing the samples

2) Then, the five samples are placed inside five measuring containers and pouring 40 g of the Toluene-MEK solution inside each container (Figure 109);
3) The samples are allowed to react with the solvent to achieve depolymerization;
4) The samples are left untouched for 6-10 hours at room temperature;

5) Once the resin is dissolved entirely inside the solvent, the fiber should be, wash with distilled water and dry it;
6) The mixture of solvent and the resin is left untouched more than 12 hours so that the solvent can vaporize and leave the resin behind.

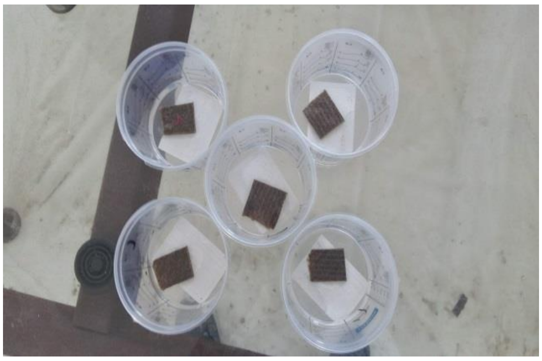

Figure 109 Composite recycling setup

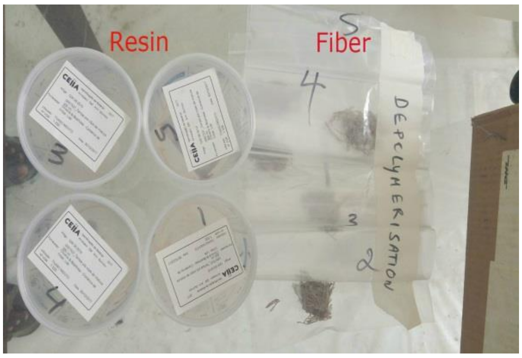

Figure 110 Recycled samples

With the help of solvent, the samples can be successfully recycled (Figure 110), and one can reuse the matrix and the reinforcement for some other application. The solvent is allowed to evaporate, as mentioned earlier, to retain the matrix. Since the solvent is an organic component and volatile in nature exposing is in a high quantity may cause health issues for the workers in the working environment. To overcome this issue, a controlled environment for recycling has to be made. The quality of the resin is related to the viscosity, in this case, calculating the theoretical values by considering a weight fraction of 50%, for comparison. The weight of the samples and the recycled samples can be seen in Table 33.

Table 33 Depolymerization Data

Specimen	Initial Weight	Wt_F Theoretical [g]	Wt_F Practical [g]	Wt_R Theoretical [g]	Wt_R Practical [g]
1	2.8556	1.4278	1.8144	1.4278	1.0412
2	2.8561	1.4280	1.7205	1.4280	1.0356
3	2.9118	1.4559	1.8545	1.4559	1.0573
4	3.3896	1.6948	2.2104	1.6948	1.1792
5	3.1019	1.5509	1.8379	1.5509	1.2640

Wt_F-Weight of fiber, Wt_R-Weight of the resin.

3.7.3 *Eco-impact of the composite*

The energy needed in the production of UK flax fibers and the energy needed for cultivating plant fibers is low (4-15 MJ/kg of processed fiber), the use of agrochemicals and retting processes significantly increase the energy consumption (by 38-110 MJ/kg of processed fiber). An independent analysis by Duigou et al. [131] on French flax fibers, based on a different set of assumptions, gives a similar conclusion. Water retting is found to be the least energy intensive, followed by dew retting and bio-retting. Conversion from fibers to semi-products through textile processes increases the energy consumption further by 2-15 and 26-40 MJ/kg of processed fiber, for slivers and yarns, respectively. The total energy needed is 54-88 MJ/kg for flax sliver and 81-126 MJ/kg for flax yarn. This compares to 55 MJ/kg for E-glass reinforcement mats and 90 MJ/kg for polypropylene fibers [132]. Hence, even regarding minimizing the environmental impact of plant fiber reinforcements, minimal processing is attractive.

Aligned plant fiber preforms have a larger eco-impact than E-glass preforms. It is worth to note that the eco-impact of part end-of-life disposal is not considered here, while landfilling or incinerated the GFRPs the energy is recovered from the resin alone, while in NFRPs the energy recovery from both the plant fibers and the resin. Unsaturated polyester resin has embodied energies of 63-78 MJ/kg [132], while the Elium® has the embodied energy of 41-68 MJ/kg [91].

One can also say that the cost of a product may be a useful indicator of the embodied energy of a product; while raw flax fibers and non-woven mats are low-cost and need low energy for production, aligned plant fiber semi-products are high-cost and need high energy inputs for production. These findings highlight that for structural applications of NFRPs to be projected as environmentally benign alternatives to GFRPs and the development of sustainable processes for the manufacture of aligned plant fiber semi-products are critical steps ahead.

CONCLUSIONS

4 CONCLUSIONS AND PROPOSALS OF FUTURE WORKS

Natural fiber composites have the capability of replacing human-made polymer reinforced composites regarding semi-structural and structural applications. The panoramic goals of this work are to investigate the feasibility and viability of using the eco-friendly and sustainable material for "Be," the autonomous car, to produce a sustainable auto part and to propose an alternative to GFRPs and CFRPs. Since this approach of using natural fiber and the sustainable matrix is a new approach in an automotive application, the primary concern of this thesis is to achieve the necessary mechanical properties required, basic human safety criteria, and the recyclable composite part.

This chapter aims to present the significant conclusions set up from work described in this thesis, concerning the subject described in *Chapter 1 and 3*. Also, several recommendations are made for future works.

4.1 CONCLUSIONS

A goal by goal conclusion is presented in this chapter for a better understanding of the work.

4.1.1 Study/Benchmarking various Natural fiber and sustainable matrix

Various natural fibers and their physical and chemical properties are studied to better understand the behavior of natural fiber. Several fibers such as Flax, Jute, Hemp, Kenaf, and sisal were studied, as well as their overall behavior. From the study, some fibers showed remarkable properties which can match the intended application and can replace GFRP or CFRP composites.

On studying and benchmarking various natural fibers in section 2.3 and 2.4.1, the following was concluded:

- ❖ Based on the weight/density criteria, coir and flax are said to be less dense fibers having 1.25 and 1.4 g/cc, respectively;
- ❖ Under tensile strength criteria, flax and hemp show a maximum tensile strength of 1500 and 900 MPa, respectively;
- ❖ Considering the strength of the fibers, flax and hemp exhibited the maximum Young's modulus of 80 and 70 GPa, respectively;
- ❖ Under failure strain consideration coir and cotton have a remarkably high strain rate of 15-25 and 3-10 %, respectively;
- ❖ Jute, cotton, and ramie fibers have the greater tendency to absorb moisture, while flax showed the best behavior;

- The price of the fibers is almost equal, thus, underprice criteria all the natural fibers are inexpensive except silk and spider silk.

On studying and benchmarking various sustainable matrices in section 2.4.2, the resins that have been studied in this work are PLA, Elium®, PEEK, and PPS.

- PLA is also called corn plastic, and it has a wide range of application in many industries. It is used in 3D printing technology and rapid prototyping because of its versatileness. The density of PLA is high, which makes the part heavier and it has low thermal resistance, and the mechanical properties are less to other resins. But, PLA is 100% biodegradable;
- Elium® is a liquid thermoplastic resin, which can be recycled efficiently using simple techniques and without investing much energy into it. Tensile strength and Young's modulus of Elium lies in the range of 557 MPa and 27 GPa, respectively, and the cost is equivalent to other thermoplastic resins available in the market. Elium is 100% recyclable;
- PEEK and PPS also have excellent mechanical properties but considering recycling and embodiment energy they are not economical. Recycling PEEK or PPS it takes remarkably high energy to break the polymer chain.

Analyzing various case studies on a bonnet system and many plastic bonnets in the market, a requirement matrix for a sustainable bonnet system was created, and some of the necessary properties at this stage of development are founded out to be:

- High Young's modulus;
- High tensile yield;
- High stiffness;
- Low density;
- High sustainability.

4.1.2 *The sustainable material selection process*

The material selection process can be done in many possible ways, but the effective and efficient way of choosing a material is by combining both Ashby and analytical methods of selection. From section 3.5.1, one can see the matrix and the fiber selection process.

The fibers selection is started by deriving a material index based on the intended application in this case. Bonnet is considered to be a flat rectangular plate, and the requirements are eco-design with high stiffness-minimum mass. The derived material index is $E^{1/3}/\rho$. Using the Density vs. Young's modulus Ashby chart and $E^{1/3}/\rho$ material index line, an area of interest is marked. Section 2.4.1 aids to select the three best materials from the area of interest. The three materials are Flax, Hemp, and Jute. From analytical calculations ***Flax*** has been selected as a suitable candidate.

The matrix selection is started by studying various sustainable resins in section 2.4.2, and again three possible resins have been chosen among them and compared their properties analytically. By the end of the calculation, ***Elium®*** shows better performance rate compared to other resin.

4.1.3 *Designing CAD part for Bonnet*

Since the Be car is still in the product development state, the cad geometry of the earlier prototype is taken as a reference geometry, and few modifications were made. The changes were made by considering a natural fiber reinforced bonnet.

The previous prototype bonnet is made of 3 mm DCPD, and the new design is of 5 mm of NFRP, and tolerance is added considering the use of adhesive between the frame and the skin in the bonnet.

4.1.4 *Design and manufacture of composite*

Based on the material selection process completed in section 3.5.1, a suitable manufacturing process is selected. The composite laminated is manufactured by the same manufacturing technique, which is the Vacuum Infusion technique, considering the bonnet section in mind. Using the same VARTM technique, two different set of samples were manufactured. As an outcome, a composite laminate with a good surface finish at a needed dimension was produced.

4.1.5 *Strength verification of composite*

The manufactured samples were cut according to standard testing coupon size as discussed in section 3.6. The mechanical characteristics of the composite are compared numerically with the experimental results. For that the composite must be modeled in numerical simulation software. Micromechanics has been used to calculate the strength of the composite in all directions which helps to model the composite adequately. The overall conclusion of experimental evaluation can be seen in Table 34.

Table 34 Strength Verification-Conclusion

Test		**Experimental**		**Numerical**
Tensile test	**E [GPa]**	4.35	Additive	7.01
		3.95	No Additive	
Bending Test	**σ_b [MPa]**	21.28	Additive	Interlaminar failure
		19.90	No Additive	
Impact test	**Visible Damage indentation [mm]**	2.1		1.4
Moisture Absorption	**EWE% Max**	1.443	Additive	
		1.339	No Additive	

In addition to the primary goals, an essential outcome of this study is that the added natural additive helps in enhancing the properties of the composite at a marginal rate. This increase in the property of the composite by the addition of natural additive might be a breakthrough in natural fiber composite usage. Further studies on the additive help in understanding and using the properties if it is in a better way.

4.1.6 *Safety criteria verification*

An automotive part, especially auto body parts, must qualify the NCAP safety criteria. In the case of Bonnet, it must qualify the safety criteria such as Head Impact Criteria, leg impact criteria, front and side pole crash criteria. In this study, HIC and front-pole impact criteria are evaluated.

The HIC tests are simulated using the conditions specified by the EURONCAP, and the tests were conducted at three critical zones on the bonnet system. The obtained HIC values are 314.62, 292.84, 806.193 at A, B, C zones, respectively, where the allowable values in those zones were 1700, 1000, and 1700, respectively. Therefore, the bonnet system is safe to manufacture and use in a car, in which regards the HIC. The final values show that the part meets the EUNCAP requirements for the HIC.

The front pole impact at 60 km/h was carried out to see the damage happened to bonnet during pole impact. The resultant stress achieved during the crash is 203.3 MPa which is marginally higher than the yield strength of the composite. In this case, the bonnet will have unrepairable damage. These results can be seen in section 3.6.5 and 3.6.6.

4.1.7 *Recycling*

The Flax/Elium® Composite is recycled at ease by both mechanical and chemical process. The composite is successfully recycled in both techniques. In the mechanical process, the composite part is shredded and remixed with Elium® resin and remanufactured using compression or hot press compression molding. The results for the mechanical recycling can be seen in section 3.7.1.

The chemical recycling process is even more straightforward. The parts to be recycled are immersed in any universal solvent/alcohol. The Elium® polymeric chains started breaking down and result in the separation of the matrix and the fiber. To reduce the process timing an initiator/catalyst is added to the solvent. In this study, the composite is successfully recycled, and the matrix and the fiber are separated. 90 % of the weight of the matrix is retained back after the recycling process.

By the end of recycling, the energy consumed, or the embodiment energy is comparatively less than other composites or other material. As a result, this composite is said to be a sustainable replacement to GFRP/CFRP/Metallic bonnets. However, a further study on the composite is necessary in order to use it in a wide range of applications instead of constraining it to a specific application. The overall conclusion of the work is tabulated in Table 35.

Table 35 Conclusions

S. No	*Goals*	*Status*
1	**Study and benchmark various natural fibers, sustainable matrix, and Bonnet system**	Achieved
2	**Sustainable material selection**	Achieved
3	**Designing a Bonnet system CAD part**	Achieved
4	**Successfully design and manufacture a sustainable composite**	Achieved
5	**Validate the physical strength of the composite by both experimentally and numerically ways**	Achieved
6	**Validate some essential safety requirements that the Bonnet must satisfy using CAE software (HIC and Crash)**	Achieved
7	**Successfully recycle the composite and reuse it**	Achieved

Achieved (green) Not achieved (red)

4.2 PROPOSALS OF FUTURE WORKS

In light of the work performed, numerous topics were proposed for future work. Some critical studies or developments that could be undertaken regarding material and manufacturing process development for a complete sustainable part and its characterization are:

- Modification of the fiber properties by chemical treatment using chemicals such as sodium hydroxide [133] and magnesium hydroxide [134]. This alkali treatment helps in improving the surface roughness of the fiber and enhances the adhesion between fiber and matrix. It also helps in enhancing the strength of the composite as well;
- To study the effect of the TSP additive by varying its content in the matrix mixture. In this study the amount of the additive added is equal to the weight of the peroxide used;
- Performing the detailed analysis on the bonnet to validate it in all the aspects and to prototype it successfully in the next "Be" prototype and manufacture it in a large scale. The detailed analysis includes complete stiffness requirement analysis, evaluating Leg injury criteria and other safety requirements as per EURONCAP requirements;
- Sandwiching the composite with natural fiber-based core materials such as flax/PP or Flax/PLA honeycomb structures Zuhri et al. [135] evaluated the mechanical properties of natural fiber-based honeycomb core structures which provided extensive knowledge in using them as an alternative to conventional foams and plastic cores. Stocchi et al. [136] evaluated the mechanical properties of flax/vinyl ester honeycomb reinforced sandwich panels;
- Analyze the properties of Hybrid natural fiber composite such as flax-Jute, Flax-Hemp, etc. reinforced composites.

In this work, the tensile, flexural, impact and moisture absorption behavior of the composite is investigated thoroughly. However, to consider this composite for structural applications, specifically bonnet and fenders of a car sometimes it becomes necessary to predict the actual response of a material/part to specific load scenarios. While this thesis does try to develop and validate all the possible predictive models (based on the rule of mixtures and conventional micro-mechanical models) on the tensile and fatigue properties of reinforced NFRPs, some aspects that require further research include:

- ❖ Stiffness and torsional evaluation of the composite must be done, as showed in Figure 49;
- ❖ The fatigue life of the composite and the fiber pullout tests had to be made to understand the composite during its life better;
- ❖ For structures manufactured through infusion processes, flow modeling is also genuinely relevant. It is of interest to investigate the effect of plant yarn structure on flow front evolution and fill time.

In this work, two ways of recycling the composite are described. Both are simple but, during depolymerization, the solvent is allowed to evaporate in the air so that the fiber and the matrix is extracted back. On using this depolymerization technique solvent to recycle the composite the recycle rate will be very high. A Chemical running bed system is created, and the fiber is placed at the center of the chamber and osmosis technique can be used to retain the matrix from the solvent. A schematic arrangement for this process is shown in Figure 111.

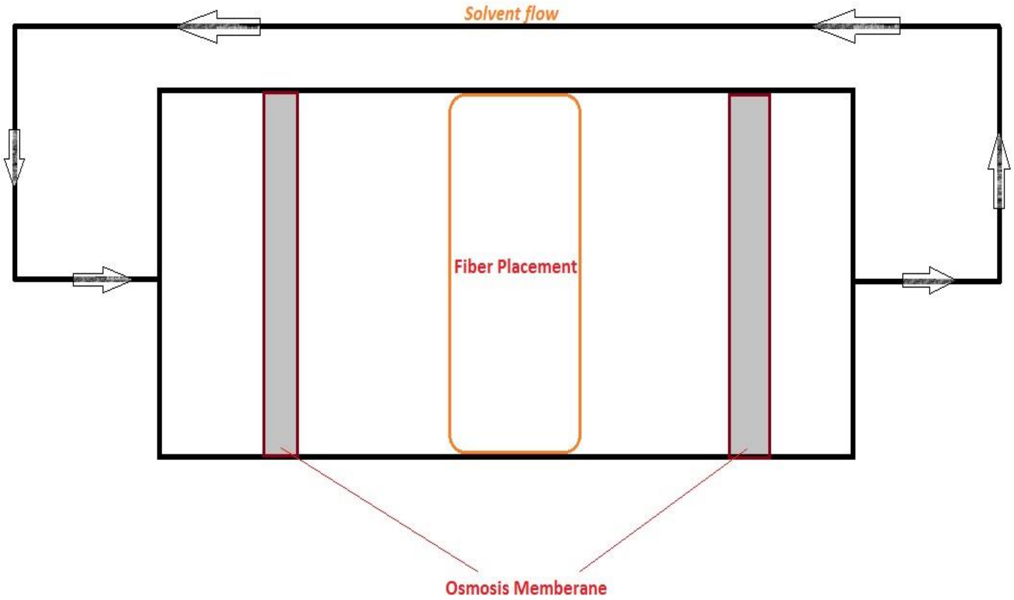

Figure 111 Simple schematic suggesting recycling technique

REFERENCES AND OTHER SOURCES OF INFORMATION

5 REFERENCES AND OTHER SOURCES OF INFORMATION

5.1 Works Cited

[1] "OICA," 2017. [Online]. Available: http://www.oica.net/category/production-statistics/2017-statistics/. [Accessed October 2017].

[2] "European comission growth sector- Automotive industry," European comission, 2017. [Online]. Available: https://ec.europa.eu/growth/sectors/automotive_en. [Accessed 05 March 2018].

[3] Plunkett Research, Ltd., "Automobile Industry Market Research," Plunkett Research, Ltd., Huston, Texas, 2017.

[4] ACEA - European Automobile Manufacturers Association, "Facts about the Automobile Industry," 2017. [Online]. Available: http://www.acea.be/automobile-industry/facts-about-the-industry. [Accessed 02 December 2017].

[5] ACEA - European Automobile Manufacturer Association, "Economic and Market Report Quater 3 2017," 2017.

[6] J. O'Brien, FORD and SYNC, "Time machine: Car Tech," Mashable- Tech.

[7] M. Popular, "Article- Evolution of Technology in cars," in *Popular Mechanics Magazine*, 2017.

[8] B. Stewart, "The 15 Most Important Automotive Tech Milestones of the Last 25 Years," Popular Mechanics, 2016.

[9] INTLAND SOFTWARE, "An outlook on Automotive Tech Trends in 2018," 2018.

[10] Z. Shahan, "1 Million Pure EVs Worldwide: EV Revolution Begins," Clean Technica, 2016.

[11] R. MATULKA, "The History of the Electric cars," U.S. Department of Energy, 2017.

[12] E. Ghassemieh, Materials in Automotive Application, State of the Art and Prospects, Sheffield, UK, 2011.

[13] A. McWilliams, "Advanced Materials, Lightweight Materials in Transportation," 2017.

[14] W. J. Witteman, "Improved Vehicle Crashworthiness Design by Control of the Energy Absorption for Different Collision Situations," *Eindhoven University of Technology-Thesis,* 2009.

[15] UK Environment-agency, 2010. [Online]. Available: http://www.environment-agency.gov.uk.

[16] CAR - Centre for Automotive Research, "Technology Roadmaps:Intelligent Mobility Technology, Materials and Manufacturing Processes, and Light Duty Vehicle Propulsion," 2017.

[17] J. Baron and S. Modi, "Assessing the Fleet-wide Material Technology and Costs to Lightweight Vehicles.," 2016.

[18] K. Behlouli, "Chapter 16: Natural Fiber Composites in Automotive Applications," in *Handbook of Green Materials*, 2014, pp. 245-253.

[19] J. Lee, G. Kim and K. Smith, "National renewable energy laboratory (NREL) U.S.," 2010. [Online]. Available: https://www.nrel.gov/vehiclesandfuels/energystorage/publications.html#p2010. [Accessed 06 March 2018].

[20] S. Peters1, G. Lanza, J. Ni, J. Xiaoning, Y. Pei-Yun and M. Colledani, "Automotive manufacturing technologies – an international viewpoint," *S. Peters et al., Published by EDP Sciences,* 2014.

[21] U. D. o. Energy, "Technical Plan — Fuel Cells," 2015. [Online]. Available: https://www1.eere.energy.gov/hydrogenandfuelcells/mypp/pdfs/fuel_cells.pdf. [Accessed 07 March 2018].

[22] Y. Wang, K. Chen, J. Mishler, S. Cho and X.C. Adroher, *Applied Energy 88,* vol. 4, 2011.

[23] D. Carter, M. Ryan and J. Wing, "Fuel Cell Today," [Online]. Available: http://www.fuelcelltoday.com/analysis/industry-review/2012/the-industry-review-2012. [Accessed 07 March 2018].

[24] "Fuel Cell Europe," [Online]. Available: http://ec.europa.eu/clima/consultations/0005/registered/88980385100-51_fuelcelleurope_en.pdf. [Accessed 07 March 2018].

[25] "Advanced Manufacturing Portal," 2015. [Online]. Available: http://www.manufacturing.gov/lm3i.html. [Accessed 07 March 2018].

[26] "Fraunhofer Institute for Chemical Technology," 2013. [Online]. Available: http://www.ict.fraunhofer.de/en/comp/pe/hfv/thermoset_RTM_process.html. [Accessed 07 March 2018].

[27] W. Hufenbach, 2015. [Online]. Available: http://www.tudresden.de/die_tu_dresden/W. Hufenbach (2013) http://www.tudresden.de/die_tu_dresden/projekt. [Accessed 14 July 2017].

[28] "Automotive Council Technology Group, UK," 2013. [Online]. Available: http://www.automotivecouncil.co.uk/wp-content/uploads/2013/09/Lightweight1.jpg. [Accessed 26 September 2017].

[29] "European Technology Platform Photonics21," 2014. [Online]. Available: https://www.photonics21.org/download/PhotonicsMultiannualRoadmap/PhotonicsMultiannualStrategicRoadmapDocument.pdf. [Accessed 2017].

[30] "Advanced Manufacturing Portal," U.S. Goverment, 2015. [Online]. Available: https://www.manufacturing.gov/nnmi_pilot_institute.html. [Accessed October 2017].

[31] Volkswagen and B. Wilhelm, "Platform and Modular Concepts at Volkswagen — Their Effects on the Assembly Process," in *Transforming Automobile Assembly*, vol. 30, Shimokawa, Koichi and Jürgens, Eds., Springer, pp. 146-156.

[32] J. Fleischer and J. Schaedel, *CIRP Journal of Manufacturing Science and Technology,* vol. 6, no. 2.

[33] J.-E. Gans, G. Lanza, R. Muller, S. Peters and L. Schoen, "wt Werkstattstechnik online," wt Werkstattstechnik online.

[34] T. Bauernhansl, interaktiv – Fraunhofer IPA.

[35] R. Lund, "Remanufacturing: United States Experience and Implications for Developing Nations," Center for Policy Alternatives, Massachusetts Institute of Technology, Massachusetts, 1983.

[36] A. Brusaferri, M. Colledani, G. Copani and N. Pedrocchi, "Implementing Sustainable Manufacturing," in *The 10th Global Conference on Sustainable Manufacturing*, Istanbul.

[37] D. Froelich, E. Maris, N. Haoues, L. Chemineau and H. Renard, "Material Engineering," in *Minerals Engineering*, 2007.

[38] N. Perry, A. Bernard, F. Laroche and S. Pompidou, *CIRP Annals – Manufacturing Technology,* vol. I, no. 61.

[39] M. F. Ashby, Materials in Mechanical Design, Elsevier Ltd., 2011.

[40] M. S. F. A.Jahan, "Classification of screening and ranking methods in materials selection," *Materials & Design,* pp. 696-705, 2010.

[41] R. Malkapuram, V. Kumar and Y. S. Negi, "Recent development in natural fiber reinforced polypropylene composites," *Journal of Reinforced Plastics and Composites,* pp. 1169-1189, 2009.

[42] K. Amar, M. Manjusri and T. and Lawrence, Natural Fibers, Biopolymers, and Bio-composites, CRC Press, Tailor & Francis., 2005.

[43] S. Taj, M. A. Munawar and S. u. Khan, "Review- NATURAL FIBER-REINFORCED POLYMER COMPOSITES," *Proc. Pakistan Acad. Sci.,* pp. 129-144, 2007.

[44] A. Nechwata, Reußmann, S. Böhm and E.Richter, "The Dependence between the Process Technologies and the Effect of MAH-PP- Adhesives in Natural Fibre Reinforced Thermoplastic Composites," *Advanced Engineering Materials,* vol. 7, no. 1-2, pp. 68-73, 2005.

[45] J. C. Sakthivel, S. Mukhopadhyay and N. K. Palanisamy, "Some Studies on Mudar Fibers," *Journal of Industrial Textiles,* vol. 35, no. 1, pp. 63-76, 2005.

[46] A.Bessadok and S.Roudesli, "Alfa fibers for unsaturated polyester composites reinforcement: Effects of chemical treatments on mechanical and permeation properties," *Composites Part A: Applied Science and Manufacturing,* vol. 40, no. 2, 2009.

[47] M. C. Symington, W. Banks, O. D. West and R. Pethrick, "Tensile Testing of Cellulose-Based Natural Fibers for Structural Composite Applications," *Journal of Composite Materials,* vol. 43, no. 9, pp. 1083-1108, 2009.

[48] V.S.Sreenivasan, S. Somasundaram and D. Ravindran, "Microstructural, physicochemical and mechanical characterization of Sansevieria cylindrica fibers – An exploratory

investigation," *Materials & Design,* vol. 32, no. 1, pp. 453-461, 2011.

[49] A. Mohanty, M. Misra, L. Drzal, S. Selke, B. Harte and G. Hinrichsen, Natural Fibers, Biopolymers and Biocomposites, Boca Raton: CRC Press, 2005.

[50] A. Sathaye, "Jute Fibre Based Composite for Automotive Headlining," *SAE Technical Paper 2011-01-0224,* 2011.

[51] K. M. Nair, S. Thomas and GGroeninckx, "Thermal and dynamic mechanical analysis of polystyrene composites reinforced with short sisal fibers," *Composites Science and Technology,* vol. 61, no. 16, pp. 2519-2529, 2001.

[52] R.M.N.Arib, S. Sapuan and M. Paridah, "Mechanical properties of pineapple leaf fiber reinforced polypropylene composites," *Materials & Design,* vol. 27, no. 5, pp. 391-396.

[53] S. L. Fávaro, M. S. Lopes, A. G. V. d. C. Neto, R. R. d. Santana and E. Radovanovic, "Chemical, morphological, and mechanical analysis of rice husk / post-consumer polyethylene composites," *Composites Part A: Applied Science and Manufacturing,* vol. 41, no. 1, pp. 154-160, 2011.

[54] L. B.Manfredi, E. S.Rodríguez and M. Wladyka-Przybylak, "Thermal degradation and fire resistance of unsaturated polyester, modified acrylic resins and their composites with natural fibers," *Polymer Degradation and Stability,* vol. 97, no. 2, pp. 255-261.

[55] M. Sain, S.HPark, F. Suhara and S. Law, "Flame retardant and mechanical properties of natural fiber–PP composites containing magnesium hydroxide," *Polymer Degradation and Stability,* vol. 83, no. 2, pp. 363-367, 2013.

[56] S. Mohanty, S. K.Verma and S. K.Nayak, "Dynamic mechanical and thermal properties of MAPE treated jute/HDPE composites," *Composites Science and Technology,* vol. 66, no. 3-4, pp. 538-547, 2007.

[57] K.Majeedab, M.Jawaid, A.Hassan, A. Bakar, H. Khalil and A.A.Salema, "Potential materials for food packaging from nanoclay/natural fibers filled hybrid composites," *Materials & Design,* vol. 46, pp. 391-410, 2013.

[58] P. Wambua, B. Vangrimde, S. Lomov and IgnaasVerpoest, "The response of natural fibre composites to ballistic impact by fragment simulating projectiles," *Composite Structures,* vol. 77, no. 2, pp. 232-240, 2007.

[59] M.S.Sreekala, M.G.Kumaran and S. Thomas, "Stress relaxation behavior in oil palm fibers," *Materials Letters,* vol. 50, no. 4, pp. 263-273, 2012.

[60] M.M.Kabir, H.Wang, K.T.Lau and F.Cardona, "Chemical treatments on plant-based natural fiber reinforced polymer composites: An overview," *Composites Part B: Engineering,* vol. 43, no. 7, pp. 2883-2892, 2012.

[61] A. Mohanty, M. AKhan and G. Hinrichsen, "Surface modification of jute and its influence on performance of biodegradable jute-fabric/Biopol composites," *Composites Science and Technology,* vol. 60, no. 7, pp. 1115-1124, 2013.

[62] J. Meredith, R. Ebsworth, S. R.Coles, B. M.Wood and K. Kirwan, "Natural fiber composite energy absorption structures," *Composites Science and Technology,* vol. 72, no. 2, pp. 211-217, 2012.

[63] P. K. Bajpai, I. Singh and J. Madaan, "Tribological behavior of natural fiber reinforced PLA composites," *Wear,* vol. 297, no. 1-2, pp. 829-840, 2013.

[64] C.W.China and B.F.Yousif, "Potential of kenaf fibers as reinforcement for tribological applications," *Wear,* pp. 1550-1557, 2009.

[65] N.S.M.El-Tayeb, "A study on the potential of sugarcane fibers/polyester composite for tribological applications," *Wear,* vol. 265, no. 1-2, pp. 223-235, 2008.

[66] M.M.Davoodi, S.M.Sapuan, D.Ahmad, A.Aidy, A.Khalina and M. Jonoobi, "Concept selection of car bumper beam with developed hybrid bio-composite material," *Materials & Design,* vol. 32, no. 10, pp. 4857-4865, 2011.

[67] P. Bajpai, I. Singh and J. Madaan, "Tribological behavior of natural fiber reinforced PLA Composites," *wear 297,* no. 1-2, pp. 829-840, 2012.

[68] A. Shalwan and B. Yousif, "In State of Art: Mechanical and tribological behavior of polymeric composites based on natural fibers," *Materials & Design,* vol. 48, pp. 14-24, 2013.

[69] O. Faruk, A. K. Bledzki, H.-P. Fink and M. Sain, "Biocomposites reinforced with natural fibers: 2000–2010," *Progress in Polymer Science,* vol. 37, no. 11, p. 1552–1596, 2012.

[70] DilipKumar, Amarnath and Rakesh, "Design and analysis of Natural fiber composite," Anna University, Chennai, 2016.

[71] N. Banthia and R. Gupta, "Influence of polypropylene fiber geometry on plastic shrinkage cracking in concrete," *Cement and Concrete Research,* vol. 36, no. 7, p. 1263–1267, 2006.

[72] S. Joshi, L.TDrzal, A.KMohanty and S. Arora, "Are natural fiber composites environmentally superior to glass fiber reinforced composites?," *Composites Part A: Applied Science and Manufacturing,* vol. 35, no. 3, pp. 371-376, 2011.

[73] M.M.Davoodi, S.M.Sapuan, D.Ahmad, AidyAliaA.Khalina and M. Jonoobi, "Mechanical properties of hybrid kenaf/glass reinforced epoxy composite for passenger car bumper beam," *Materials & Design,* vol. 31, no. 10, pp. 4927-4932, 2010.

[74] A. C. a. Kılınc, C. Durmus¸kahya and M. €. O. Seydibeyog˘lu, "Natural fibers," in *Fiber Technology for Fiber-Reinforced Composites*, Woodhead Publishing, 2017, pp. 210-235.

[75] f. Wild, "Wild Fibres - Natural fibres for spinning & felting," 11 April 2018. [Online]. Available: http://www.wildfibres.co.uk/html/jute.html.

[76] Saheb, D. Nabi, Jog and J. P, "Natural fiber polymer composites: a review," *Advances in polymer technology,* pp. 351-363, 1999.

[77] S. Biswas, S. Shahinur, M. Hasan and Q. Ahsan, "Physical, Mechanical and Thermal Properties of Jute and Bamboo Fiber Reinforced Unidirectional Epoxy Composites," in *6th BSME International Conference on Thermal Engineering*, 2015.

[78] C. Alves, P. Ferrão, A. Silva, L. Reis and M. Freitas, "Ecodesign of automotive components making use of natural jute fiber composites," *Journal of Cleaner Production,* vol. 18, no. 4, pp. 313-327, 2010.

[79] F. Cristiano, P. Ana and S. Carlo, "Mechanical and impact characterization of flax and basalt fiber vinyl ester composites and their hybrids," *Composites Part B: Engineering,* pp. 247-259, 2018.

[80] C. Kong, H. Lee and HyunbumPark, "Design and manufacturing of automobile hood using natural composite structure," *Composites Part B: Engineering,* pp. 18-26, 2016.

[81] S.Sair, A.Oushabi, A.Kammouni, O.Tanane, Y.Abboud and A. Bouari, "Mechanical and thermal conductivity properties of hemp fiber reinforced polyurethane composites," *Case Studies in Construction Materials,* pp. 203-212, 2018.

[82] B. Zuccarello, G. Marannano and A. Mancino, "Optimal Manufacturing and Mechanical Characterization of High-Performance Biocomposites Reinforced by Sisal Fibers," *Composite Structures,* 2018.

[83] F. Food and Agriculture Organization-United Nation, "Future Fibers," FAO-United Nation, New York, 2016.

[84] W. D. (. Brouwer, "Natural Fibre Composites in Structural Components: Alternative Applications for Sisal?," *Common Fund for Commodities - Alternative Applications for Sisal and Henequen - Technical Paper No. 14,* 2000.

[85] L. Xiao, B. Wang, G. Yang and M. Gauthier, "PLA-Based Biomaterials: Synthesis, Modification and Applications, Biomedical Science," *Engineering and Technology,* 2012.

[86] B. Bax and J. Müssig, "Impact and tensile properties of PLA/Cordenka and PLA/flax composites," *Composites Science and Technology,* pp. 1601-1607, 2008.

[87] M. A.Sawpana, K. L.Pickering and AlanFernyhough, "Improvement of mechanical performance of industrial hemp fiber reinforced polylactide biocomposites," *Composites Part A: Applied Science and Manufacturing,* pp. 301-319, 2011.

[88] A. Couture, G. Lebrun and L. Laperrière, "Mechanical properties of polylactic acid (PLA) composite reinforced with unidirectional flax and flax-paper layers," *Composite Structures,* pp. 286-295, 2016.

[89] Arkema, *Press Release,* 2014.

[90] "Liquid thermoplastic resins processable with thermoset composite techniques.," March 2014. [Online]. Available: https://www.plasticstoday.com/content/liquid-thermoplastic-resins-processable-thermoset-composite-techniques/1953251020169.

[91] Arkema, "Elium Liquid thermoplastic composite," Arkema International, Colombes Cedex.

[92] D. Parker, J. Bussink, T. G. H, W. W. G, D. E and R. K. ,. S. F. ,. J. O. a. W. R. Ostlinning E., "Polymers, High-Temperature," *Ullmann's Encyclopedia of Industrial Chemistry,* 2012.

[93] L. Jonsson and M. Lundborg, "Dry transformer bushings with composite insulators," *In Central America and Panama Convention (CONCAPAN XXXIV), IEEE,* 2014.

[94] "Properties of PEEK material," 31 August 2018. [Online]. Available: https://www.uplandfab.com/peek-machining.

[95] Harry R. Luzetsky; John Michasiow, "Design Development of Lightweight Thermoplastic Composite Cargo Floor for Helicopter Application," *AHS International 74rd Annual Forum & Technology Display.*

[96] David Hauber; Zachary August, "Manufacturing Optimization of Thermoplastic Composite Pressure Vessels: Presentation," *AHS International 74rd Annual Forum &*

Technology Display, 2018.

[97] M. Roux, C. Dransfeld and N. Eguémannb, "PROCESSING AND RECYCLING OF A THERMOPLASTIC COMPOSITE FIBRE/PEEK AEROSPACE PART," *ECCM16 - 16th EUROPEAN CONFERENCE ON COMPOSITE MATERIALS,* 2014.

[98] "Tamarind seeds," 2016. [Online]. Available: http://www.agriculturalproductsindia.com/seeds/seeds-tamarind-seeds.html.

[99] "Agro Products-Seeds," Agro Products India, [Online]. Available: http://www.agriculturalproductsindia.com/seeds/seeds-tamarind-seeds.html. [Accessed 11 April 2018].

[100] S. Krishna and T. P. Ghose, Indian Ephedras, Delhi: Government of India Central Pub. Branch, p. 32.

[101] M.-p. Ho, H. Wang, J.-H. Lee, C.-k. Ho, K.-t. Lau, J. Leng and D. Hui, "Critical factors on manufacturing processes of natural fiber composites," *Composites: Part B,* pp. 3549-3562, 2012.

[102] K. G. Swift and J. D. Booker, Process Selection From design to manufacture, Butterworth-Heinemann, 2003.

[103] N. L. Moigne, M. v. d. Oever and T. Budtova, "A statistical analysis of fiber size and shape distribution after compounding in composites reinforced by natural fibers," *Composites Part A: Applied Science and Manufacturing,* pp. 1542-1550, 2011.

[104] S. K. Mazumdar, COMPOSITES MANUFACTURING Materials, Product, and Process Engineering, CRC Press LLC, 2002.

[105] C. Kong, H. Lee and H. Park, "Design and manufacturing of automobile hood using natural composite structure," *Composites Part B,* pp. 18-26, 2016.

[106] volvo car corporation, "Design prerequisites," Gothenburg, Sweden.

[107] EuroNCAP, "Pedestrian safety results of Renault Twingo, BMW i3 and Volvo XC90," EuroNCAP, 2017. [Online]. Available: http://www.euroncap.com/en/ratings-rewards/latest-safety-ratings/#?selectedMake=0&selectedMakeName=Select&selectedModel=0&includeFullSafetyPackage=true&includeStandardSafetyPackage=true&selectedModelName=All&selectedProtocols=26061&selectedClasses=1202,11. [Accessed 12 March 2018].

[108] Porsche, "The new porsche 911 rs," Porsche, [Online]. Available: https://newsroom.porsche.com/en/products/. [Accessed 13 March 2018].

[109] t. Materials, "Ford develops prototype carbon composite bonnet," [Online]. Available: http://www.materialstoday.com/composite-applications/. [Accessed 12 March 2018].

[110] Y. Yanga, R. Boom, B. Irion, D.-J. v. Heerden, P. Kuiper and H. d. Wit, "Recycling of composite materials," *Chemical Engineering and Processing: Process Intensification,* pp. 53-68, 2012.

[111] S.J.Pickering, "Recycling technologies for thermoset composite materials—current status," *Composites Part A: Applied Science and Manufacturing,* pp. 1206-1215, 2006.

[112] D. Weiss, "Recycling and disposal of metal–matrix composites," in *ASM Handbook, Volume 21: Composites*, ASM International®, 2001, pp. 1013-1016.

[113] CEiiA, "CEiiA-Mobility," CEiiA, [Online]. Available: https://www.ceiia.com/mobility. [Accessed 2018 September 11].

[114] A.Masoumi, M. H. Shojaeefard and A. Najib, "Comparison of steel, aluminum and composite bonnet in term of pedestrian head impact," *Safety Science,* pp. 1371-1380, 2011.

[115] A. Michael F, The CES EduPack database of natural and man-made materials, Cambridge, UK: Cambridge University and Granta Design, 2008.

[116] D. Hull and T. Clyne, An Introduction to Composite Materials, second edition, Cambridge: Cambridge University Press, 1996.

[117] W. Callister, "Composites," in *Materials Science and Engineering An Introduction*, Utah, 2010, pp. 577-617.

[118] A. S. Virk, "Numerical models for natural fiber composites," University of Plymouth, Plymouth, 2010.

[119] B. Harris, Engineering Composite materials, London: The Institute of materials London, 1999.

[120] M. E. Messiry, "Theoretical analysis of natural fiber volume fraction of reinforced composites," *Alexandria Engineering Journal,* pp. 301-306, 2013.

[121] AkzoNobel, "Perkadox CH-50X Product Data sheet," AkzoNobel, 2012.

[122] D. G. R. William D. Callister Jr, Materials Science and Engineering: An Introduction, 8th Edition, Utah: Library of Congress , 2010.

[123] ASTM, "Standard Test Method for Tensile Properties of Polymer Matrix Composite Material," ASTM.

[124] R. K. Bansal, A Textbook Of Strength Of Materials, Laxmi Publications Pvt Limited, 2007.

[125] ASTM, "Standard method for testing short beam strength for polymer matrix composite and their laminates," ASTM International, 2006.

[126] ASTM, "Standard Test Method for Moisture Absorption Properties and Equilibrium Conditioning of Polymer Matrix Composite Materials," ASTM International, 2014.

[127] I.-. I. I. f. H. Safety, "Side Impact Injury Measures Rating," Insurance Institute for Highway Safety, Ruckersville, 2014.

[128] EuroNCAP, "Pedestrian safety tests and results," EuroNCAP, 2017. [Online]. Available: http://www.euroncap.com/en/ratings-rewards/latest-safety-ratings/#?selectedMake=0&selectedMakeName=Select&selectedModel=0&includeFullSafetyPackage=true&includeStandardSafetyPackage=true&selectedModelName=All&selectedProtocols=26061&selectedClasses=1202,11. [Accessed 12 March 2018].

[129] UNECE, "DRAFT REGULATION ON PEDESTRIAN SAFETY," United Nation, 2009.

[130] S. Pal, Design of Artificial Human Joints & Organs, Springer, 2013.

[131] A. L. Duigou, P. Davies. and C. Baley, "Environmental impact analysis of the production of flax fibers to be used as composite material reinforcement.," *Journal of Biobased Materials and Bioenergy,* pp. 153-165, 2011.

[132] D. N. V. A. H. W. Summerscales J, "A review of bast fibers and their composites.," *Part 2 – Composites. Composites Part A: Applied Science and Manufacturing,* pp. 1336-1344, 2010.

[133] A. Amiri, C. A. Ulven and S. Huo, "Effect of Chemical Treatment of Flax Fiber and Resin Manipulation on Service Life of Their Composites Using Time-Temperature Superposition," *Polymers,* no. 7, pp. 1965-1978, 2015.

[134] Y. Wu, C. Xia, L. Cai, A. C. Garcia and S. Q. Shi, "Development of natural fiber-reinforced composite with comparable mechanical properties and reduced energy consumption and environmental impacts for replacing automotive glass-fiber sheet molding

compound," *Journal of Cleaner Production,* no. 184, pp. 92-100, 2018.

[135] M.Y.M.Zuhri, Z.W.Guan and W.J.Cantwell, "The mechanical properties of natural fibre based honeycomb core materials," *Composites Part B: Engineering,* vol. 58, pp. 1-9, 2014.

[136] A. Stocchi, L. Colabella, A. Cisilino and V. Álvarez, "Manufacturing and testing of a sandwich panel honeycomb core reinforced with natural-fiber fabrics," *Materials & Design,* vol. 55, pp. 394-403, 2014.

ANNEXES

6 ANNEXES

6.1 ANNEX1

This section is to present the support documents for the chapter STATE OF THE ART.

6.1.1 Passenger car trade

Table 36 EU passenger car trade

	Jan-Sep 2017	Jan-Sep 2017	% change
Imports	29,874	27,779	+7.5
Exports	94,519	92,362	+2.3
Trade Balance	64,644	64,583	+0.1
Trade in volume (Units)	**Jan-Sep 2017**	**Jan-Sep 2017**	**% change**
Imports	2,282,445	2,084,231	+9.5
Exports	4,195,727	4,009,484	+4.5

Source 5 EUROSTAT

6.1.2 Passenger car imports

Table 37 Origin of most passenger car imports

Trade in value (€M)	Jan-Sep 2017	Jan-Sep 2017	% change
WORLD	29,874	27,779	+7.5
JAPAN	5,719	6,816	-16.1
TURKEY	5,658	4,372	+29.4
UNITED STATES	4,642	5,454	-14.9
SOUTH KOREA	4,176	3,598	+16.1
MEXICO	3,027	1,482	+ 104.3
Trade in volume (Units)	**Jan-Sep 2017**	**Jan-Sep 2017**	**% change**
WORLD	2,282,445	2,084,231	+9.5
TURKEY	551,776	450,611	+22.5
JAPAN	406,596	423,244	-3.9
SOUTH KOREA	348,509	306,261	+13.8
UNITED STATES	174,497	190,936	-8.6
MOROCCO	169,765	137,454	+23.5

Source 6 EUROSTAT

6.1.3 *Passenger car Exports*

Table 38 EU passenger car exports

Trade in value (€M)	Jan-Sep 2017	Jan-Sep 2017	% change
WORLD	94,519	92,362	+2.3
UNITED STATES	27,398	27,143	+0.9
CHINA	16,360	14,714	+11.2
JAPAN	5,940	5,405	+9.9
SWITZERLAND	5,508	5,374	+2.5
TURKEY	4,528	6,112	-25.9
Trade in volume (Units)	**Jan-Sep 2017**	**Jan-Sep 2017**	**% change**
WORLD	4,195,727	4,009,484	+4.7
UNITED STATES	828,846	847,104	-2.2
CHINA	425,075	359,477	+18.3
TURKEY	321,249	412,259	-22.1
NIGERIA	239,212	90,627	+164.0

Source 7 EUROSTAT

6.2 *ANNEX2*

6.2.1 *Property Importance calculation for fiber and matrix*

Table 39 Property importance detailed calculation

Prop	(1/2)	(1/3)	(1/4)		Importance
1	55	55	60	$\frac{Property\ 1}{Property\ 1}=\frac{55}{55}=1.00$	$\frac{\boldsymbol{Individual\ importance}}{\boldsymbol{Total\ importance}}=\frac{\mathbf{1.00}}{\mathbf{3.303}}=\mathbf{0.3028}$
2	45			$\frac{Property\ 1}{Property\ 2}=\frac{45}{55}=0.8182$	$\frac{\boldsymbol{Individual\ importance}}{\boldsymbol{Total\ importance}}=\mathbf{0.2477}$
3		45		$\frac{Property\ 1}{Property\ 3}=\frac{45}{55}=0.8182$	$\frac{\boldsymbol{Individual\ importance}}{\boldsymbol{Total\ importance}}=\mathbf{0.2477}$
4			40	$\frac{Property\ 1}{Property\ 4}=\frac{60}{40}=0.6667$	$\frac{\boldsymbol{Individual\ importance}}{\boldsymbol{Total\ importance}}=\mathbf{0.2018}$
				Total ***3.3031***	***1.000***

6.2.2 *Tensile Curves*

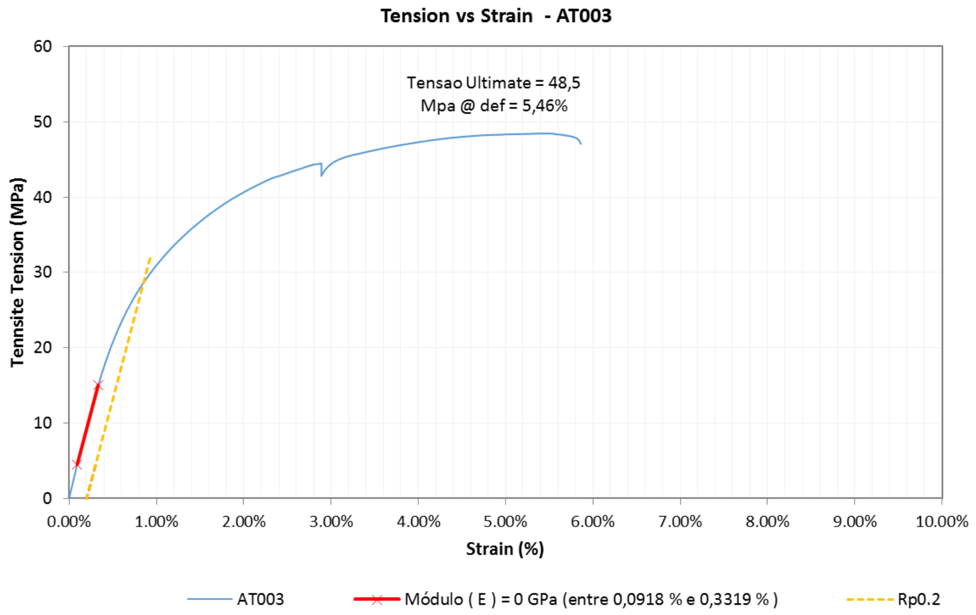

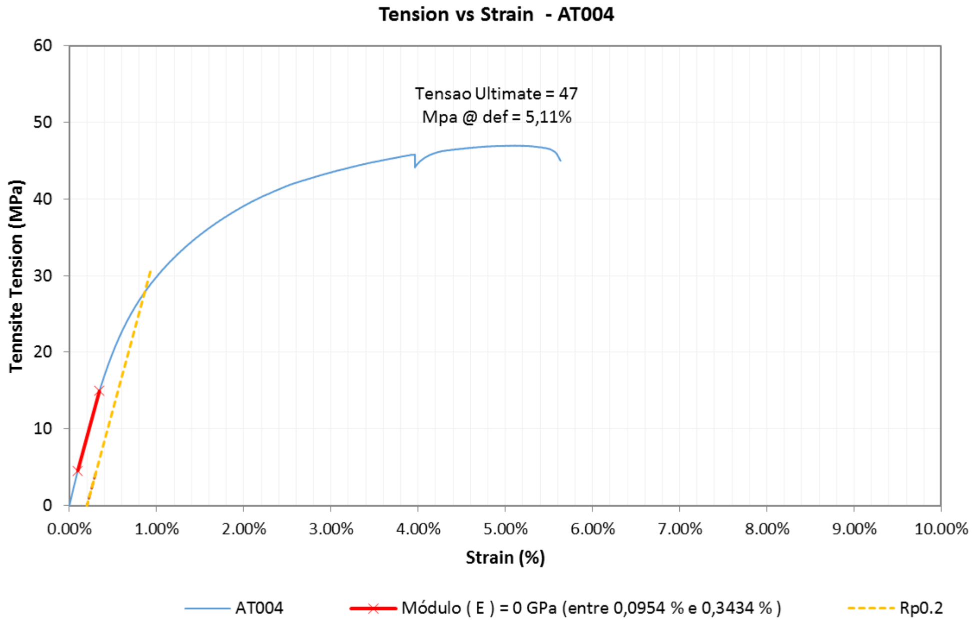

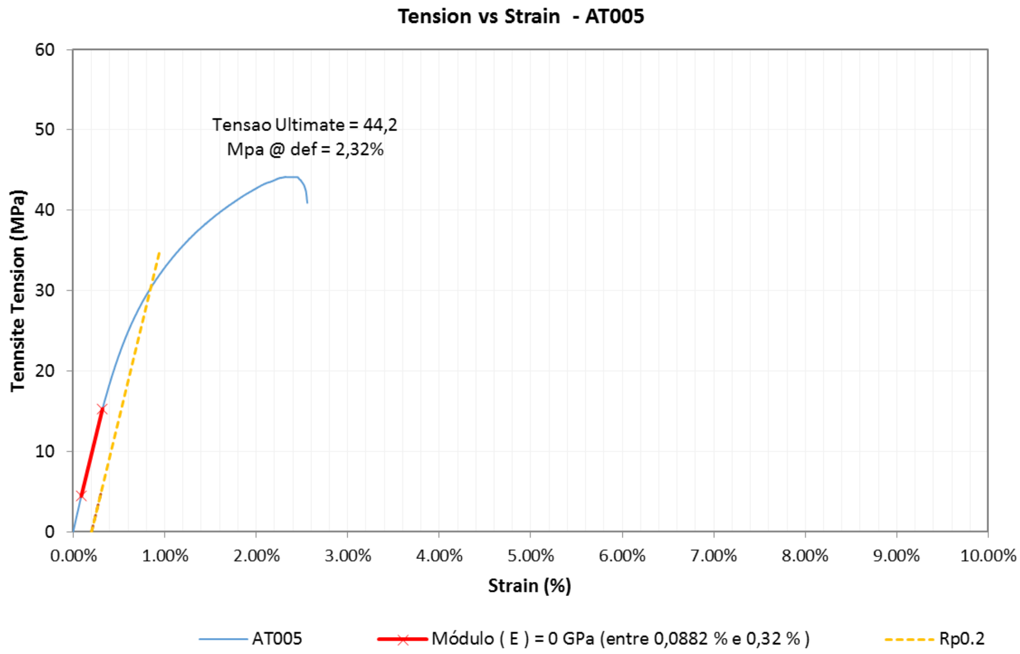
Tension vs Strain - AT005
Tensao Ultimate = 44,2 Mpa @ def = 2,32%
Tennsite Tension (MPa)
Strain (%)
AT005
Módulo (E) = 0 GPa (entre 0,0882 % e 0,32 %)
Rp0.2

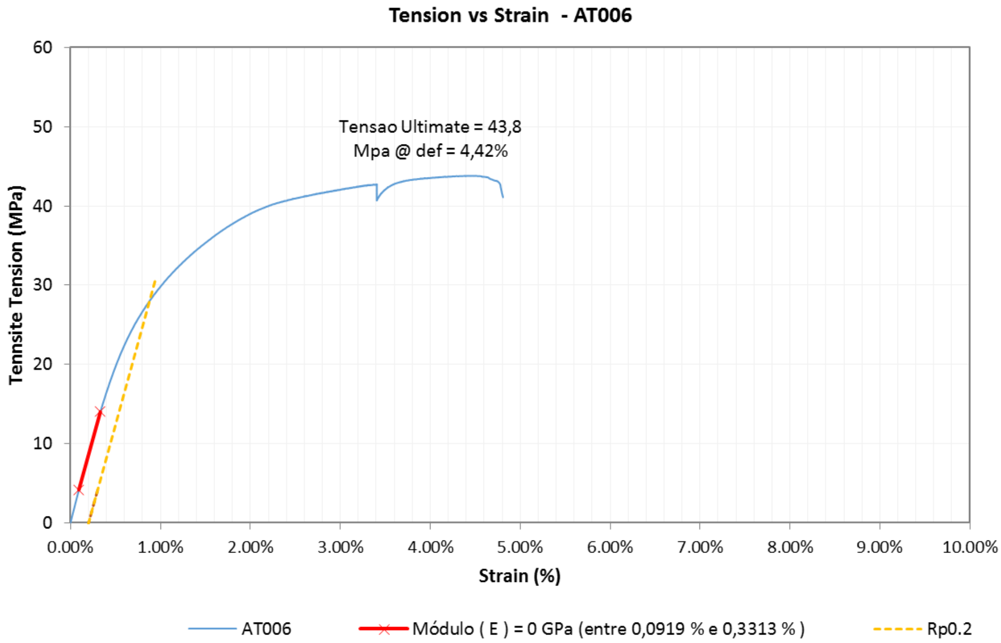
Tension vs Strain - AT006
Tensao Ultimate = 43,8 Mpa @ def = 4,42%
Tennsite Tension (MPa)
Strain (%)
AT006
Módulo (E) = 0 GPa (entre 0,0919 % e 0,3313 %)
Rp0.2

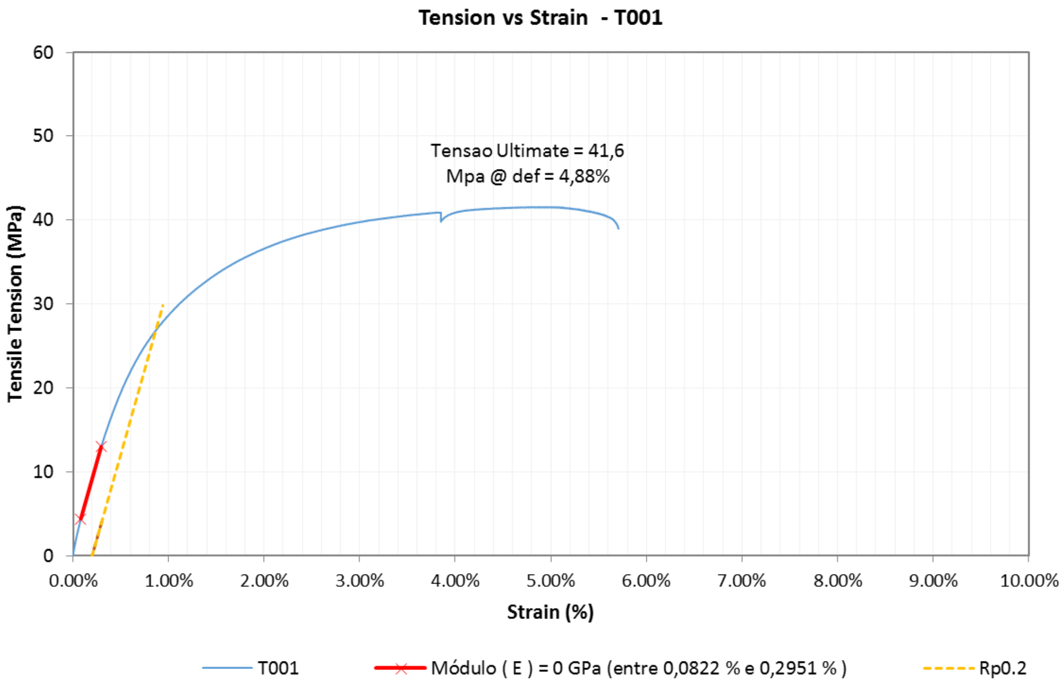
Tension vs Strain - T001
Tensao Ultimate = 41,6
Mpa @ def = 4,88%
Tensile Tension (MPa)
60
50
40
30
20
10
0
0.00%
1.00%
2.00%
3.00%
4.00%
5.00%
6.00%
7.00%
8.00%
9.00%
10.00%
Strain (%)
T001
Módulo (E) = 0 GPa (entre 0,0822 % e 0,2951 %)
Rp0.2

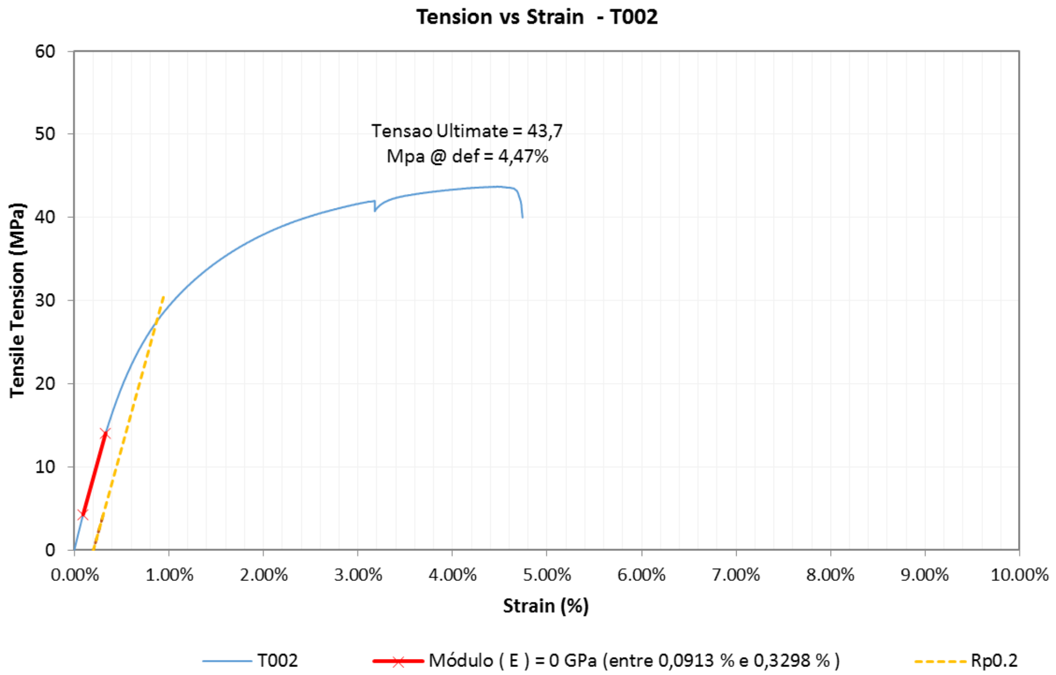
Tension vs Strain - T002
Tensao Ultimate = 43,7
Mpa @ def = 4,47%
Tensile Tension (MPa)
60
50
40
30
20
10
0
0.00%
1.00%
2.00%
3.00%
4.00%
5.00%
6.00%
7.00%
8.00%
9.00%
10.00%
Strain (%)
T002
Módulo (E) = 0 GPa (entre 0,0913 % e 0,3298 %)
Rp0.2

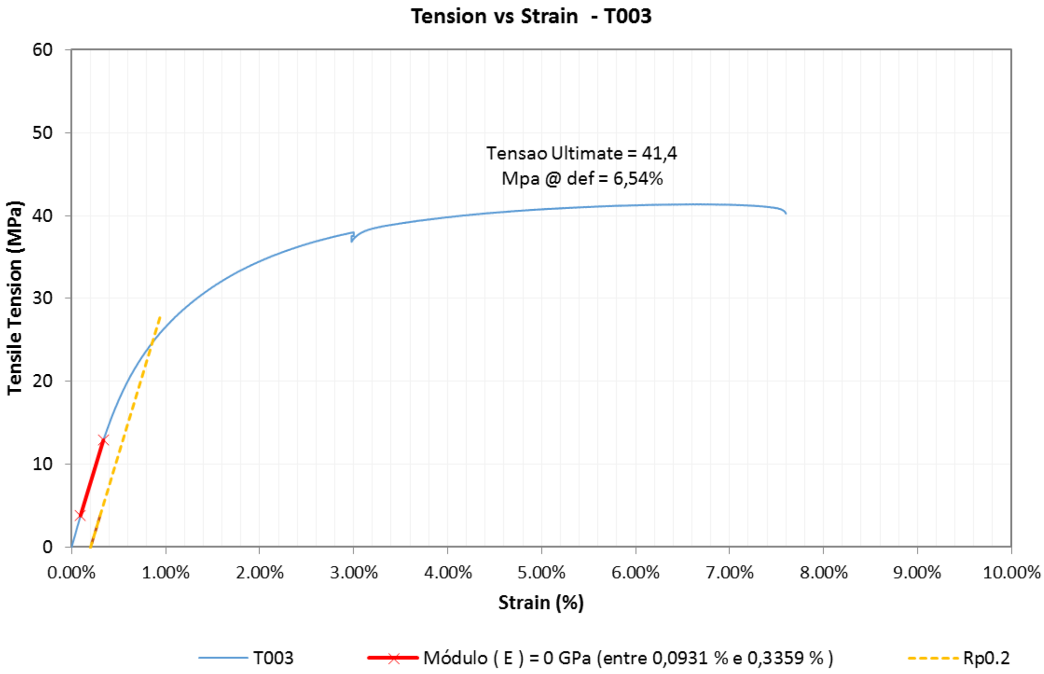
Tension vs Strain - T003
Tensao Ultimate = 41,4
Mpa @ def = 6,54%
Tensile Tension (MPa)
Strain (%)
T003
Módulo (E) = 0 GPa (entre 0,0931 % e 0,3359 %)
Rp0.2

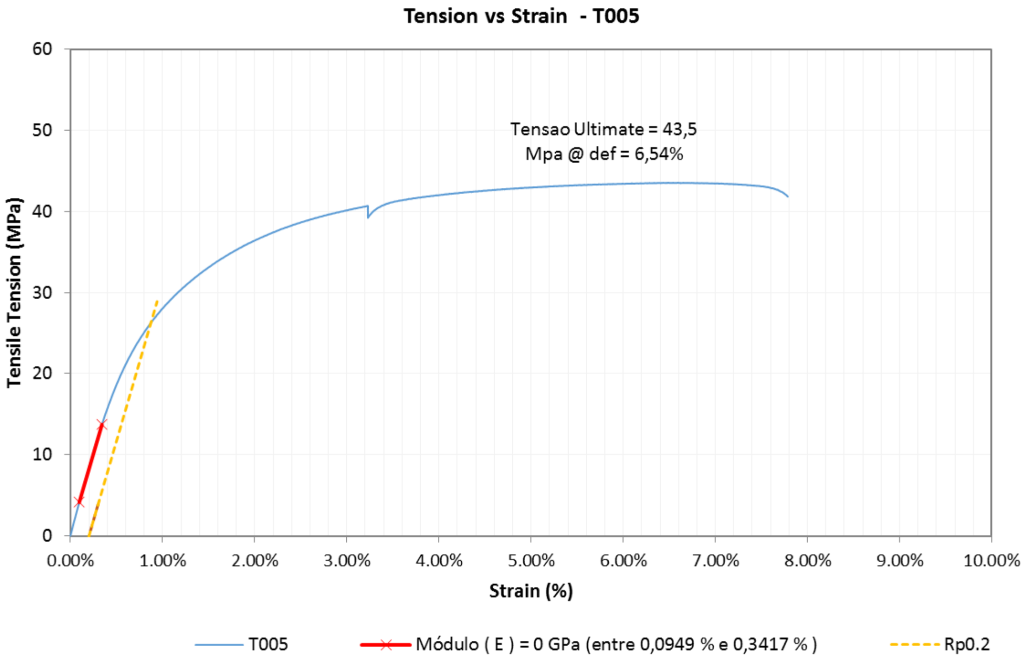
Tension vs Strain - T005
Tensao Ultimate = 43,5
Mpa @ def = 6,54%
Tensile Tension (MPa)
Strain (%)
T005
Módulo (E) = 0 GPa (entre 0,0949 % e 0,3417 %)
Rp0.2

6.2.3 *Short beam strength model calculation*

Table 40 Short beam strength model calculation

Equation	Maximum Load [N]	Area[mm^2]	Beam strength[MPa]
$\frac{3P_m}{2bh}$=strength	1456.89	**12x4.7=56.40**	$\frac{1456.89}{56.40} = 19.37$
	1573.15		$\frac{1573.15}{56.40} = 20.92$
	1460.40		$\frac{1460.40}{56.40} = 19.42$
	Average		**19.90**

6.2.4 *HIC calculation*

Table 41 HIC manual Calculation

$$HIC_A = \left[\frac{1}{0.03 - 0.015}\int_{0.015}^{0.030} 53.54\, dt\right]^{2.5} (0.030 - 0.015) = 314.62$$

$$HIC_B = \left[\frac{1}{0.03 - 0.015}\int_{0.015}^{0.030} 52.026\, dt\right]^{2.5} (0.030 - 0.015) = 292.84$$

$$HIC_C = \left[\frac{1}{0.03 - 0.015}\int_{0.015}^{0.030} 78.008\, dt\right]^{2.5} (0.030 - 0.015) = 806.193$$